AD NUMBER

AD482498

NEW LIMITATION CHANGE

TO

Approved for public release, distribution unlimited

FROM

Distribution authorized to U.S. Gov't. agencies and their contractors; Critical Technology; MAY 1966. Other requests shall be referred to Air Force Systems Command, Space Systems Division, Los Angeles, CA.

AUTHORITY

SAMSO ltr, 24 Jan 1972

Air Force Report No.
SSD-TR-66-73 Vol I

Aerospace Report No.
TR-669(6220-10)-3, Vol I

LIFTING REENTRY COMMUNICATIONS
VOLUME I: A COMPARATIVE EVALUATION OF POTENTIAL SYSTEMS

Prepared by

REENTRY AND PLASMA-ELECTROMAGNETICS DEPARTMENT
Plasma Research Laboratory

Laboratories Division
Laboratory Operations
AEROSPACE CORPORATION

May 1966

Prepared for

BALLISTIC SYSTEMS AND SPACE SYSTEMS DIVISIONS
AIR FORCE SYSTEMS COMMAND
LOS ANGELES AIR FORCE STATION
Los Angeles, California

NOTICE

This document is subject to special export controls and each transmittal to foreign governments or foreign nationals may be made only with prior approval of SSD(SSTRT).

FOREWORD

This report is published by the Aerospace Corporation, El Segundo, California, under Air Force Contract No. AF04(695)-669. The report was authored by the following members of the ad hoc Working Group on Reentry Communications:

Donald M. Dix
Kurt E. Golden
Edward C. Taylor
Marc A. Kolpin
Paul R. Caron

This working group was organized by Richard H. Huddlestone, Head, Reentry and Plasma-Electromagnetics Department, Plasma Research Laboratory in anticipation of the requirements of the Space Systems Division. The authors gratefully acknowledge Dr. Huddlestone's many suggestions and his constructive criticism.

The following figures have been adapted as indicated: Fig. 1, from D. R. Chapman, TN 4276, NACA, 1958; Fig. 3, from Ref. 6; Fig. 4, from Ref. 7; Fig. 5, from Ref. 9; Fig. 6, from Refs. 4 and 5; Fig. 13, from Ref. 25; Fig. 41, from Ref. 58.

This report, which documents research carried out from 1 July 1965 through 1 February 1966, was submitted on 16 May 1966 to Capt. R. F. Jones, SSTRT, for review and approval.

Information in this report is embargoed under the U.S. Export Control Act of 1949, administered by the Department of Commerce. This report may be released by departments or agencies of the U.S Government to departments or agencies of foreign governments with which the United States has defense treaty commitments. Private individuals or firms must comply with Department of Commerce export control regulations.

Approved

R. X. Meyer

R. X. Meyer, Director
Plasma Research Laboratory
Laboratories Division
Laboratory Operations

Publication of this report does not constitute Air Force approval of the report's findings or conclusions. It is published only for the exchange and stimulation of ideas.

Robert F. Jones

Robert F. Jones, Captain
Space Systems Division
Air Force Systems Command

ABSTRACT

Aerodynamic and electromagnetic calculations are performed to evaluate quantitatively the magnitude and duration of communications blackout for lifting reentry vehicles. A comprehensive list of proposed alleviation techniques is compiled and evaluated on the basis of communication quality, weight, flexibility, and required research. It is concluded that the techniques of local aerodynamic shaping, injection of coolant into the nonexpanding part of the flow, injection of electronegative species into the expanding part of the flow, and use of magnetic window are apparently feasible. A program of further research, which is required for a solution of the blackout problem, is delineated.

CONTENTS

CONTENTS (Continued)

CONTENTS (Continued)

FIGURES

FIGURES (Continued)

TABLES

I. INTRODUCTION

A. BACKGROUND

It is well known that radio communication to and from vehicles reentering the earth's atmosphere is virtually impossible for a substantial portion of the reentry flight path, and it is understood that this difficulty is due to a sheath of ionized air and ablation products that forms about the vehicle. This radio blackout problem is not considered critical in most ballistic missile development programs since the blackout is of relatively short duration (30 sec), the trajectories are well defined, and information storage during blackout for transmission after recovery of radio contact is feasible. The problem is not considered critical at the present time in the manned space flight program for the same reasons, yet it is more serious here since it is desirable to communicate with manned vehicles during the critical reentry phase of missions.

With the proposed use of lifting reentry vehicles for both manned and unmanned missions, the requirement for real-time communications becomes critical. The reasons are twofold: lifting reentry trajectories cannot be predetermined with as much precision as ballistic trajectories, and the periods of blackout are considerably longer (5 to 10 min). Thus, lifting reentry missions provide a strong impetus for efforts devoted to solving the reentry blackout problem.

The technical community has expended considerable effort in attempts to find feasible solutions to this problem (Refs. 1 - 3). Proposed solutions include cooling the plasma by fluid injection, modifying the plasma by aerodynamic shaping, using electronegative species to reduce the free electron concentration, using a magnetic field to constrain electron motion and enhance transmission, and using transmission frequencies well outside the standard telemetry range. Most of the previous investigations have been concerned with a single technique. This fact and the fact that the solutions proposed to date have posed several problems indicate that examination of possible solutions in a broader setting and on a more common basis is appropriate at this time.

B. OBJECTIVES OF THE PRESENT STUDY

The primary aim of this report is to recommend a program of research and development that can yield a solution to the lifting reentry vehicle communications problem. In order to provide a sound technical basis for the recommended program, several subsidiary requirements must be met: the magnitude of the lifting reentry communications problem must be established, proposed alleviant techniques must be evaluated to assess their feasibility; and the most promising methods must be determined. A large portion of this report is devoted to satisfying these subsidiary requirements, and hence it is essentially a preliminary systems study.

It is emphasized that this study is not intended to provide a complete catalogue of information of the type most useful for design purposes; such calculations as are performed are primarily intended only to be approximations that are accurate enough to assess feasibility and indicate relative merits and individual problem areas of the various techniques. In some cases, the results presented are certainly adequate for design purposes, and a more detailed parameterization of results than those presented would be possible. However, it is our view that such parameterizations would not contribute to the primary objectives of this study in a way commensurate with the effort involved in obtaining them, and hence they are beyond the scope of this report. In some areas, although a more detailed parameterization is possible, it would tend to be misleading due to the limited technical knowledge available in these areas.

Finally, it is pointed out that although lifting reentry is the major consideration in this report, some of the results are equally applicable to ballistic reentry. In fact, most of the techniques to be investigated were first proposed in connection with the ballistic reentry communications problem.

C. CONTENTS OF THE REPORT

To emphasize the logical merit of the recommended program as clearly as possible, the supporting technical detail has largely been eliminated from this volume. This material is presented in Volumes II and III of this report

in the form of appendices that are referenced in appropriate sections of this Volume.

The arrangement of the contents has been governed by the specific requirements that must be fulfilled. Section II of this Volume is devoted to the model employed for the lifting reentry communications problem. This involves four phases:

1. Consideration of trajectories, vehicle geometries, and aerodynamics of flow fields to determine the plasma conditions likely to be encountered at an antenna location.
2. Consideration of the electromagnetic aspects of the communications problem to obtain the signal attenuation to be expected from given plasma conditions.
3. Combination of the results of the first two phases to yield attenuation as a function of time for representative lifting reentry conditions.
4. Specification of representative communications systems, which are used to define blackout and prescribe the magnitude of the alleviation problem.

Section III contains the results of feasibility studies of a comprehensive list of proposed solutions for the communications problem. For some of these, the feasibility analysis was performed to a point where an estimate of the associated system weight could be made. In other cases, the analysis could not proceed this far either because of gaps in present technology, or because the potential applicability of the proposed solution did not warrant it. In all cases, however, the aim has been to evaluate critically each technique in terms of the unresolved problem areas, their likely influence on system feasibility, and the type of effort required to resolve them.

Finally, Section IV contains the conclusions and recommendations resulting from this study. Systems studied are classified according to feasibility. The amount and type of effort required to develop each feasible system to the point where flight demonstration can be undertaken is discussed. Volume I concludes with a recommended research program designed to resolve problem areas and provide quantitative design information which is presently unavailable.

II. FORMULATION OF THE MODEL

A. AERODYNAMIC CALCULATIONS

1. TRAJECTORIES

In order to estimate the magnitude and duration of the lifting reentry communications problem, one must determine the properties of the plasma surrounding the vehicle as a function of time. The pertinent plasma parameters may be obtained from standard aerodynamic calculations if the velocity, altitude, and shape of the vehicle are specified. It is the purpose of this Section to present such results for a typical reentry vehicle.

The study will be limited to the types of gliding reentry vehicles that are likely to dominate the next decade, and prototypes under development now such as the USAF SV-5 and the NASA M2 and LH-10 are taken as representative. These vehicles are characterized by lift-to-drag ratios (L/D) of the order of unity and ballistic parameters ($W/C_L S$) between 100 and 200 lb/ft^2. An analysis of the dynamics of such vehicles is presented in Volume II, Appendix A, and the pertinent conclusions are presented in Figs. 1 and 2. (Figure 1 is taken from D. R. Chapman, "An Approximation Analytical Method for Studying Entry into Planetary Atmospheres," NACA TN 4276, May 1958.)

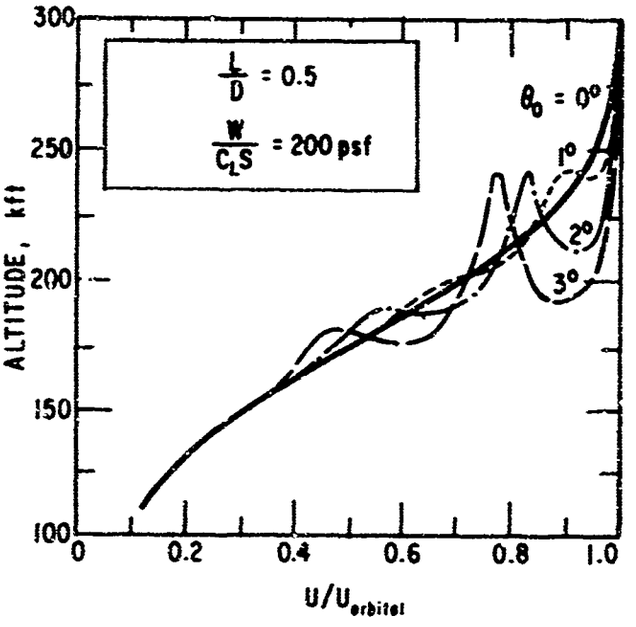

Fig. 1. Lifting Reentry Trajectories

Figure 1 illustrates the dependence of altitude on velocity for a vehicle with a L/D ratio of 0.5 and a ballistic parameter of 200 lb/ft^2 as a function of the initial path angle θ_0 (the path angle is defined as the angle made by the velocity vector of the vehicle

with a plane parallel to the surface of the earth). For an initial path angle of zero, the trajectory is a smooth descent through the atmosphere with an approximate balance among gravitational, lifting, and centrifugal forces. For small deviations from a zero initial path angle, the trajectory executes large oscillations in the altitude-velocity plane. This results in a characteristic high-speed dive of the vehicle into the denser layers of the atmosphere, which greatly increases the severity of signal attenuation. Such trajectories must be included if the model is to provide a realistic appraisal of communication difficulties.

In order to represent adequately the situation described above, two trajectories are defined: an equilibrium trajectory (also referred to as Trajectory 1) which is calculated for an initial path angle of zero, and a non-equilibrium trajectory (also referred to as Trajectory 2) which is an envelope of trajectories calculated on a digital computer for several nonzero initial path angles. These two trajectories are presented in Fig. 2-A.

An assessment of the value of a given alleviation technique requires an estimate of the duration of radio blackout. Representative values of altitude and velocity have been calculated as a function of time for this purpose, and the results are presented in Fig. 2-B. The values for Trajectory 2 were obtained by compiling several exact solutions and represent average values such that the maximum discrepancy is less than 10%. These data will be taken as the basis for our model of lifting reentry.

2. VEHICLE GEOMETRIES

Lifting reentry vehicle geometries are complex shapes from the point of view of aerodynamic flow field calculation. An exact calculation for a realistic vehicle shape is expensive and is not warranted for the present purposes. Instead we have computed and compiled aerodynamic information for flows about axisymmetric stagnation points and sharp cones and wedges. This information is assumed to be representative of conditions encountered during lifting reentry, both in the magnitude of plasma parameters obtained and in the altitude-velocity trends indicated. To partially confirm this assumption, a comparison has been made of the plasma parameters obtained from a 40-deg sharp wedge inviscid flow field calculated assuming uncontaminated air in thermodynamic equilibrium vs the plasma parameters

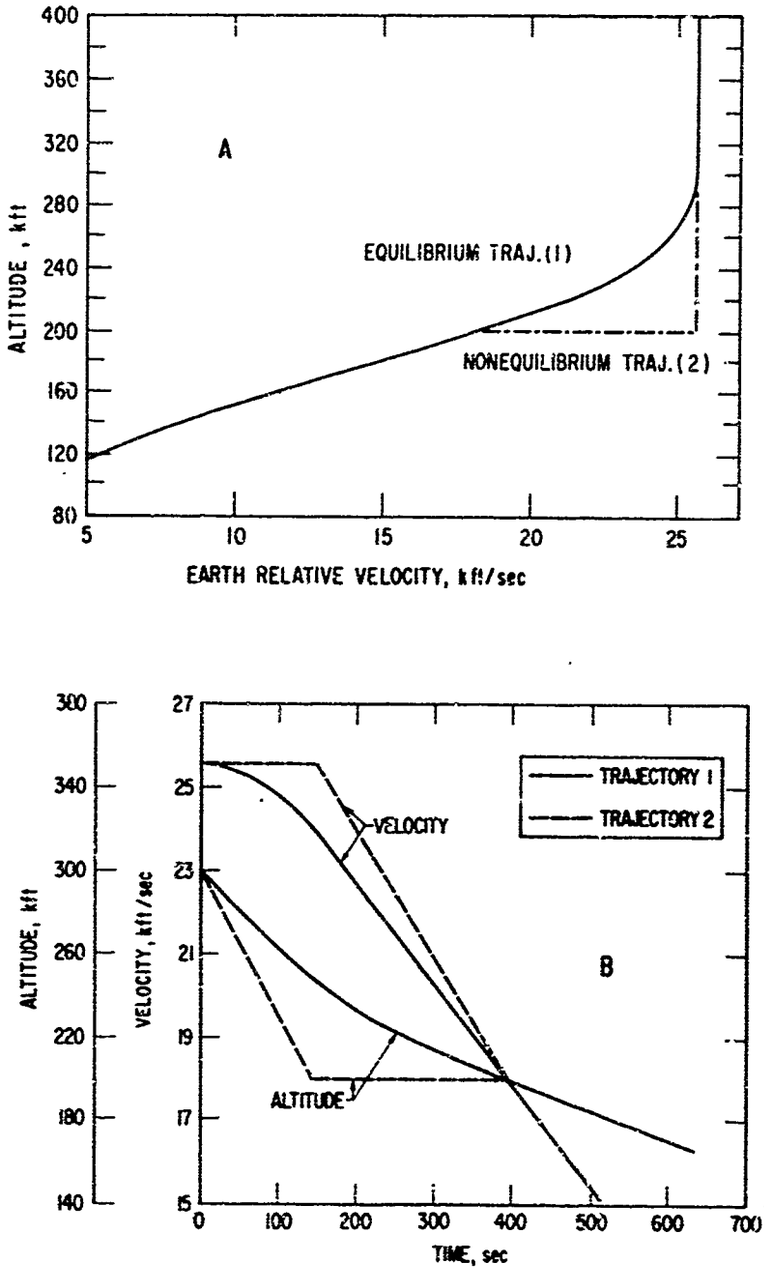

Fig. 2. Representative Trajectories: (A) Altitude vs Velocity; (B) Altitude and Velocity vs Time

obtained from an exact method of characteristics plus boundary layer circulation[1] for a 40-deg cone with a 3-in. nose radius, again assuming clean air in thermodynamic equilibrium. The results of this comparison are listed:

Altitude, kft	260	210	210
Velocity, kft/sec	26	26	19.2
Plasma Frequency at Shock, GHz			
40° sharp wedge, 12 in. from apex	16.5	49	7.6
40° blunt cone, 34 in. from stagnation point	14.1	44	3.5
Maximum Plasma Frequency in Flow, GHz			
40° sharp wedge, 12 in. from apex	16.5	49	7.6
40° blunt cone, 34 in. from stagnation point	14.1	48.5	5.6
Characteristic Collision Frequency, GHz			
40° sharp wedge, 12 in. from apex	0.60	5.0	3.0
40° blunt cone, 34 in. from stagnation point	0.52	4.4	3.0
Plasma Thickness, in.			
40° sharp wedge, 12 in. from apex	0.90	0.99	1.13
40° blunt cone, 34 in. from stagnation point	1.05	0.99	1.12

Thus, in this case, the conditions calculated for a sharp wedge, 1 ft from the apex, are representative of those encountered on a more realistically shaped vehicle some 34 in. from the stagnation point. This observation serves to illustrate the spirit in which the calculations have been made.

It is pointed out that the flow fields obtained for the class of shapes considered here are basically nonexpanding flows (i.e., there is no abrupt decrease in pressure after the shock wave). The reasons for employing this type of flow as the primary basis for this study are:

1. Such flows are common to all lifting reentry vehicles;
2. Flow properties are not sensitive to relatively small changes in vehicle geometry and attitude (as contrasted to expanding, afterbody flows);

[1] The authors are indebted to Mr. F. A. Vicente for supplying these results.

3. Although these flows represent a generally more severe communications problem than do afterbody flows, their spatially restricted nature makes them more amenable to alleviation techniques.

The important aspects of expanding flows are considered in Section III-G.

3. AERODYNAMIC CALCULATIONS

The techniques employed here are standard and do not merit detailed discussion.[2] The basic flow is that of clean air in thermodynamic equilibrium: effects of chemical nonequilibrium and contamination will be briefly treated in subsequent paragraphs. The flow field is treated in the usual manner of an outer inviscid flow, where viscous effects are unimportant (the shock layer), and a boundary layer on the vehicle surface, where viscous effects are dominant. Interaction effects between the inviscid and viscous flows are not considered since they do not affect the character of the results at the conditions of interest here. It should be remarked that uncertainties of the order of a factor of two in the properties of air, particularly those most relevant to the communications problem, are not uncommon. Thus these calculations are aimed at providing a representative estimate of lifting reentry conditions rather than obtaining the maximum available theoretical accuracy.

The properties of the flow of most interest for estimating the communications problem are the magnitudes and distributions of the electron density[3] and the electron collision frequency. For the inviscid portion of the flow, the distributions of these quantities are relatively uniform; this is exactly true in the case of wedges and approximately true at stagnation points (Ref. 4) and in conical shock layers (Ref. 5). Thus the inviscid flow is adequately represented by the values of electron density and collision frequency immediately behind the shock wave and by the thickness of the shock layer.

---

[2] More detail on the results of aerodynamic calculations presented here is contained in Volume II, Appendix B.

[3] Electron density is used synonymously with plasma frequency in this report. The two are, of course, related by $f_p = 8.79 \times 10^3 \sqrt{n_e}$, where f_p is in Hz and n_e in electrons/cc.

The plasma frequency f_p and the electron collision frequency ν for clean air in thermodynamic equilibrium behind normal shock waves is shown as a function of altitude and velocity in Fig. 3, which is taken from Ref. 6 with the addition of some interpolated curves. These results are accepted as standard and agree with every reliable published calculation. With the interpretation indicated on Fig. 3, i.e., employing the velocity component normal to the shock wave as the appropriate velocity, these results are equally applicable to oblique shock waves. Hence they may be used to define the plasma state for flows about cones and wedges, as well as at stagnation point conditions.

Although the plasma frequency and collision frequency are the most relevant state properties for determining the magnitude of the communications problem, it is also useful to know the temperature and mass density, particularly with reference to evaluating alleviation techniques. The temperature and mass density presented in Fig. 4 were obtained from Ref. 7. The molecular composition of equilibrium air is also of interest, and the data given in Refs. 7 and 8 were used in this study.

To complete the specification of the inviscid flow field, it is necessary to estimate the thickness of the shock layer. For axisymmetric stagnation points, this thickness is the shock detachment distance, shown in Fig. 5, normalized with respect to the nose radius. These values are based on the correlation of Serbin (Ref. 9), which agrees quite well with experimental results. To obtain the inviscid shock layer thickness for cones and wedges of a specified semivertex angle, it is necessary only to relate this angle with the shock angle. Figure 6 shows this relation, which, for wedges, was obtained from Feldman (Ref. 4), and for cones, was obtained from Romig (Ref. 5). It should be pointed out that these relationships are actually slight functions of altitude and velocity and, thus, cannot be exhibited exactly in terms of the similarity parameter ($U_\infty \sin \Theta$, where U_∞ is the freestream velocity, and Θ is either the body or shock angle). This may yield errors of the order of 20% in the difference between shock angle and body angle; such errors are not deemed important for this study. Thus, Figs. 3 through 6

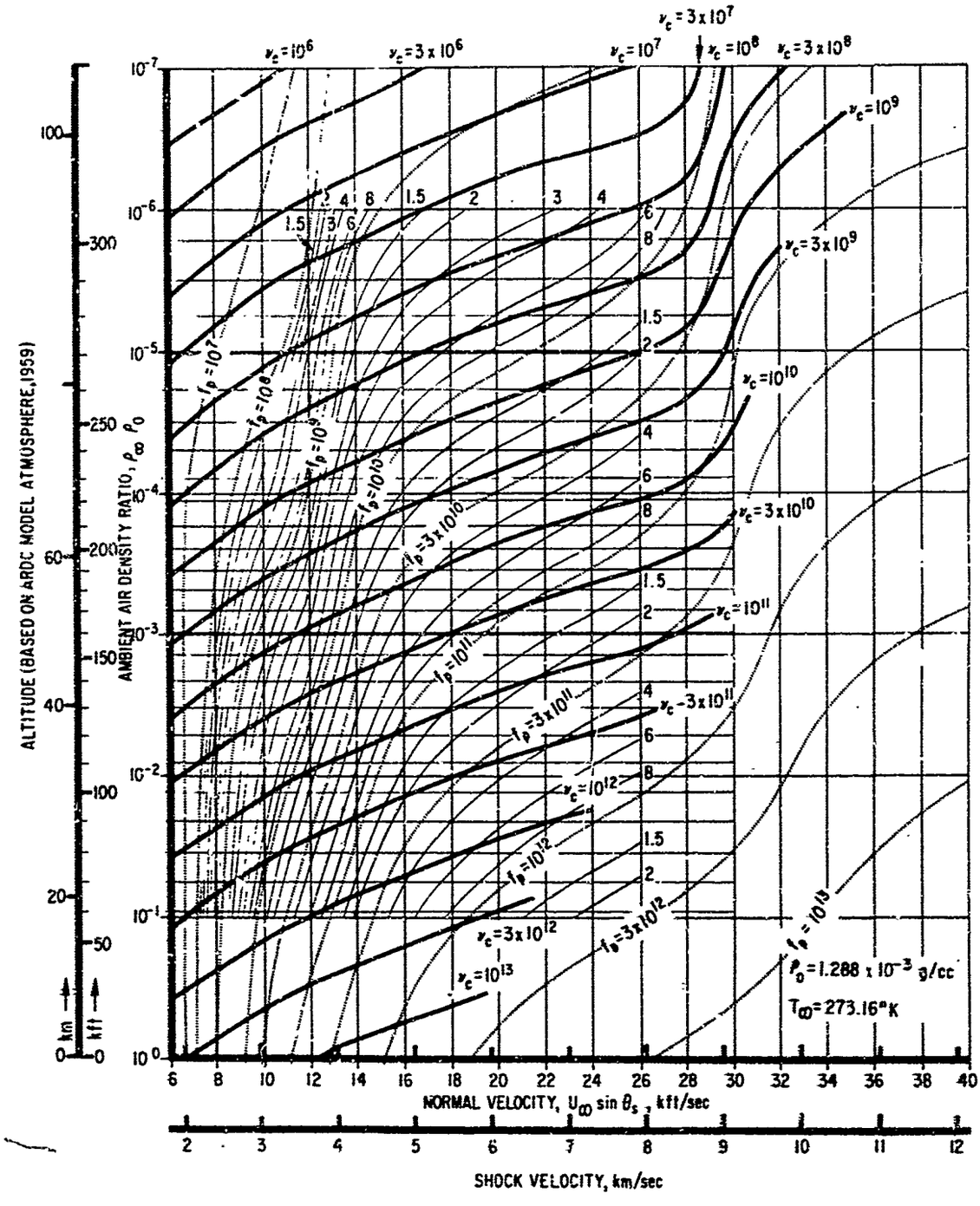

Fig. 3. Plasma Frequency and Electron Collision Frequency in Equilibrium Air Behind Normal Shocks

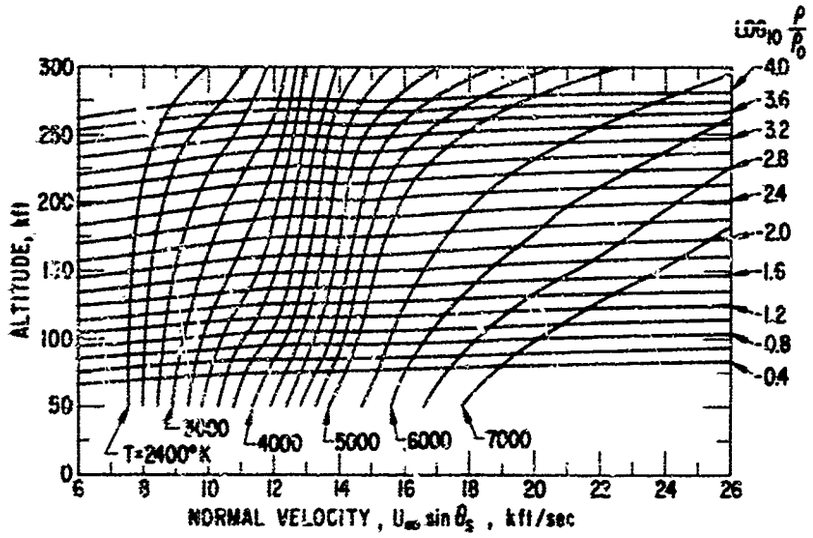

Fig. 4. Temperature and Density Behind Normal and Oblique Shocks

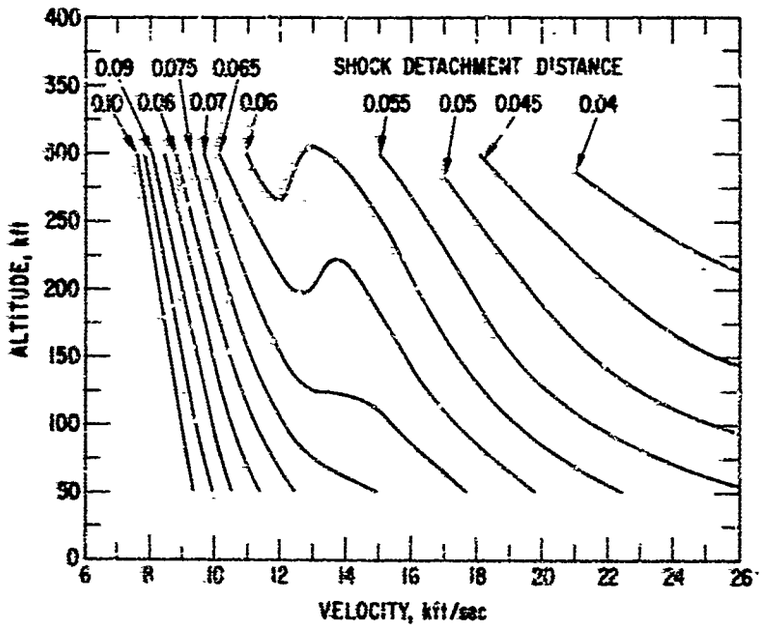

Fig. 5. Normalized Blunt Body Shock Detachment $\Delta/R = 2/[3(\rho_2/\rho_1 - 1)]$

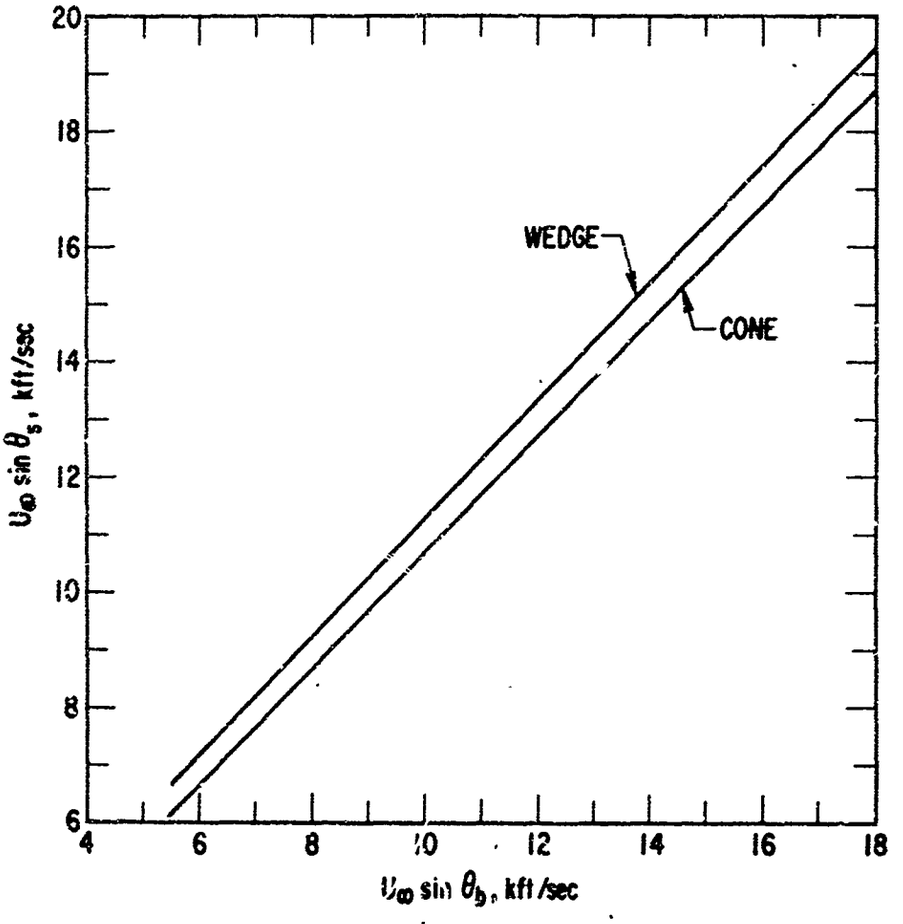

Fig. 6. Shock Angle vs Body Angle for Wedges and Cones

completely specify the inviscid flow properties about cones, wedges, and axisymmetric stagnation points; these figures are included primarily because the inviscid flow plays a dominant role in the subsequent analyses.

Properties relevant to the viscous boundary layer on sharp cones and wedges are portrayed graphically in Volume II, Appendix B. These properties were obtained from an existing computer program, a complete description of which can be found in Ref. 10. In brief, the boundary layer properties are computed using a standard integral technique (described in Ref. 11) wherein a linear velocity profile is assumed, the local density is assumed to be inversely proportional to the local static enthalpy, and the local enthalpy h is related to the local velocity U by a modified Crocco relation:

$$\frac{h + R(U^2/2) - h_w}{h_e + R\left(U_e^2/2\right) - h_w} = \frac{U}{U_e}$$

where R is the recovery factor (~0.86 for laminar flow), and the subscripts e and w refer to conditions at the outer edge of the boundary layer and at the vehicle surface, respectively. The wall enthalpy was specified as 600 Btu/lb (T_w = 1220°K), which is typical of high-temperature ablation materials. This of course yields boundary layer properties that are more severe from a communications view than those obtained with lower wall enthalpies. For computational purposes, the relevant properties of equilibrium air were represented by analytical expressions and introduced a noticeable error in the results; specifically, both plasma frequency and collision frequency could be in error by as much as 50%. This error is tolerable in the present context, as the results obtained remain representative of lifting reentry. It should be pointed out that the boundary layer thickness tends to be underestimated by the technique just described; to compensate, the thickness was calculated assuming an adiabatic wall but with the transport properties modified by the actual wall temperature. This yields results in fair agreement with those of Van Driest (Ref. 12).

The main features of the results of these boundary laver calculations are that the boundary layer is laminar over those portions of the trajectories where the communications are severe, and that the clean, equilibrium air boundary layer is not of primary consideration from the communications view for body angles greater than 35 deg, approximately.

The preceding discussion is based upon the assumption of thermodynamic equilibrium. It is well known that at the altitudes and velocities of interest, there may be insufficient collisions between the constituent particles to maintain equilibrium, and some assessment of the importance of nonequilibrium effects is therefore necessary. The character of nonequilibrium is not the same for both nonexpanding and expanding flows, and the difference must be carefully distinguished at the outset.

For nonexpanding flows behind shock waves, which are of primary interest here, the shock wave represents an increase in the energy invested in the translational and rotational degrees of freedom of the original air constituents, which takes place in the distance equal to a few mean paths. Subsequently, some of this energy is utilized, by means of particle collisions, to dissociate and ionize the original air constituents. The distance required to reach the final equilibrium state is generally of the order of hundreds of mean free paths and is controlled by the rates of the dissociation and ionization processes. During the major portion of this interval, the levels of dissociation and ionization are below that of the final equilibrium state.

For expanding flows, such as occur over the afterbodies of blunt shapes, the air usually has time to reach an equilibrium state before the expansion begins. Upon expansion, the energy in the translational and rotational degrees of freedom decreases quite rapidly, whereas, the energy invested in dissociation and ionization requires many collisions to equilibrate with the translational and rotational modes, the distance now being controlled by the rates of the atomic and ionic recombination processes. During the equilibration interval, the levels of dissociation and ionization are above those of the equilibrium state.

As indicated previously, the nonexpanding flow is of most interest to the present study and some feeling of the importance of nonequilibrium can be gained from Fig. 7, obtained from the results presented in Ref. 13. The figure indicates the distance behind a shock wave (measured normal to the shock wave) required for the electron density to reach one-half of the equilibrium value. The broken lines in the figure indicate typical conditions encountered during lifting reentry, and it is observed that the ionization incubation period can be appreciable. The resulting effects on signal attenuation estimates are discussed in Section II-C-2. Nonequilibrium effects in expanding flows are discussed briefly in Section III-G.

The other aspect relevant to aerodynamic calculations based upon the assumption of clean air in thermodynamic equilibrium concerns the effect of ablation products from the vehicle heat shield that contaminate the boundary layer. To perform a fairly exact calculation of such effects is at present beyond the state of the art. However, there exists limited evidence that the major effect of the ablation products upon the electron density in the boundary layer is attributable to the amount of easily ionizable species, e.g., alkali impurities, contained in the ablation material (see Refs. 14, 15). Our consideration of ablation product contamination in the boundary layer is therefore based upon this assumption. Specifically, we have considered the electron density produced by trace amounts of sodium in equilibrium air. These results are shown in Fig. 8, wherein the equilibrium electron density produced by various amounts of sodium (assuming that the presence of the air constituents does not affect the sodium equilibrium) is compared with the prevailing electron density in equilibrium air.

For a given air density and sodium contamination level there exists a temperature below which the effects of the sodium become significant. This is better demonstrated by Fig. 9, where this minimum temperature, determined by a given ratio of mixture electron density to air electron density, is shown as a function of both mass fraction of sodium and air density. It should be pointed out that sodium contamination levels, as used here, refer to concentrations in the air, and not in the ablation material. Ablation

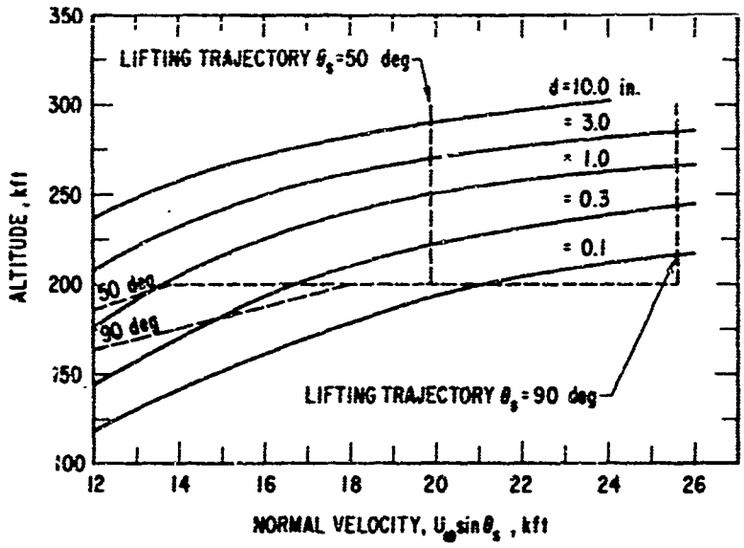

Fig. 7. Characteristic Nonequilibrium Distance Behind Shock Waves in Air

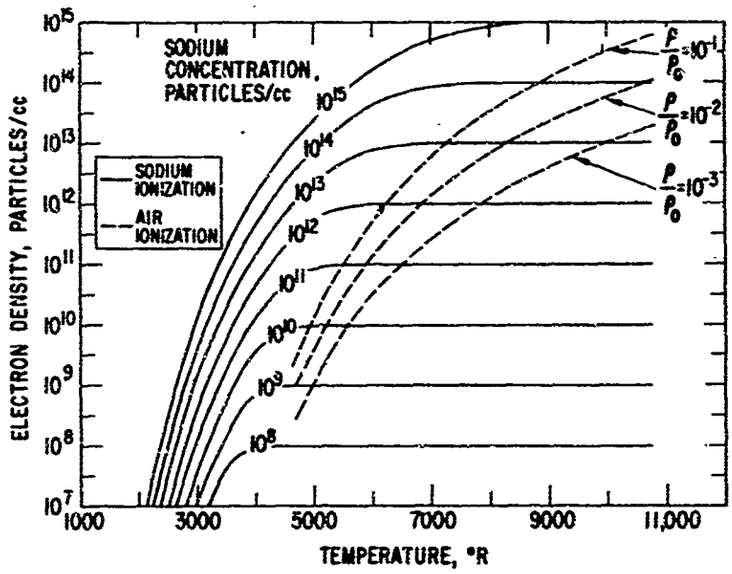

Fig. 8. Ionization in Sodium Compared with Ionization in Equilibrium Air

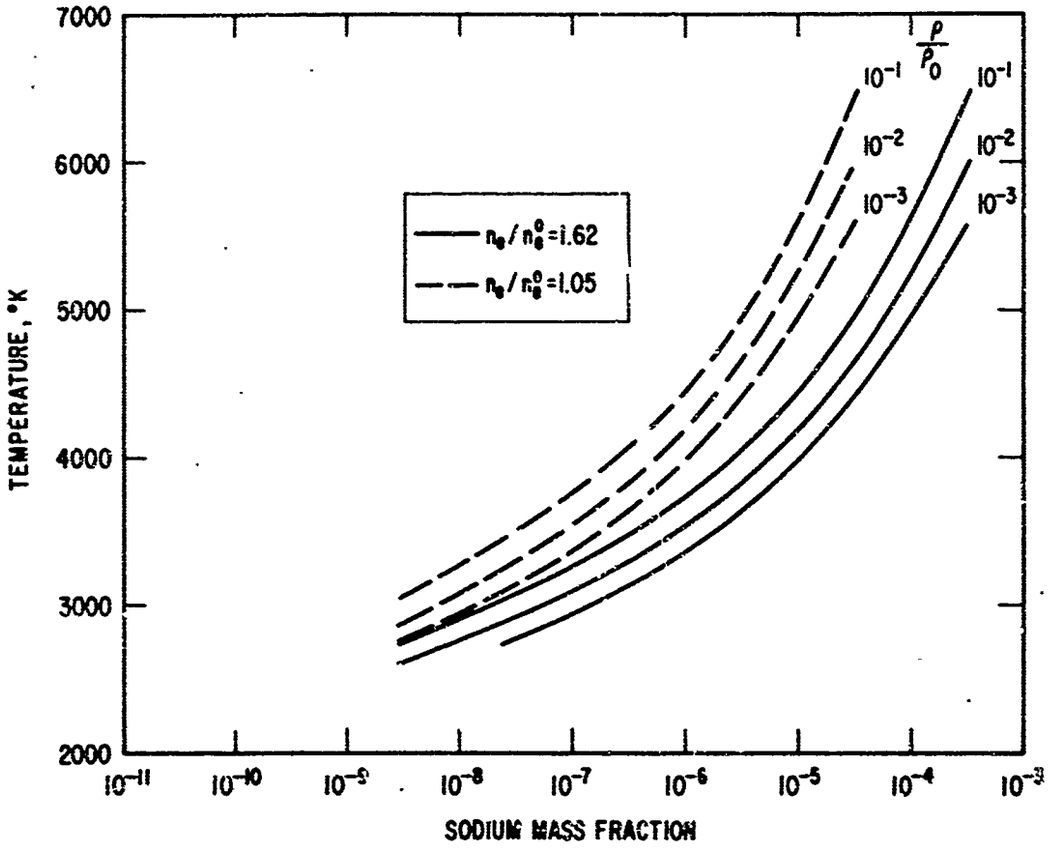

Fig. 9. Effects of Sodium Contamination in Equilibrium Air

calculations have indicated that the sodium mass fraction in the air is approximately 10% of that in the ablation material. The effect of contamination on signal attenuation estimates is discussed in Section II-C, where it can be seen that under many lifting reentry conditions these effects may be neglected.

B. ELECTROMAGNETIC CONSIDERATIONS

1. ATTENUATION ESTIMATES

In order to assess the severity of the communications problem in lifting reentry, it is necessary to estimate the signal attenuation due to the presence of the plasma sheath in front of the antenna. This is done here by assuming that the attenuation is equal to that of a plane wave normally incident upon a homogeneous plasma slab, for which computational techniques are readily available (Ref. 16).

A more detailed discussion of the correspondence between this estimate and the reentry antenna geometry appears below. There it will be shown that the plane-wave predictions closely approximate the attenuation in the reentry geometry if the cross-sectional dimensions of the antenna aperture are much greater than the attenuation length in the plasma and the sheath is highly overdense.

The plane-wave transmission coefficient was evaluated by digital computation, resulting in an extensive set of plasma attenuation tables (see Volume III). The relevant plasma parameters were varied over the following ranges:

$$0.6 \leq W = \omega_p/\omega \leq 900$$

$$0 \leq V = \nu/\omega \leq 100$$

$$10^{-4} \leq d/\lambda_0 \leq 10$$

where ω_p $(=2\pi f_p)$ is the plasma frequency, ν is the collision frequency, ω is the signal frequency, d is the plasma slab thickness, and λ_0 is the free space wavelength. This variation in parameters adequately covers the reentry situations considered.

In order to more fully appreciate the nature of the communications problem, it is helpful to have a graphical portrayal of the general functional dependence of the plasma attenuation on the plasma parameters. For this purpose, we have constructed, from the tabulated results, attenuation contour maps as functions of d/λ_0 and $(\omega_p/\omega)^2$ for various values of the parameter $V\lambda_0/W^2d$, which is independent of signal frequency, and is approximately equal to 10^{-2} in this study. The general shape of the constant attenuation contours is illustrated in Fig. 10. The two dashed lines in Fig. 10 are contours for typical plasma conditions and varying signal frequencies (specifically, they approximately represent conditions at maximum attenuation for a 50-deg wedge on Trajectory 2 and for a 40-deg wedge on Trajectory 1, respectively; see Section II-C). These variable frequency contours illustrate two points worthy of note:

1. For the typical severe reentry condition of a highly overdense, lossy plasma, the attenuation increases with increasing signal frequency and approaches a maximum at a frequency roughly one order of magnitude less than the plasma frequency (e.g., for the 50-deg wedge case, the attenuation increases up to a signal frequency of 5 GHz approximately).
2. Beyond the maximum attenuation point, no substantial reduction in attenuation is achieved until the signal frequency is roughly equal to the plasma frequency.

2. EFFECTS OF PLASMA INHOMOGENEITIES

The equivalent dielectric properties of the plasma have been assumed to be homogeneous throughout the sheath for computational reasons. The magnitude of the errors incurred in a homogeneous approximation are given in the following tabulation, which shows the correlation between the attenuation of a plasma layer of thickness $\lambda_0/2$, having a triangular electron density profile, and the attenuation of an equivalent homogeneous plasma slab.

ν/ω	$(\omega_p/\omega)_{peak} = 1.2$		$(\omega_p/\omega)_{peak} = 1.4$		$(\omega_p/\omega)_{peak} = 2.0$	
	Exact	Homog	Exact	Homog	Exact	Homog
0.01	-3.7 dB	-4.7 dB	-9.2 dB	-9.7 dB	-20.3 dB	-18.9 dB
1.0	-6.0 dB	-5.9 dB	-9.7 dB	-9.2 dB	-16.9 dB	-15.5 dB

The exact transmission coefficient was obtained from the results of Gold (Ref. 17). The homogeneous slab was calculated using an electron density equal to the peak electron density in the inhomogeneous case, and an equivalent thickness such that the total number of electrons in the slab equals the total number of electrons in the inhomogeneous sheath. Although the conditions at which this comparison is made are not typical of reentry, the comparison at more typical conditions (thinner sheaths and higher ratios of ω_p/ω) is not expected to yield significantly different results. Further, better agreement between the inhomogeneous and equivalent uniform slab calculations would be expected in the lifting reentry geometry for those cases in which the inviscid shock layer flow is the dominant plasma, since the resulting sheaths are nearly homogeneous. It is therefore concluded that nonuniformities in the plasma sheath have no important effect on our attenuation estimates.

3. APERTURE EFFECTS

Effects due to finite sources that are not taken into account by the plane-wave model include far-field pattern distortion (Refs. 18-20) and modification of the antenna impedance by the presence of the plasma sheath in the near field of the antenna (Ref. 20). Calculations of radiation patterns of a rectangular slot antenna in the presence of a plasma sheath indicate that the first effect is insignificant for highly overdense plasmas. The results of the calculations are presented in Fig. 11, where it may be observed that the major effect of the plasma on the radiation system is an increase in attenuation and that pattern distortion is insignificant when ω_p/ω is much

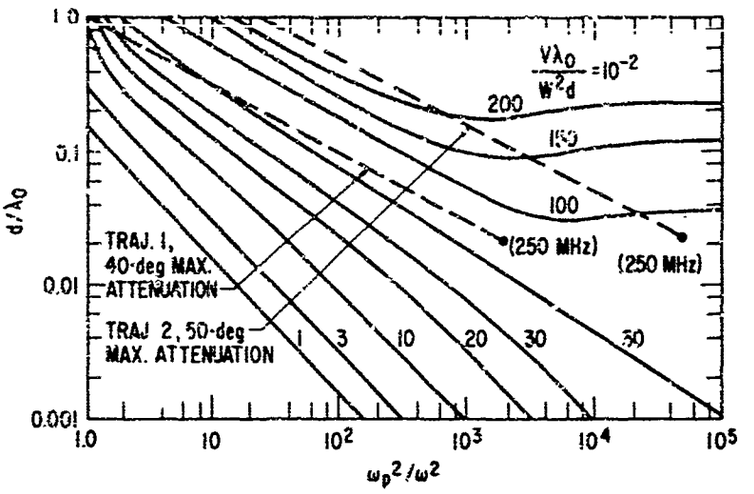

Fig. 10. Plasma Slab Attenuation

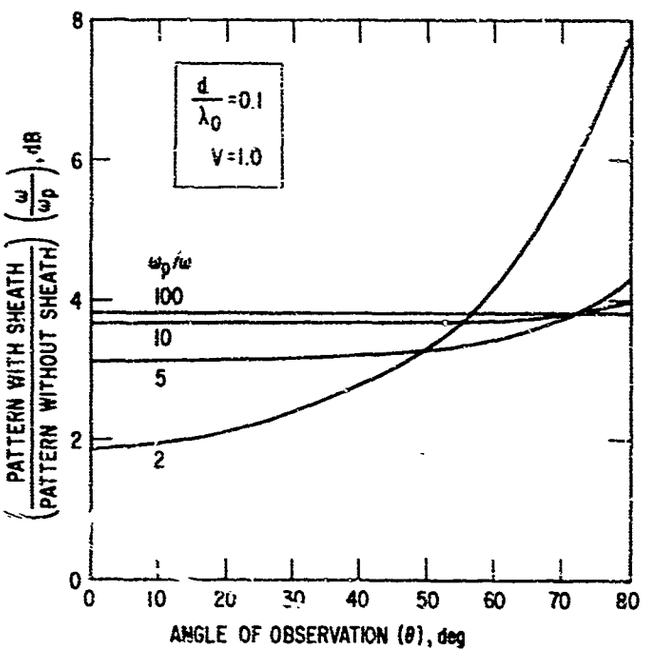

Fig. 11. Radiation Patterns for Rectangular Slot Antenna

greater than unity (more precisely, when the attenuation length in the plasma is much less than the sheath thickness).

A modification of antenna impedance causes a mismatch in the radiating system so that some of the power generated by the transmitter is reflected back into the transmitting system. We will presume that the system is designed so that the transmitter is isolated from reflected waves and that the only effect of an impedance mismatch is a loss of power from the free-space radiation pattern. In order to estimate this effect, the radiation pattern of a slot with a specified field distribution has been calculated and the magnitude of the field in the slot from the plane-wave reflection coefficient of the plasma has been estimated. A comparison of these results with plane-wave attenuation estimates is given in Fig. 12, and it is concluded that the plane-wave model is sufficiently accurate for overdense plasmas.

On a more general basis, it has been shown that the effects of plasma sheath on signal attenuation can be estimated using a plane-wave analysis when the radiating aperture is sufficiently large (Ref. 21). It has also been observed experimentally (Ref. 22) that the measured attenuation in a rectangular slot geometry radiating through an overdense sheath closely approximates the plane-wave transmission coefficient. If the antenna aperture has cross-sectional dimensions which are much greater than the attenuation length in the plasma and if the plasma is highly overdense, the driving point impedance of the aperture can be approximately determined from an appropriate plane-wave reflection coefficient (Ref. 23). In other words, diffraction effects can be neglected due to the highly attenuating nature of the plasma. The criterion for determining more precisely when the plane-wave computations approximate the attenuation observed in a slot geometry is given by the following inequality (Ref. 23)

$$\frac{\ell}{\lambda_0} \operatorname{Im}\left[1 - \frac{\omega_p^2}{\omega(\omega + i\nu)}\right]^{1/2} > 1$$

where ℓ is the width of the slot antenna. For the types of plasma sheaths encountered in lifting reentry the minimum slot width ranges from $\lambda_0/100$ to $\lambda_0/10$ (at 250 MHz). Further, it is well established (Ref. 24) that the linear dimensions of a slot type antenna can be as small as $\lambda_0/10$ (approximately) without degrading the free-space electrical characteristics of the radiator. In the present study the antenna apertures will therefore be assumed to be greater than $\lambda_0/10$, for which the plane-wave estimates are adequate.

4. RADIO-FREQUENCY BREAKDOWN

When electromagnetic signals are transmitted through a narrow layer of ionized air, it is found experimentally that the layer typically exhibits the nonlinear power transfer characteristics sketched in Fig. 13 (Ref. 25). In both the underdense and the overdense cases, there is a linear region of the characteristic response in which the attenuation may be estimated by calculations such as those presented in Section II-B-1. The breakdown power level is that level of input power which corresponds to the termination of the linear regime, and an estimate of it is necessary to determine the range of applicability of the attenuation calculations.

Radio frequency (rf) breakdown occurs when the electron density in a region increases rapidly due to the presence of the field. For continuous wave signals, the condition for breakdown is simply that, in some region, the time rate of change of electron density is greater than zero. The rate of change in any region is determined by several factors, and the most important of these are the rate at which the electrons ionize neutrals, the rate at which the electrons attach to neutrals, the rate of diffusion of electrons, and the rates at which electrons are convected to and from the region. The purpose here is to determine a range of signal levels for which breakdown is not likely to be a problem; for this purpose we can safely ignore diffusion and convection, since these effects act to alleviate the breakdown problem. The condition for breakdown, then, may be written

$$\frac{\partial n_e}{\partial t} = (\nu_i - \nu_a) n_e \geq 0 \qquad (1)$$

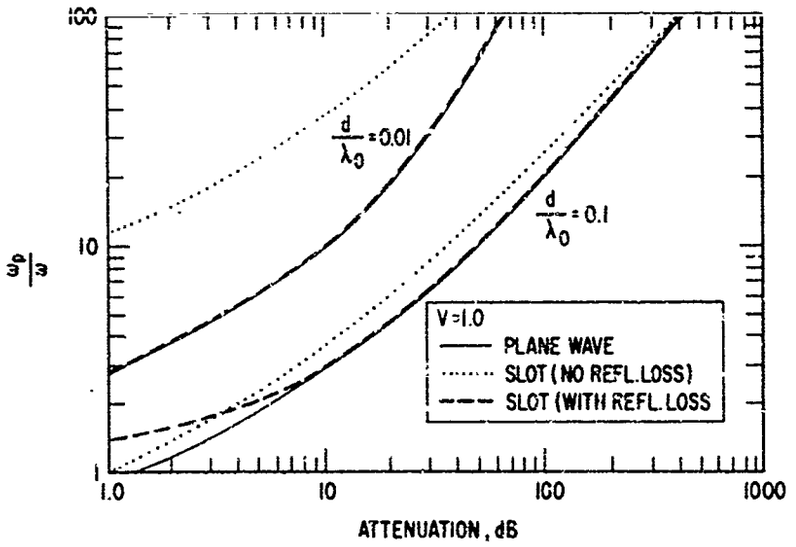

Fig. 12. Plasma Impedance Effects

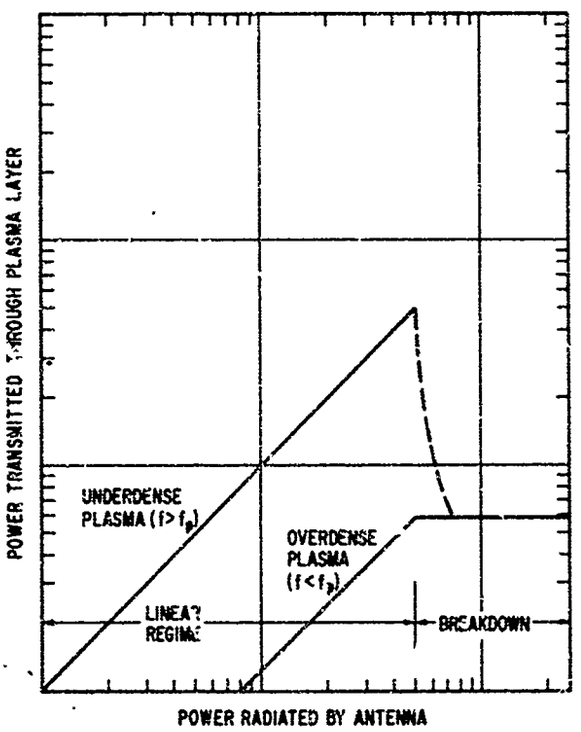

Fig. 13. Manifestation of rf Breakdown on Incident-Transmitted Power Relation

where n_e is the electron density, ν_i is the frequency of ionizing electron-neutral collisions, and ν_a is the frequency of attaching electron-neutral collisions. If we define a net ionization frequency ν_{net} as the difference between the ionizing electron-neutral collisions and the attaching electron-neutral collisions, then the problem is to determine the electric field intensity E_b which will cause ν_{net} to exceed zero. The breakdown field E_b is a function of both the frequency of the radio signal and the state of the air.

For gases at room temperature the breakdown phenomenon is well understood (Ref. 26) and it is clear that ν_{net} is a function of the average energy of the electrons. The average energy of the electrons is in turn a function of an effective dc field E_e (defined such that the electron energy gain from the ac field E_b is equal to that from a dc field E_e) and the electron collision frequency ν_c. The effective dc field E_e is related to the ac field E_b by the relationship

$$E_b = \left[1 + \left(\frac{2\pi f}{\nu_c}\right)^2\right]^{1/2} E_e \qquad (2)$$

where f is the signal frequency. When diffusion and convection are neglected, it was shown by Gould and Roberts (Ref. 27) that the effective field E_e for breakdown of air at room temperature is given by

$$E_e \cong 30\left(\frac{\nu_c}{5.3 \times 10^9}\right) \text{ V/cm} \qquad (3)$$

Although no quantitative study of breakdown for high temperature air exists at the present time, qualitative discussions of the effects that must be considered in modifying the Gould and Roberts theory have been presented by Reilly (Ref. 28) and Epstein (Ref. 29). It was pointed out that as the temperature of the air is raised to reentry levels, the reactions $O_2 \rightleftharpoons 2O$ and $N + O \rightleftharpoons NO^+ + e$ proceed to the right so that the composition of the air

is considerably altered. Furthermore, the N_2 molecules are easier to ionize because the outer electrons are more likely to exist in excited states. Unfortunately the data required to estimate the pertinent reaction rates for high temperature air are not presently available, but it does not seem likely that the breakdown fields would be altered from the cold air levels by more than 50%. Another effect arises from the fact that the electron density is so high in the case of lifting reentry that the plasma frequency is higher than frequencies normally used for communication; therefore, most of the power directed towards the plasma is reflected. Account is taken of this effect by recognizing that the breakdown field is associated with the actual power delivered into the plasma, and not the power delivered to the antenna.

For the case of a 373 MHz signal emitted from a 0.5×17 in.^{2} slot, breakdown occurs in the previously described experiment (Fig. 13) when the net power delivered to the plasma is 4.5 W. The amplitude of the electric field associated with a plane wave with a power density of 4.5 W over an area of 8.5 in.^{2} is 8 V/cm. Since the experimental air pressure was 0.2 mm, and ν_c for air may be taken to be $5.3 \times 10^9 p$, Eq. (2) indicates an effective electric field of 2 V/cm. The results of the experiment can be crudely extrapolated to the reentry plasma by recognizing that the background gas in the experiment is cold, and that in this situation the theoretical value of the effective electric field is 6 V/cm, which is larger by a factor of three than the indicated experimental value. The discrepancy is attributed to the effect of the near field of the antenna, which must also be a consideration in the reentry estimate. Using a factor of one-third for the near-field effect and a factor of one-half for the high temperature effects, we may proceed from Eqs. (2) and (3) to calculate the breakdown power density S_b, and we obtain

$$S_b \approx 0.08 \left[1 + 40\left(\frac{f}{\nu_c}\right)^2\right]\left(\frac{\nu_c}{5 \times 10^9}\right)^2 \text{ W/cm}^2 \qquad (4)$$

It must be emphasized that the quantity S_b represents the net power density delivered to the plasma: it is computed by subtracting the reflected power density from the incident power density at breakdown.

A typical slot antenna is taken to have a width of 1 cm and a length of a one-half wavelength. Using these dimensions and Eq. (4), we find that the net power delivered to the plasma at breakdown is given by

$$P = 5 \times 10^{-11}\left(\nu_c^2 + f^2\right)/f \quad \text{Watts} \tag{5}$$

According to Eq. (5), the minimum breakdown level occurs when $f = \nu_c/6$ with a power of $6 \times 10^{-10}\ \nu_c$ W. Since ν_c is typically greater than 10^9, (1.6×10^9, say), it is concluded that breakdown is most likely to occur in the vhf region of the spectrum with a delivered power of about 1 W. A typical vhf reentry system has an output of 7 W with a 30 dB margin. During reentry, a large fraction (greater than 95%) of the transmitter power is reflected by the plasma, so that the power actually delivered is considerably less than 1 W. We conclude that it is legitimate to use the linear calculations to estimate signal attenuations for our reentry model. This conclusion is further supported by the fact that in the region of severe plasma attenuation, the collision frequency is likely to be at least 3 times (or perhaps 10 times) greater than that selected above, and hence the breakdown level would be increased by roughly an order of magnitude.

C. REPRESENTATIVE LIFTING REENTRY ATTENUATION

1. RESULTS FOR CLEAN EQUILIBRIUM AIR

The preceding sections provide a basis for calculating signal attenuation for lifting reentry conditions. In this section such calculations are presented, from which the pertinent features of the lifting reentry communications problem will be extracted.

For the two trajectories selected previously (Section II-A-1), the signal attenuation was estimated for the simplified body shapes under consideration (Section II-A-2), as indicated below:

Configuration	Body Station	Flow Field
Stagnation Point	nose (3 in. radius)	Shock Layer
Sharp Wedge (50°)	1 ft 5 ft	Shock Layer
Sharp Wedge (30°, 40°)	1 ft 5 ft	Shock Layer Boundary Layer
Sharp Wedge (20°)	1 ft 5 ft	Boundary Layer
Sharp Cone (50°)	1 ft 5 ft	Shock Layer
Sharp Cone (30°, 40°)	1 ft 5 ft	Shock Layer Boundary Layer
Sharp Cone (20°)	1 ft 5 ft	Boundary Layer

The results of the first two cases of the preceding list are given in tabular form in Tables I and II. Results for the remaining cases are presented in Volume II, Appendix C. The flow field properties were computed by the procedures indicated in Section II-A-2. The resultant signal attenuation was obtained for five frequencies (0.25, 0.50, 1.0, 5.0, 10.0 GHz) from the plane-wave, homogeneous slab model discussed in Section II-B-1 (extensively tabulated in Volume III). The frequencies selected cover the standard range for space and reentry vehicle communications systems.

In our flow field approximation, the shock layer possesses uniform properties, and its relationship to the homogeneous slab calculation is clear. The boundary layer is approximated by a slab of equal thickness possessing uniform properties equal to peak boundary layer conditions, which overestimates this contribution somewhat.

Table I. Stagnation Point Attenuation

Time, sec	Altitude, kft	Velocity kft/sec	f_p, GHz	ν, rad/sec	d, in.	Attenuation, dB					Traject 1 = Equil. 2 = Trans.
						f = 250 MHz	f = 500 MHz	f = 1 GHz	f = 5 GHz	f = 10 GHz	
0	300	25.6	6.5	1.5×10^8	0.102	13	6.5	3.8	0.25	0.0	1
100	266	2	18.0	1.2×10^9	0.111	29	26.0	22.5	7.8	3.0	1
150	247	24.0	28.0	2.8×10^9	0.118	34	34.0	30.5	18.0	11.0	1
190	236	23.0	32.0	4.0×10^9	0.123	34	35.0	35.0	22.0	15.0	1
230	227	22.0	35.0	5.0×10^9	0.132	35	35.0	36.0	26.0	18.0	1
275	220	21.0	36.0	5.5×10^9	0.136	34	36.0	35.0	28.0	22.0	1
320	214	20.0	37.0	6.2×10^9	0.144	35	36.0	37.0	29.0	23.0	1
365	207	19.0	38.0	7.0×10^9	0.153	35	35.0	38.0	32.0	25.0	1
0	300	25.6	6.5	1.5×10^8	0.102	13	6.5	3.8	0.25	0.0	2
30	280	25.6	13.0	5.5×10^8	0.105	26	20.0	14.0	3.3	1.2	2
60	260	25.6	25.0	1.6×10^9	0.111	36	33.0	28.0	15.0	9.3	2
90	240	25.6	42.0	4.4×10^9	0.117	39	40.0	40.0	28.0	24.0	2
120	220	25.6	65.0	9.8×10^9	0.120	39	41.0	44.0	36.0	39.0	2
150	200	25.6	100.0	2.0×10^{10}	0.123	42	44.0	47.0	62.0	60.0	2
170	200	25.0	95.0	2.0×10^{10}	0.126	41	42.0	46.0	60.0	58.0	2
205	200	24.0	82.0	1.8×10^{10}	0.129	42	40.0	44.0	55.0	53.0	2
240	200	23.0	75.0	1.5×10^{10}	0.132	38	40.0	42.0	54.0	50.0	2
275	200	22.0	65.0	1.5×10^{10}	0.136	36	37.0	40.0	43.0	43.0	2
305	200	21.0	58.0	1.3×10^{10}	0.141	36	38.0	42.0	42.0	40.0	2
340	200	20.0	50.0	1.1×10^{10}	0.147	35	38.0	40.0	40.0	35.0	2
375	200	19.0	43.0	8.2×10^9	0.154	34	38.0	39.0	36 0	28.0	2
410	200	18.0	38.0	8.1×10^9	0.162	35	36.0	38 0	34.0	27.0	1,2
450	194	17.0	37.0	9.1×10^9	0.174	33	35.0	38.0	34.0	28.0	1,2
495	188	16.0	31.0	9.0×10^9	0.183	31	32.0	34.0	30.0	24.0	1,2
540	182	15.0	22.0	8.8×10^9	0.195	26	26.0	27.1	20.0	13.0	1,2
585	176	14.0	16.0	9.0×10^9	0.201	20	20.0	20.0	13.0	7.0	1,2
625	170	13.0	8.0	9.2×10^9	0.201	10	12.0	10.0	2.9	0.7	1,2
670	164	12.0	4.0	9.2×10^9	0.207	4	3.8	3.2	0.5	0.1	1,2

Table II. Shock Layer Attenuation, 50-deg Wedge

Time, sec	Altitude, kft	Velocity, kft/sec	f_p, GHz	ν, rad/sec	d(1 ft), in.	d(5 ft), in.	Attenuation, dB										Traject. 1 = Equil. 2 = Trans.
							f = 250 MHz		f = 500 MHz		f = 1 GHz		f = 5 GHz		f = 10 GHz		
							1 ft	5 ft	1 ft	5 ft	1 ft	5 ft	1 ft	5 ft	1 ft	5 ft	
0	300	25.5	3.4	9.0×10^{7}	1.04	5.22	26.0	91	21.0	85	14.0	71	0.4	0.1	0.0	0.0	1
100	266	25.0	10.0	6.5×10^{8}	1.09	5.44	68.0	Large	42.0	261	37.0	257	38.0	212.0	10.0	27.0	1
150	247	24.0	17.0	1.5×10^{9}	1.17	5.85	97.0	Large	96.0	Large	95.0	466	77.0	440.0	63.0	366.0	1
190	235	23.0	20.0	1.3×10^{9}	1.19	5.95	100.0	Large	104.0	Large	118.0	541	105.0	Large	90.0	472.0	1
230	227	22.0	22.0	2.9×10^{9}	1.28	6.38	102.0	Large	123.0	Large	130.0	604	128.0	Large	103.0	572.0	1
275	220	21.0	22.0	3.2×10^{9}	1.34	6.70	100.0	Large	124.0	Large	139.0	643	134.0	Large	110.0	604.0	1
320	214	20.0	21.0	3.8×10^{9}	1.38	6.90	91.0	Large	117.0	Large	133.0	609	131.0	Large	109.0	561.0	1
365	207	19.0	20.5	4.4×10^{9}	1.46	7.31	88.0	Large	114.0	Large	131.0	611	139.0	Large	112.0	589.0	1
0	300	25.6	3.4	9.0×10^{7}	1.04	5.22	26.0	91	21.0	85	7.7	711	0.4	0.5	0.0	< 1	2
30	280	25.6	6.9	2.0×10^{8}	1.04	5.22	50.0	182	44.0	175	37.0	169	18.0	108.0	0.4	1.0	2
60	260	25.6	13.5	9.8×10^{8}	1.04	5.22	80.0	Large	79.0	Large	70.0	329	57.0	298.0	38.0	213.0	2
90	240	25.6	22.2	2.5×10^{9}	1.04	5.22	94.0	Large	106.0	Large	118.0	518	104.0	498.0	80.0	471.0	2
120	220	25.6	35.0	3.6×10^{9}	1.04	5.22	117.0	Large	148.0	Large	168.0	Large	171.0	Large	159.0	Large	2
150	200	25.6	56.0	1.2×10^{10}	1.04	5.22	100.0	Large	131.0	Large	165.0	Large	260.0	Large	270.0	Large	2
170	200	25.0	55.0	1.2×10^{10}	1.09	5.44	100.0	Large	133.0	Large	181.0	Large	269.0	Large	233.0	Large	2
205	200	24.0	50.0	1.1×10^{10}	1.17	5.85	105.0	Large	138.0	Large	192.0	Large	268.0	Large	265.0	Large	2
240	200	23.0	45.0	9.5×10^{9}	1.19	5.95	102.0	Large	134.0	Large	184.0	Large	243.0	Large	236.0	Large	2
275	200	22.0	40.0	8.3×10^{9}	1.28	6.38	103.0	Large	139.0	Large	188.0	Large	230.0	Large	213.0	Large	2
305	200	21.0	34.0	7.3×10^{9}	1.34	6.70	98.0	Large	125.0	Large	184.0	Large	200.0	Large	206.0	Large	2
340	200	20.0	29.0	6.5×10^{9}	1.38	6.90	83.0	Large	119.0	Large	160.0	Large	180.0	Large	170.0	Large	2
375	200	19.0	22.0	5.5×10^{9}	1.46	7.31	80.0	Large	113.0	Large	133.0	612	150.0	Large	128.0	Large	2
410	200	18.0	18.0	4.9×10^{9}	1.46	7.31	75.0	Large	97.0	Large	123.0	519	115.0	Large	96.0	499.0	1,2
450	194	17.0	14.5	5.5×10^{9}	1.54	7.72	62.0	236	78.0	Large	93.0	423	94.0	Large	69.0	365.0	1,2
495	188	16.0	9.0	5.9×10^{9}	1.65	8.25	43.0	159	53.0	323	61.0	281	52.0	276.0	7.9	83.0	1,2
540	182	15.0	5.5	5.8×10^{9}	1.78	8.88	28.0	101	34.0	138	39.0	180	17.0	83.0	1.6	< 10	1,2
585	176	14.0	3.3	6.1×10^{9}	1.90	9.50	17.0	61	19.0	80	22.0	105	2.4	12.3	0.5	< 10	1,2
625	170	13.0	2.2	6.5×10^{9}	2.06	10.30	11.0	43	12.0	57	12.0	68	1.1	< 10	0.2	< 10	1,2
670	164	12.0	1.6	7.2×10^{9}	2.29	11.40	7.5	30	8.0	38	5.2	31	0.6	< 10	0.0	< 10	1,2

The first feature of note in these results is the relatively unimportant contribution of the boundary layer to the total signal attenuation at the larger body angles. This is illustrated in Table III, which gives, for three different frequencies, signal attenuation due to the shock layer and the boundary layer at a station 1 ft from the apex of a 40-deg wedge at various points along the typical trajectories. It must be understood that these attenuations are reported separately for the shock layer and for the boundary layer, and that the total attenuation due to both is in general less than the sum of these separate attenuations. (This is because reflection losses are substantial and not additive.) For example, at 340 sec on Trajectory 2, the plasma and collision frequencies characterizing both the shock layer and the boundary layer are nearly equal. The separate attenuations at 250 MHz are 53 dB for the shock layer and 20 dB for the boundary layer; however, the total attenuation due to a plasma slab of thickness equal to that of the shock layer plus boundary layer for the same plasma properties is 58 dB. Thus the boundary layer contributes only 5 dB. Similarly, at 90 sec on Trajectory 2, the separate attenuations are 72 and 52 dB, whereas, the total attenuation based on a homogeneous slab model is 79 dB.

Noting from Table III that variations in signal frequency do not significantly change the relative importance of the boundary layer, it is concluded that for a 40-deg wedge, the boundary layer contributes little to the total signal attenuation (and contributes less at stations further aft, since it is thinner relative to the shock layer). The boundary layer contribution to total signal attenuation increases with decreasing wedge angle, such that at 30 deg it is almost equal to that due to the shock layer, whereas, at 20 deg it is the dominant contribution. For cones, the boundary layer contribution is somewhat greater than for wedges, since the boundary layer thickness relative to that of the shock layer is greater for cones. It should be emphasized that this discussion considers only uncontaminated air; as will be seen (Section II-C-2), the presence of contaminants increases the importance of the boundary layer.

Table III. Shock Layer (SL) and Boundary Layer (BL) Signal Attenuations for a 40-deg Wedge, 1 ft from Apex

Time, sec	Altitude, kft	Velocity, kft/sec	Attenuation, dB					
			f = 250 MHz		f = 1 GHz		f = 10 GHz	
			SL	BL	SL	BL	SL	BL
Traj. 1								
0	300	25.6	16	--	4	--	0	--
100	266	25	46	--	35	--	0.1	--
150	247	24	61	44	50	34	13	10
190	236	23	62	35	65	27	24	7
230	227	22	61	30	69	24	27	5
275	220	21	57	21	61	18	19	1.4
320	214	20	40	16	54	10	5.2	0.3
365	207	19	31	10	40	6	0.5	0.1
Traj. 2								
0	300	25.6	16	--	4	--	0	--
30	280	25.6	33	--	7	--	0	--
60	260	25.6	55	--	46	--	2	--
90	240	25.6	72	52	76	44	42	27
120	220	25.6	87	48	108	50	95	31
150	200	25.6	80	44	150	48	151	36
170	200	25	74	40	145	42	145	30
205	200	24	74	37	144	37	121	23
240	200	23	64	32	103	30	96	15
275	200	22	61	27	95	23	80	8
305	200	21	53	20	72	16	52	2.5
340	200	20	41	15	63	10	24.5	0.9
375	200	19	35	9	45	5	3.2	0.2

Table III. Shock Layer (SL) and Boundary Layer (BL) Signal Attenuations for a 40-deg Wedge, 1 ft from Apex (Continued)

Time, sec	Altitude, kft	Velocity, kft/sec	Attenuation, dB					
			f = 250 MHz		f = 1 GHz		f = 10 GHz	
			SL	BL	SL	BL	SL	BL
Traj. 1 and 2								
410	200	18	19	4	17	2.2	0	0
450	194	17	16	3	13	1.2	0	0
495	188	16	10	1	5	0.4	0	0
540	182	15	5	0.3	2.5	0.2	0	0
585	176	14	2	0.1	1	0	0	0
625	170	13	1.5	0	0.6	0	0	0
670	164	12	1	0	0.3	0	0	0

The preceding discussion justifies the approximate procedure used in the subsequent representation of total signal attenuation. Unless otherwise stated, this consists of neglecting boundary layer contributions entirely for body angles greater than 30 deg (including stagnation points), adding the separate shock layer and boundary layer attenuation for 30-deg body angles, and neglecting shock layer contributions entirely for body angles of 20 deg or less.

A second feature of these results is the time duration of severe signal attenuation. This is illustrated in Figs. 14 and 15, which show, for wedges and cones, respectively, the duration for which attenuation exceeds 10 dB along the two selected trajectories. The blackout duration is of the order of 10 min, and could be appreciably greater for conditions further aft on a vehicle. The body angle affects the blackout duration markedly; for body angles of approximately 20 deg or less, no communications problem is expected (from uncontaminated air). Figures 14 and 15 also indicate that the duration of blackout is appreciably reduced at higher signal frequencies. This effect is further demonstrated by Fig. 16, wherein duration is shown as a function of frequency for the 50-deg wedge on the transient trajectory. Also indicated in this figure is the sensitivity of the result to the attenuation level used to define blackout.

The depth of blackout is another quantity of interest, since it fixes the magnitude of the problem perhaps more definitively than the blackout duration. Table IV shows the maximum signal attenuation due to the plasma sheath encountered along the two trajectories for five frequencies and several geometries. It should be noted that the signal attenuation can be extremely large (>100 dB). Furthermore, increasing signal frequency in the range from 250 MHz to 10 GHz is evidently ineffective since the peak attenuation tends to peak around 5 GHz. This is in agreement with the previous general considerations of plane-wave attenuation (Section II-B-1). For body angles of 30 deg or less, the fact that increasing the signal frequency to 10 GHz does reduce the attenuation appreciably is also in agreement with previous considerations, since here the plasma frequency is near 10 GHz.

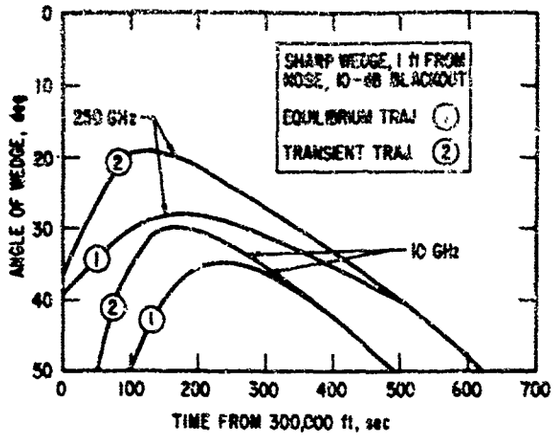

Fig. 14. Representative Blackout Region for Lifting Reentry (Sharp Wedge)

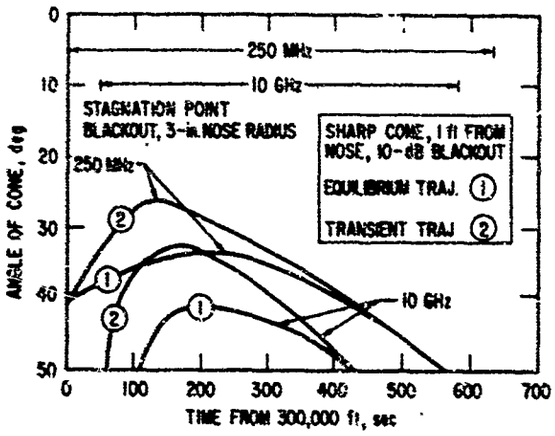

Fig. 15. Representative Blackout Region for Lifting Reentry (Sharp Cone)

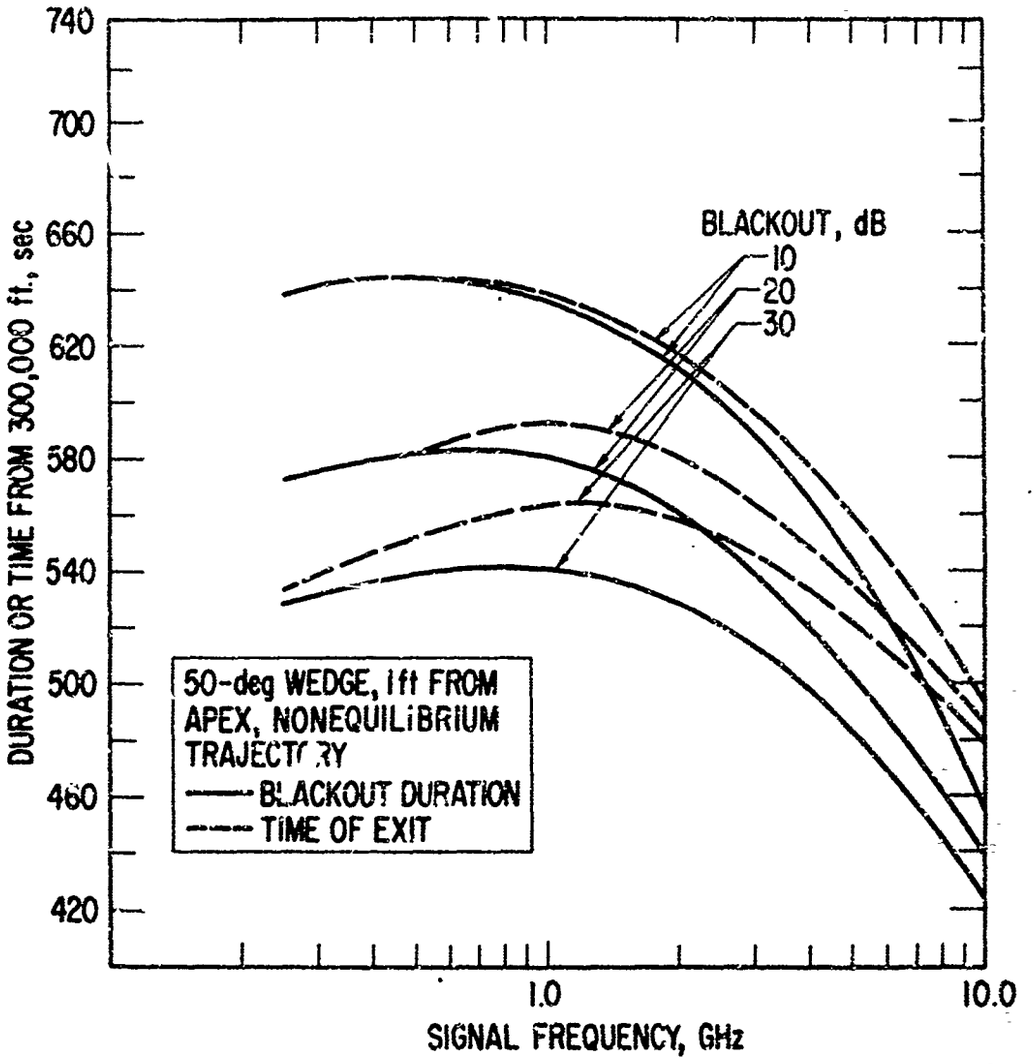

Fig. 16. Blackout Duration and Time of Exit from Blackout

Table IV. Peak Signal Attenuations Representative of Lifting Reentry Conditions

Signal Frequency, GHz	Attenuation, dB						
	Stagnation Point (3-in. Nose Radius)	Wedge				Cone	
		50 deg, 1 ft	40 deg, 1 ft	30 deg, 1 ft	20 deg, 1 ft	50 deg, 1 ft	40 deg, 1 ft
Equilibrium Trajectory							
0.25	35	102	62	24	1.7	59	38
0.50	36	124	64	15	0.5	63	35
1.0	38	134	69	9	0.2	67	30
5.0	34	139	53	0.2	0	56	14
10.0	28	112	27	0	0	44	4.2
Nonequilibrium Trajectory							
0.25	42	117	87	67	11	62	47
0.50	44	148	150	65	8	77	61
1.0	47	185	150	62	4	98	67
5.0	62	269	165	25	0.2	129	72
10.0	60	265	151	18	0	124	60

Although these conclusions are based on clean equilibrium air calculations, the influence of nonequilibrium and contamination effects are shown below to be relatively unimportant.

2. CHEMICAL NONEQUILIBRIUM EFFECTS

The effects of chemical nonequilibrium on the preceding equilibrium results are selectively portrayed in Figs. 17 through 19 in the form of attenuation vs time for both equilibrium and nonequilibrium flow. All of the latter results have been obtained by reducing the effective plasma slab thickness at a particular location by the distance normal to the shock wave required for the electron density to reach one-half the equilibrium value (as has been indicated in Section II-A-3). Figure 17 portrays the nonequilibrium effects for a relatively insensitive case (that is, far back on a large angle cone). It is observed that the effects are more pronounced on the equilibrium glide trajectory than on the transient trajectory, due to the higher altitude of the former. A quite significant feature is that the entry into the blackout region is more strongly affected than the exit therefrom.

Figure 18 indicates the nonequilibrium effects for a more sensitive case; the salient feature here is that the nonequilibrium flow situation 2 ft from the apex is roughly equivalent to the equilibrium flow situation 1 ft from the apex, with the exception of the increased time before entry into blackout. Nonequilibrium flow effects are somewhat less for wedges than for cones, but in both cases the effects increase substantially with decreasing body angle. For body angles of 30 deg or less, nonequilibrium considerations indicate that electrons will not be formed in any quantity in the shock layer for the equilibrium glide trajectory and only for a very short period during the transient trajectory. All of the preceding information is contained in a detailed tabulation of the characteristic electron incubation distance behind plane shock waves compared with appropriate shock layer thicknesses presented in Volume II, Appendix C. Figure 19 shows nonequilibrium effects on stagnation point flows; the indication here is, of course that these effects are quite pronounced for small nose radii.

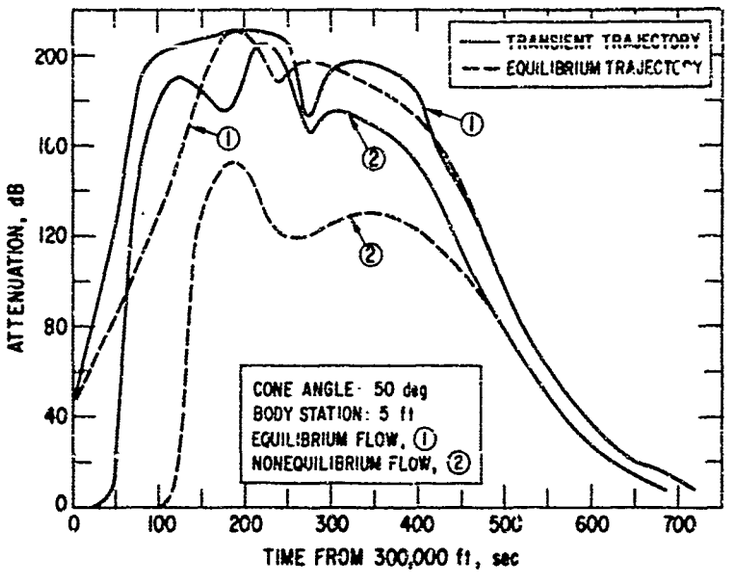

Fig. 17. Nonequilibrium Effects 5 ft from Nose

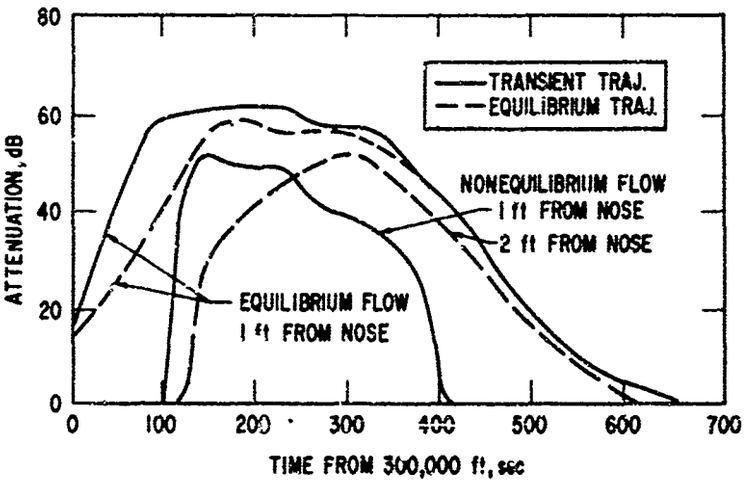

Fig. 18. Nonequilibrium Effects 1 ft from Nose

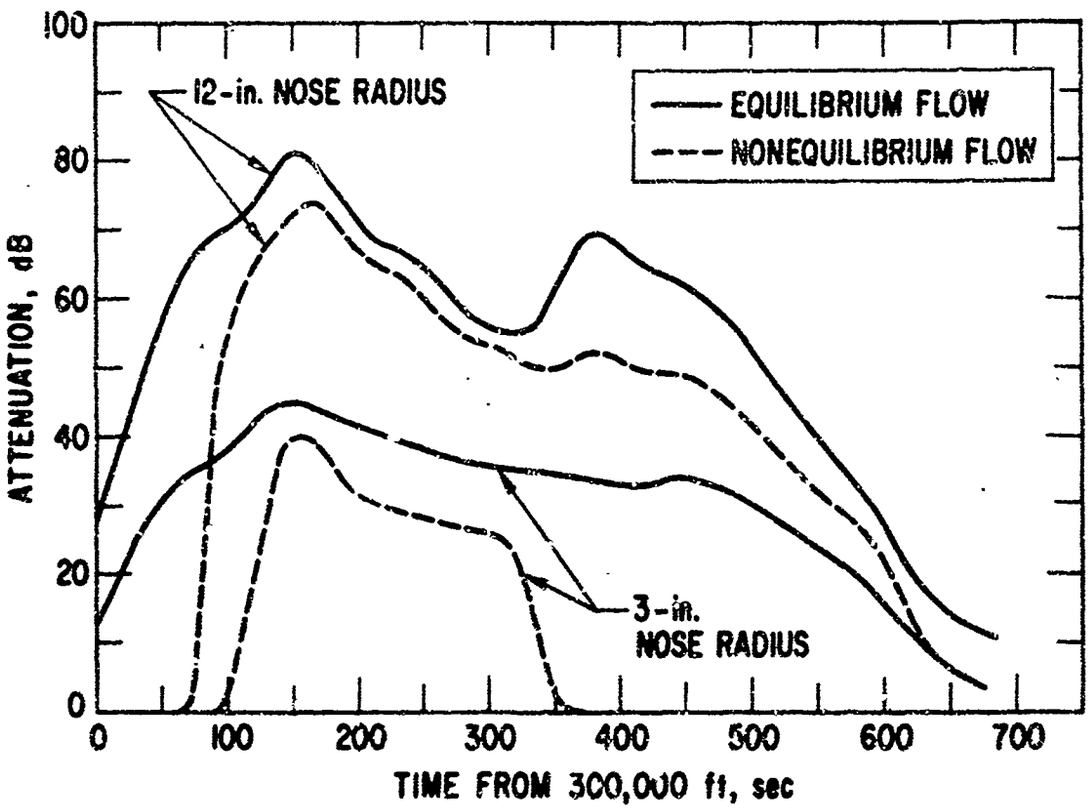

Fig. 19. Nonequilibrium Effects at Stagnation Point

The most outstanding feature of chemical nonequilibrium is the effect on the time of onset of signal attenuation. Hence, the only quantitative representation of chemical nonequilibrium effects which has been incorporated into our subsequent considerations is a modification of the time of onset, taken to be 90 sec after the vehicle reaches an altitude of 300,000 ft. The other effects of chemical nonequilibrium can be interpreted in the previously indicated sense that equilibrium flow conditions at a given station are representative of the nonequilibrium flow conditions at a station somewhat further aft, which is adequate for our purposes.

3. CONTAMINANTS EFFECTS

The effect of trace amounts of sodium in the boundary layer on the resultant signal attenuation is portrayed in Figs. 20 and 21. The figures present both shock layer and contaminated boundary layer attenuation for wedges with a 50- and 40-deg shock angle, respectively, at an altitude of 200,000 ft as a function of velocity. The conditions are representative of the transient trajectory for body angles roughly 5 deg less than the shock angles. Sodium concentrations considered are 10, 100, and 1000 ppm in the boundary layer corresponding to concentrations in the heat shield of approximately 100, 1000 and 10,000 ppm, respectively. A concentration of 100 ppm corresponds to a standard heat shield material, whereas, 10,000 ppm represents an extremely high contamination level.

The most significant feature indicated by the figures is that contamination effects become important only at lower velocities, and are not significant in the higher velocity ranges of interest (due to the fact that the equilibrium air ionization is already quite high). Hence, these effects are not important during peak attenuation periods. Specifically, from Fig. 20 we observe that a sodium concentration of 10 ppm will not increase the signal attenuation to a noticeable extent until the velocity is less than 18,000 fps. With reference to the transient trajectory, this implies that the attenuation is unaffected for approximately 340 sec after the vehicle has reached 300,000 ft. On the lower velocity portion of the trajectory, 10 ppm would increase by 140 sec the time

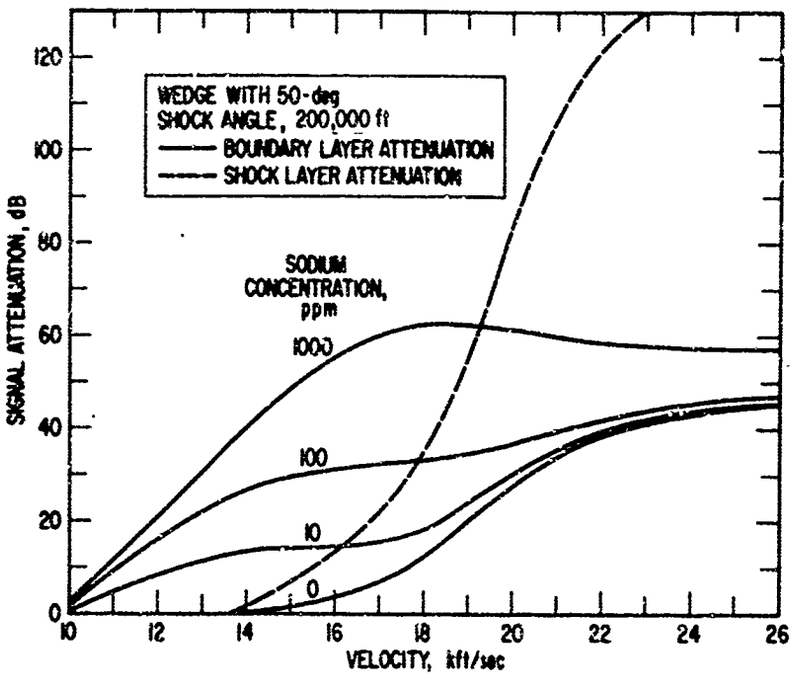

Fig. 20. Sodium Contamination Effects on 250-MHz Signal Attenuation (50-deg Shock Angle)

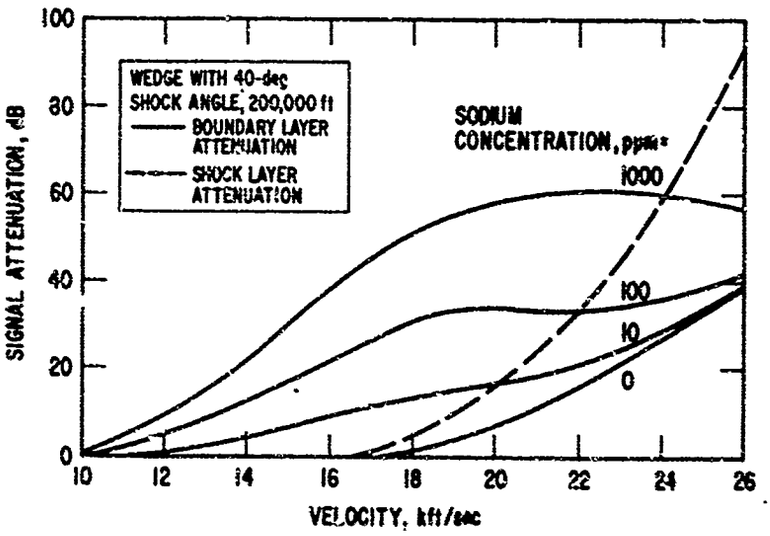

Fig. 21. Sodium Contamination Effects on 250-MHz Signal Attenuation (40-deg Shock Angle)

that the attenuation exceeded 10 dB, but would have no effect on the time that the attenuation exceeded 20 dB. The larger concentrations of sodium have somewhat greater effects, although the qualitative nature is unchanged.

Another feature indicated by the figures is that contamination effects are larger for smaller body angles (since even the uncontaminated boundary layer is relatively more important here). It is also noted that contamination effects are somewhat larger at lower altitudes (the contribution of the absolute density increase of the contaminant outweighs that of the thinner boundary layer) and are greater for cones than for wedges (again reflecting the importance of the uncontaminated boundary layer), although neither of these effects are indicated graphically.

It is concluded that the effects of sodium contamination in representative cases (concentrations of 10 ppm, approximately) are not sufficiently large to merit quantitative corrections. However, these effects will be discussed qualitatively with reference to specific alleviation techniques, as the need arises.

D. THE COMMUNICATIONS SYSTEM

1. SYSTEM MARGINS

The preceding discussions have been devoted to an assessment of signal attenuation due to the plasma sheath in typical lifting reentry situations. The effect of this plasma attenuation on the capability of communications systems can be determined only if certain parameters of the remainder of the communications link are known. It is the purpose here to specify the parameters of typical vehicular communications systems so that blackout can be defined and a framework provided for the evaluation of alleviation schemes.

The elements of typical communications systems are illustrated in Fig. 22, which indicates the path of the signal from the information source to the receiver. The parameters that determine the capability of the system are listed in the figure and discussed in Ref. 30. Such systems are normally designed to deliver information at a specified message rate C (bits/sec) when the signal-to-noise ratio (S/N) exceeds a certain threshold value,

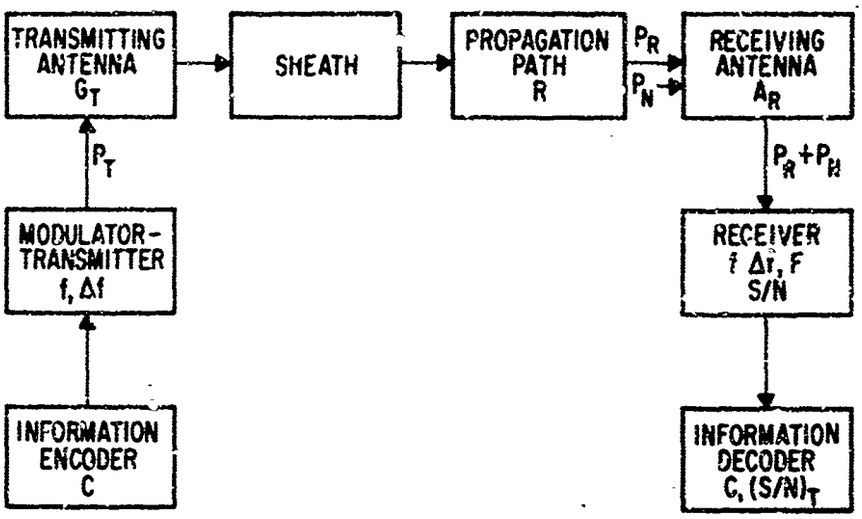

PARAMETERS

A_R = EFFECTIVE RECEIVING APERTURE
C = INFORMATION RATE
F = RECEIVER NOISE FIGURE
f = RF SIGNAL FREQUENCY
Δf = RF BANDWIDTH
G_T = TRANSMITTING ANTENNA GAIN
L = MISCELLANEOUS SYSTEM LOSSES
P_N = NOISE POWER
P_R = RECEIVED POWER
P_T = TRANSMITTER POWER
R = RANGE
S/N = SIGNAL-TO-NOISE RATIO
$(S/N)_t$ = THRESHOLD SIGNAL-TO-NOISE

Fig. 22. Communications System

designated $(S/N)_T$. When the signal-to-noise ratio is below the threshold value, the communications link becomes inoperative due to excessive error rates.

In the absence of the plasma, the signal-to-noise ratio is given by

$$\frac{S}{N} = \frac{P_T G_T A_R}{4\pi R^2 k T_e L F}$$

where T_e is an effective temperature which depends upon thermal, atmospheric, and galactic noise, and k is Boltzmann's constant. The theoretical maximum message rate C_{MAX} is given by

$$C_{MAX} = \Delta f \log_2 [1 + (S/N)_T]$$

The actual message rate C is typically considerably less than the theoretical maximum. Values of the ratio C/C_{MAX} for standard telemetry systems range from 0.02 to 0.2, depending on the type of modulation. A discussion of this point is beyond the scope of this report, but the interested reader is referred to Ref. 30 for detailed information.

A useful composite parameter is the system margin, defined as $10 \log_{10}[(S/N)/(S/N)_T]$ dB. The system margin represents the amount of plasma attenuation that can be tolerated by the system while it delivers information. If we assume that the transmitting antenna system is omnidirectional, that the range of the system is 100 miles, and that the effective area of the receiving antenna, the noise figure, and the miscellaneous losses are state-of-the-art optima, then the system margin is a function of only the transmitted power P_T, the signal frequency f, the rf bandwidth Δf, and the threshold signal-to-noise ratio $(S/N)_T$.

Typical telemetry systems are characterized by bandwidths of 300 kc and signal-to-noise thresholds of 10 (Ref. 31). These quantities and the scheme described above have been used to calculate margins for 1-W systems (Volume II,

Appendix D), and the results are presented in Fig. 23. Since the system margin is directly proportional to transmitted power and inversely proportional to rf bandwidth, the square of the range, and the signal-to-noise threshold, system margins for other values of these parameters can be readily obtained from Fig. 23. Such transformations have been made to obtain the isolated points in the figure from actual reentry systems (Refs. 32 and 33). These points serve to illustrate the adequacy of the approximations employed in the construction of the curve.

2. BLACKOUT AND ALLEVIATION

A representative frequency range for typical telemetry systems, as previously indicated, is 250 MHz to 10 GHz. Transmitter power levels range from 1 to 10 W at the lower end of this band and from 0.1 to 1 W at the higher end. These specifications and the typical specifications incorporated in Fig. 23 indicate that system margins range between 15 and 30 dB. Since plasma attenuation is typically greater than 100 dB during a 10-min period of lifting reentry, it is clear that typical communications systems will be inoperative (blacked out), and that the requirements for alleviation schemes are severe in that the schemes must either provide for or eliminate losses of the order of 70 dB.

3. SPECIFICATION OF A REPRESENTATIVE COMMUNICATIONS SYSTEM

In order to evaluate alleviation schemes, we will assume that the vehicle carries a system of the type just described operating between a frequency of 250 MHz and 10 GHz with a bandwidth of 300 kHz and further characterized by power levels in the range 0.1 to 10 W and system margins in the range from 10 to 30 dB. Within the stated limits, we will presume that the frequency is arbitrary, and that it may be selected to benefit any given alleviation scheme without penalty. If an alleviation scheme requires a modification of the representative system, such as the addition of a power amplifier, then a weight penalty will be assigned only to the modification. If the transmitting system is to be replaced, as it must be if an alleviant involves signals with

frequencies other than those prescribed above, then a weight penalty will be assigned to the entire alternate transmitting system.

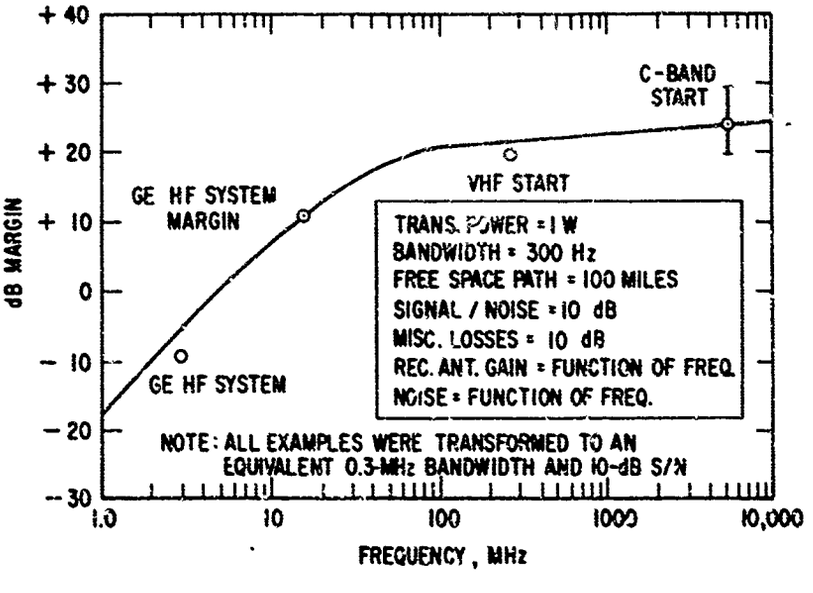

Fig. 23. Typical Free Space System Margin

III. EVALUATION OF ALLEVIATION TECHNIQUES

A. INTRODUCTION

1. EVALUATION CRITERIA

This section is devoted to presenting the results of preliminary systems analyses for a variety of techniques for alleviating the lifting reentry communications problem. The four principal criteria used as a basis for comparison are: (1) quality of communication, (2) weight penalty, (3) flexibility, and (4) further research and development effort. The quality of communication of a given system is dependent on frequency range, information rate capability, and possible effects of weather conditions. The weight penalty of a given system is a basic systems consideration, and the flexibility of a system in terms of the weight penalty involved for different trajectories or vehicles of different sizes or shapes, or both, is also very important. The further research and development effort required to bring a given technique to a point where a reasonable preliminary design of a flight item can be made involves consideration of the nature of the problem areas, the amount and type of effort required to resolve them, and their likely influence on the other evaluation criteria. Our systems analyses are oriented toward yielding an appraisal of each alleviation technique in terms of these four factors.

2. SYSTEM ANALYSIS

Two facts concerning the systems analyses presented should be emphasized at the outset. First, the alleviation techniques to be discussed have been, without exception, proposed previously in some form; we have endeavored to give due credit to the previous proposals. Second, these alleviation techniques collectively cover a broad spectrum of states of technological development and our associated analyses will vary in accordance with this spectrum. At one end of this spectrum are techniques based on well established concepts (such as coolant injection). These techniques have been

analyzed in some detail, and the amount and type of further research and development effort required has been assessed fairly accurately (simply because the magnitude of this effort has been defined by similar previous efforts). At the other end of this spectrum are techniques based on concepts which are relatively new and not too well established (such as the use of lasers). These techniques have not been analyzed in nearly as much detail simply because the state of the art does not permit it. Similarly, the amount and type of further research and development effort has not been so clearly defined; our approach to the assessment of the required effort has been to indicate the problem areas as they appear to us.

B. MODIFICATION OF THE COMMUNICATIONS SYSTEM

The most obvious way in which the lifting reentry communications problem can in principle be alleviated is by designing the communications system with a free space system margin greater than the plasma signal attenuation encountered during reentry. Two methods, which may be used separately or in combination, exist for improving the system margin: increasing the transmitted power (by a power amplifier, for example) and decreasing the rate at which information is transmitted. The analysis in Section II indicates that a typical plasma attenuation to be expected is 100 dB, whereas, typical reentry communications systems have margins in the range of 20 to 30 dB; thus the improvement in system margin which would be required (70 to 80 dB) is unrealistically large and cannot be achieved in practice. The detailed considerations presented here will of course establish this fact more quantitatively and will provide a basis for employing system margin improvement in conjunction with other alleviation schemes.

The system margin improvement which can be obtained by increasing the power of the transmitter is limited both by breakdown (Section II-B-4) and by the additional weight associated with the increased power. Previous considerations have indicated that breakdown will occur at transmitted power levels of the order of from 10^3 to 10^4 W in typical reentry situations; hence, the maximum system margin improvement that can be realized is of the order

of 30 to 40 dB. This is clearly inadequate for purposes of complete alleviation. The practicality of obtaining even this improvement is determined by weight requirements. The weight of power amplifiers in the conventional frequency range is, roughly, directly proportional to operating frequency and output power (Ref. 34). A representative relation for the weight as a function of frequency and amplification is derived in Volume II, Appendix E, and the resulting weights associated with various system margin improvements are shown.

System Margin Improvement, dB	Weight of Power Amplifier, lb			
	1-W initial power		10-W initial power	
	250 MHz	2500 MHz	250 MHz	2500 MHz
10	0.18	1.8	1.8	18
20	2.0	20	20	200
30	20	200	200	2000

It is seen that the use of a power amplifier to improve system margins by more than 30 dB is impractical, regardless of breakdown considerations.

Given a constant average transmitted power, the system margin can be increased by reducing the bandwidth of the receiver or the duty cycle of the transmitter (pulsed operation) or both. The information transmission rate is directly proportional to both of these quantities, thus, the increase in system margin is equal to the decrease in information transmission rate when both quantities are expressed in decibels. Hence, if the typical information rate of 3×10^4 bits/sec (corresponding roughly to a 300-kHz bandwidth) is reduced to the minimum useful rate of 1 bit during the entire reentry period (1 bit in 10 min, say), it is theoretically possible to obtain a system margin improvement of 70 dB. Even if such low information rates were acceptable, it is not likely that they would be achievable, since practical considerations place a lower limit on the attainable bandwidth with a given carrier frequency, and plasma breakdown considerations place a lower useful

limit on the duty cycle of a transmitter of given average power (see Volume II, Appendix E).

We conclude that the complete alleviation of blackout by simply modifying the communications system is impracticable. If such techniques are to be used at all, they must be in combination with schemes that reduce the plasma attenuation. This possibility will be discussed in subsequent sections.

C. AERODYNAMIC SHAPING

1. BASIC PRINCIPLES

Aerodynamic shaping has often been proposed (Refs. 35, 36, 37) as a technique for alleviating the communications problem. The general aim of the technique is to modify the vehicle shape to change the flow field, which reduces the thickness of the plasma sheath in the vicinity of the antenna or reduces the electron density in the plasma sheath, or both. The shaping can be of two general types, distinguished by the scale of the modification: vehicle shaping or localized shaping.

Great success has been achieved with vehicle shaping in eliminating blackout from ballistic trajectories by employing slender, slightly blunted reentry vehicles rather than the classical blunt shape. For lifting reentry purposes, however, the vehicle will have to maintain a large angle of attack to achieve the desired lift, and as the calculations of Section II have shown, even a perfectly sharp vehicle will exhibit prohibitively high electron densities in the windward shock layer. Thus, the global change of vehicle shape does not seem to offer much promise for lifting reentry, and it is not further considered in this report.

Localized shaping (i. e., modification of the vehicle shape in a restricted area) will therefore have to be employed for lifting reentry. The specific technique that has the most promise is the use of a slender fin extending through the primary shock layer on the windward side of the vehicle, as shown in Fig. 24. As the analysis in Section II has shown, an antenna location 1 ft from the apex of a sharp wedge with a half-angle of less than 25 deg (approximately) will yield an attenuation less than 10 dB throughout the entire trajectory.

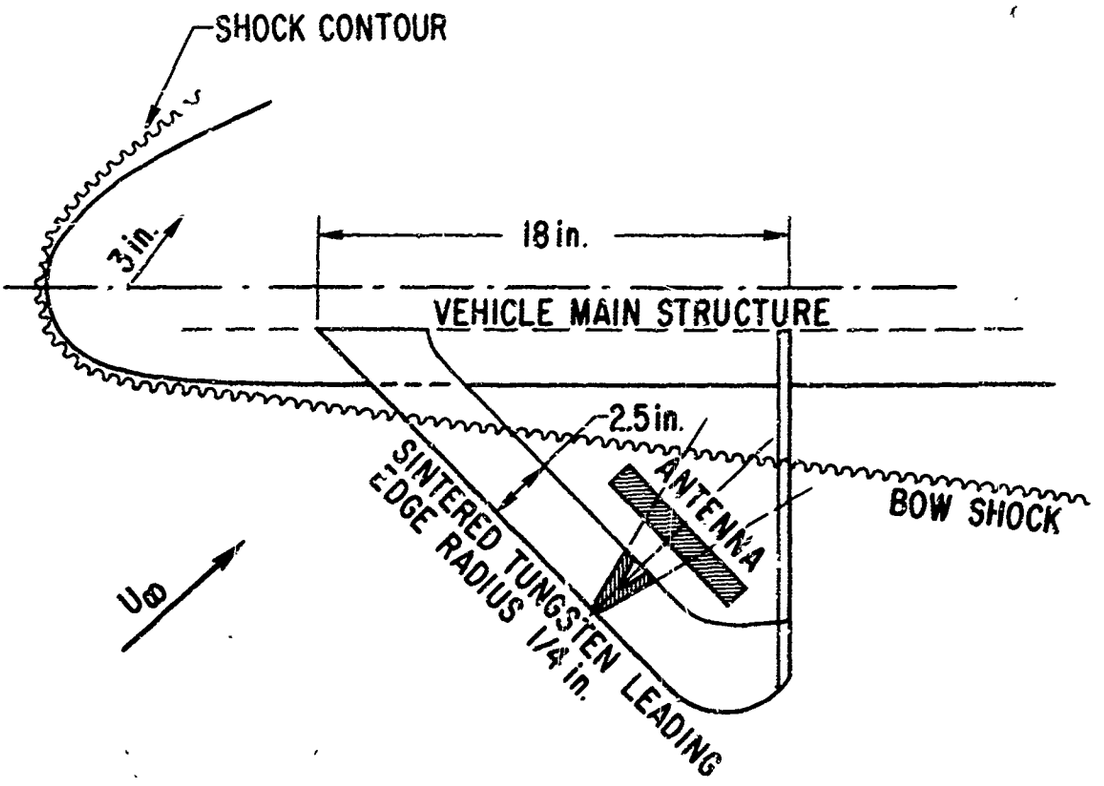

Fig. 24. Communications Fin

Hence, such a fin will provide two-way communication over the conventional frequency range, provided its structural integrity can be ensured. The two subsequent subsections are devoted to an analysis of such a structure and the areas requiring further investigation. There are many other forms of localized shaping; for completeness, these will be reviewed in the final section.

The basic problem of maintaining aerodynamic stability of the vehicle is an extremely important consideration when aerodynamic shaping techniques are contemplated. This is due to the fact that the essence of the technique is appropriate modification of the flow field, and this must affect the stability of the vehicle. Maintaining adequate stability margins in these circumstances may require a redistribution of weight or control surfaces, or both. Consequently, although the subsequent weight estimate of the fin and supporting structure is relevant, it may not reflect the total weight associated with its integration into the vehicle. Finally, it is pointed out that the stability problem requires that aerodynamic shaping techniques must be incorporated into the early stages of vehicle design.

2. FIN-DESIGN CONSIDERATIONS

The main problems in the design of the proposed fin are those associated with maintaining the structural integrity of a shape that will in fact reduce the plasma layer to negligible proportions. The configuration selected here is as indicated in Fig. 24; in the plan view, the fin presents the cross section of a 15-deg half-angle wedge with a 0.25-in. leading-edge nose radius. The effects of the nose bluntness are generally absorbed by the boundary layer in a distance of roughly 10 nose radii downstream from the leading-edge stagnation line. Thus, at the antenna location, the flow is similar to that over a sharp wedge, and the plasma attenuation is less than 10 dB throughout either of the typical trajectories. The overall dimensions of the fin shown in Fig. 24 are selected on the basis of accommodating a 6-in. slot antenna at a station roughly 2 ft from the nose of the vehicle.

The heat transfer to various portions of the fin were computed by standard techniques (Refs. 38, 39); details of these calculations are given in Volume II, Appendix F. Pertinent results are shown in Fig. 25, wherein the heating rate at the 0.25-in. radius stagnation line and at a point 1 ft from the leading edge of the fin are shown as a function of time along the transient trajectory. Considering the stagnation line heating rate, data presented in Ref. 40 show measured recession rates for sintered tungsten (the candidate leading edge material) of 0.003 in./sec at 2260 Btu/sec-ft^2 and 0.0005 in./sec at 750 Btu/sec-ft^2. From the results of Fig. 25, it is thus concluded that the leading-edge shape should be stable; indeed, the total recession of the stagnation line (~0.2 in.) is less than the leading-edge radius. The heating rate at the side of the fin is not high enough to present any difficulty; a standard ablation material will suffice.

The preceding heat transfer considerations have not considered the effects of the interaction of the shock pattern with the flow field. The effect of a vehicle bow-shock impinging on a fin has been experimentally investigated in Refs. 41 and 42. The results indicated that the heat transfer rate in the interaction zone is approximately 4 times greater than that on other portions of the leading edge. Since the bow shock lies relatively close to the body, the heat transfer rate may be reduced in the interaction zone by locally increasing the radius of the leading edge, without interfering with the communications capability of the fin. Some erosion of the material is still to be expected, however. A local increase in heat transfer rate is also to be expected in the area where the shock produced by the fin interacts with the flow over the bottom of the vehicle. No data are available on the magnitude of this increase, but it seems that a moderate local reinforcement of the bottom heat shield should be adequate.

The weight of this fin, including ablation material and supporting structure is estimated to be somewhat less than 20 lb.

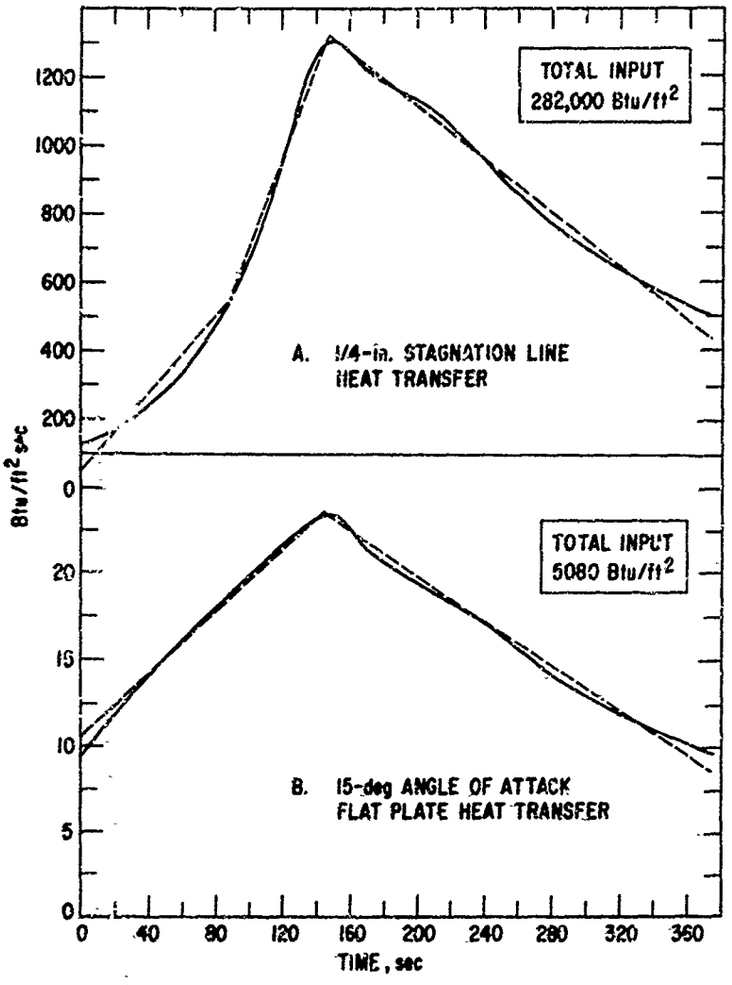

Fig. 25. Heat Transfer Rate for Communications Fin

3. AREAS REQUIRING FURTHER RESEARCH AND DEVELOPMENT

The main aspect requiring further development effort of the fin system is its effect on the aerodynamic stability of the vehicle. This requires extensive wind tunnel testing at higher Mach numbers with at least a few varieties of vehicle shapes. The primary information desired is an estimate of the total weight associated with the fin system when aerodynamic stability is maintained.

Another aspect requiring further effort is an evaluation of the increase in heat transfer rate expected due to the interaction of the fin shock with the flow on the bottom of the vehicle. It is also important to determine the effects on the flow field caused by any subsequent degradation of the bottom surface. Again, wind tunnel testing is indicated.

A final problem area requiring further effort is the actual construction of the fin to incorporate sintered tungsten leading edge without suffering degradation of the rema of the fin under prolonged high heat transfer rates. This will of course require detailed design and heating rate testing.

4. REVIEW OF PREVIOUS PROPOSALS

In this subsection, some previous proposals for localized aerodynamic shaping techniques are discussed, primarily for the sake of completeness. Some of these techniques were suggested initially with relation to ballistic reentry; the present discussion is of course oriented toward lifting reentry.

a. Flow Diverters

Flow diverters are small obstacles placed in the flow near the transmitting antenna. Their purpose is to thin the plasma layer and expand the flow in the vicinity of the antenna so as to reduce the severity of the plasma attenuation. Their small size should make them less detrimental to the overall vehicle stability than the proposed fin technique. References 35 and 36 are fairly comprehensive studies of two different flow diverter geometries.

Their results indicate that flow diverters will work best if the bulk of the attenuation takes place very near the vehicle surface. For a gliding vehicle at large angles of attack, the electron density is fairly uniformly distributed across the shock layer, making it more difficult to bypass the attenuating layer. Figure 26 indicates the maximum allowable sheath thickness for a given attenuation along a transient trajectory for a 10-deg cone. A 20 dB attenuation will require the flow diverter to be brought to within 0.010 in. of the outer shock; i.e., the whole shock layer will have to be diverted. Such a diverter will in fact be a small fin, and will show no worthwhile improvement over the communication fin described in the preceding section.

b. Aerospike Antenna

The aerospike antenna system proposed in Ref. 37 consists of an antenna enclosed in a small cylindrical casing (1.5 × 3 in.) mounted on a pylon. The flow around the antenna body is modified by the projection of a small jet of gas (helium) upstream of the forward stagnation point, thus reducing the electron density in the sheath around the casing and thermally protecting it. The reduction of electron density is brought about by two mechanisms: modification of the shock shape (i.e., making the antenna body look more slender than it is), and cooling by the mixing of the cold helium with the hot plasma sheath. For a typical reentry trajectory, the aerospike being located in the freestream, a total mass flow of the order of 6 lb/in.^{2} of casing frontal area is reported to be sufficient to properly detach the normal shock. The mass flow requirement is lessened if the antenna is located within the envelope of the bow shock. Two assumptions are implied in the concept of the aerospike antenna: (1) the antenna casing can be made to stay at zero angle of attack with the local flow all during reentry; (2) the pylon holding it can be thermally protected without becoming too bulky. Had a more complete study been made, it is suspected that the weight requirement for the aerospike antenna system would not have compared favorably with other systems, and would have remained fairly complicated and, hence, unreliable.

D. MAGNETIC WINDOW

1. PRINCIPLE OF OPERATION

The use of a magnetic field as an alleviant for signal attenuation has been proposed previously (Ref. 43, for example), and the analysis offered here is based on the same fundamental principle. This principle is simply that the presence of a dc magnetic field in the sheath with a component in the direction of signal propagation will reduce the ability of the free electrons to react to the transverse electric field associated with the signal and, hence, will reduce attenuation. If the magnetic field is made sufficiently strong, signal attenuation can be reduced to negligible levels.

The practical application of this principle, as envisioned here, is the use of a coil placed as close as possible to the vehicle skin to produce a magnetic field with large components normal to the vehicle surface; the radiating aperture is located in the central region of the coil (see Fig. 27). Configurations similar to this have been proposed previously for both conventional air core magnets (Ref. 43) and for superconducting coils (Ref. 44). The subsequent detailed analysis is concerned primarily with the use of conventional magnets since they are state-of-the-art devices. Brief consideration will be given to superconductors in the conclusion of this section.

Assuming that such a system has an operational capability, the quality of communications afforded is excellent in that the operating frequency is in the standard range, weather conditions are of no consequence, and the information rate capability is not severely limited by plasma effects.

2. MAGNETIC FIELD REQUIREMENTS

The first step in analyzing a magnetic field system is to estimate the plasma attenuation produced in the presence of a given magnetic field. The basic procedure employed here is to compute attenuation on the basis of a linearly polarized plane-wave normally incident on a homogeneous plasma slab in the presence of a uniform magnetic field in the direction of propagation. This model is of course highly idealized, but nevertheless it does seem

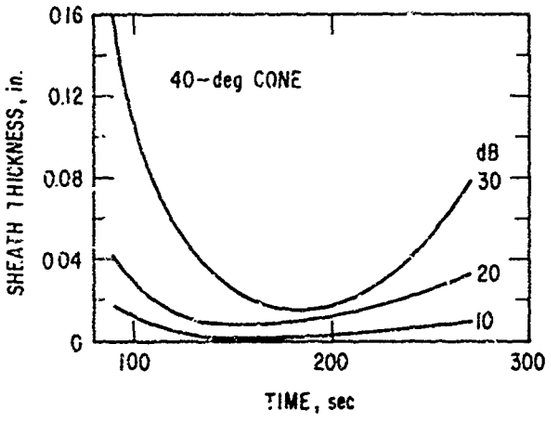

Fig. 26. Sheath Thickness vs Time for Given Attenuation

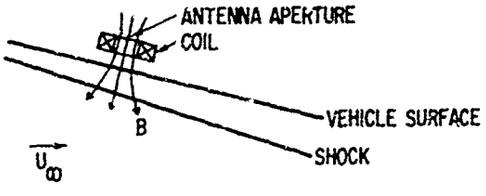

Fig. 27. Magnetic Window Technique

to approximate the actual situation of an aperture type antenna located at the inner surface of a plasma sheath (Ref. 45).

It is well known that in the model just described, the total plasma attenuation is given by (Ref. 43):

$$\text{Attenuation} = \frac{1}{2}(|T_{RH}| + |T_{LH}|)$$

where T_{RH} is the transmission coefficient for a right-hand (RH) circularly polarized wave, and T_{LH} is the transmission coefficient for a left-hand (LH) circularly polarized wave. The LH circularly polarized component is much more highly attenuated than the RH circularly polarized component, and is neglected for the purpose of our estimates.

The transmission coefficient for the RH circularly polarized component was evaluated by digital computations. A characteristic feature of the results is a highly oscillatory transmission coefficient, as illustrated in Fig. 28. In order to represent the maximum possible plasma attenuation fairly, the exact transmission coefficient was used only up to the first minimum, which occurs at

$$\frac{d}{\lambda_0} \simeq \frac{1}{4} \frac{\omega_p}{\omega}\left(\frac{\omega_c}{\omega} - 1\right)^{1/2}$$

and beyond this point the maximum attenuation envelope was used in place of the exact computation (see Fig. 28). As collisions become more predominant, the highly oscillatory transmission resonances become less severe and eventually insignificant.

The nature of the plasma attenuation in the presence of a magnetic field is illustrated in an attenuation contour map (Fig. 29). The parameter $V\lambda_0/W^2 d$ is a measure of collisional effects, independent of the signal frequency, and approximately 10^{-2} for the plasmas considered here. The dashed curves in Fig. 29 are contours for fixed plasma conditions and

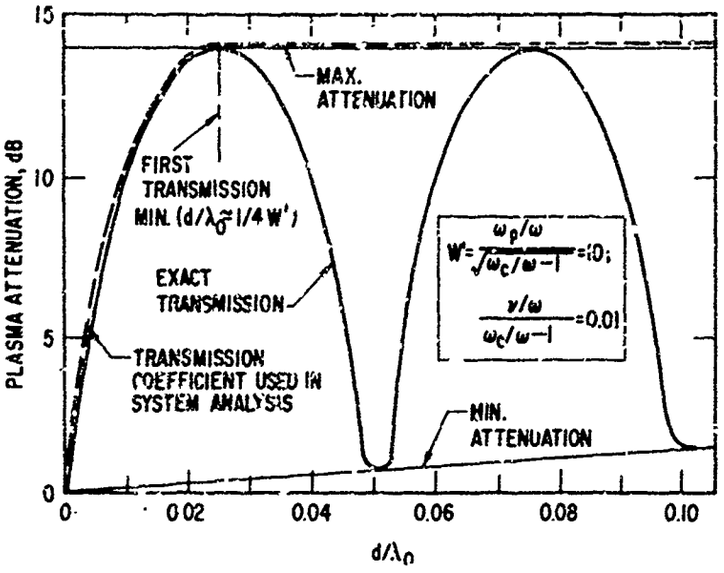

Fig. 28. Behavior of Transmission Coefficient in Magnetic Fields

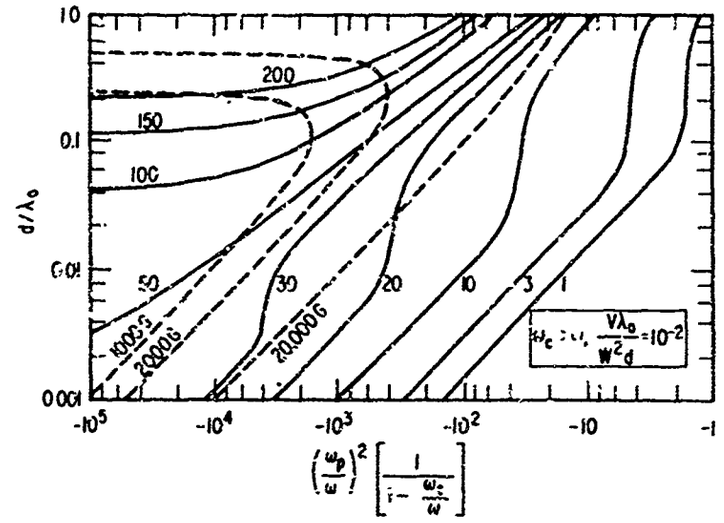

Fig. 29. Attenuation Contour Map for Typical Reentry Conditions with Magnetic Field (Attenuation in dB)

magnetic field as the signal frequency is varied. These curves correspond to the plasma conditions at maximum attenuation for a 50-deg wedge on the transient trajectory and magnetic field strengths of 1000, 2000, and 10,000 G. With conventional magnetic field strengths, increasing signal frequency beyond 250 MHz results in substantial increases in attenuation until the electron cyclotron frequency is reached. Accordingly, in the subsequent analysis of conventional magnetic field systems, we have considered only 250 MHz. For higher field strengths, increasing the signal frequency up to approximately 5 GHz will yield further decreases in attenuation.

High magnetic field strengths may cause appreciable disturbances in the flow field and, hence, in the aerodynamic characteristics of the vehicle. The importance of this interaction is governed by the ratio of magnetic forces to inertial forces -- roughly $\sigma B^2 L/\rho U$ where σ is the conductivity, L is the antenna width, ρ is the air density, and U is the air velocity. For typical reentry applications, $\sigma \sim 100$ mho/m, $\rho \sim 10^{-2}$ kg/m^3, $L \sim 0.1$ m, and $U \sim 5 \times 10^3$ m/sec, so that the ratio is about $0.2B^2$. Thus, for conventional magnets ($B \sim 0.3$ Wb/m^2) little interaction is expected, but for superconducting magnets ($B \sim 2$ Wb/m^2) the interaction may be significant.

The final step in estimating the magnetic field required to produce a given attenuation is to relate the uniform magnetic field results just discussed to the case of the non-uniform magnetic field produced by a coil. For this purpose, we have assumed that an equivalent uniform field, equal in magnitude to the field produced by the coil on axis at the outer edge of the sheath, used in conjunction with the uniform field model will adequately predict the actual signal attenuation in the non-uniform field environment. Further effort to determine signal attenuation in non-uniform fields is indicated.

3. ESTIMATE OF WEIGHT REQUIREMENTS

a. Calculation Technique

For a given vehicle shape, antenna location, trajectory, and desired attenuation level, the design point for purposes of sizing the magnet system is selected as that trajectory point which requires the largest magnetic field.

The subsequent weight estimate is based on maintaining this value of magnetic field throughout that portion of the trajectory during which the unalleviated signal attenuation exceeds the desired value. This procedure of course results in a greater system weight than would result if the magnetic field were varied continuously over the trajectory to maintain the desired level of attenuation. Typical calculations indicate that this constant magnetic field system is roughly 1.5 times as heavy as a variable magnetic field system.

The details of the procedure employed here to estimate the weight of the magnet system required to produce a given magnetic field at the sheath edge are given in Volume II, Appendix G; only the main features will be indicated here. The first step is to relate the desired value of magnetic field to the required properties of the coil. This is accomplished by assuming that the field produced by the coil is the same as if the total current in a cross section of the coil (i.e., the number of ampere-turns) were concentrated at the mean diameter of the coil at the inside edge of the sheath, as indicated in Fig. 30.

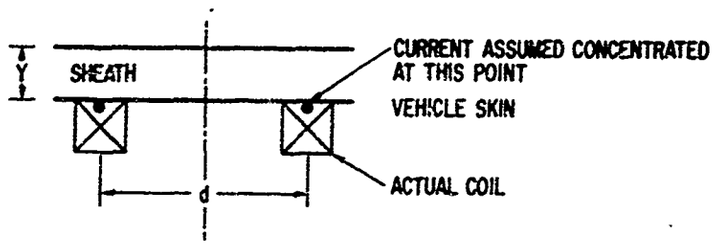

Fig. 30. Magnetic Field Calculation

This yields a relation between the number of turns and the coil current for a given coil diameter. This procedure underestimates the required ampere-turns, and is adopted primarily for consistency and ease of calculation. Conservative assumptions regarding the effect of the non-uniform magnetic field on signal attenuation should largely offset this factor. Detailed calculations indicate that actual magnet system weights will differ by less than a factor of two from those reported here.

For purposes of calculation, the weight of the coil is computed as that of the wire plus an additional 10% for structure. The power dissipated by the coil is assumed to be supplied by a battery with energy capacity of 30 W-h/lb, a conservative figure selected on the basis that a fast discharge is required. The coil is cooled by boiling water at 100°C and an additional amount of structure equal in weight to that of the water is assumed.

For a given magnetic field and coil diameter, an optimum weight system is obtained by adjusting the current and the number of turns so that the weight of coil plus structure is equal to the weight of battery plus coolant. Weight estimates are based on operation at this optimum condition. In the results to be discussed subsequently, a mean coil diameter of 4 in. has been selected to provide an adequate aperture.

b. Typical Magnet Systems

An indication of the characteristics of the required magnet systems is given by the following data for two coil systems, one of copper and another of aluminum wire, designed to limit the signal attenuation to 40 dB at a station 1 ft from the apex of a 50-deg wedge during the transient trajectory:

	No. 10 Copper Wire	No. 10 Aluminum Wire
Magnetic field at sheath edge, G	1600	1600
Magnetic field at coil center, G	2290	2290
Coil current, A	78.1	32.4
System weight, lb	17.1	12.5
Battery weight, lb	7.05	5.15

	No. 10 Copper Wire	No. 10 Aluminum Wire
Coolant weight, lb	1.45	1.06
Power dissipated, W	1905	1390
Voltage, V	24.4	42.9
Coil width (square cross section), in.	1.56	2.43
Coil mean diameter, in.	4	4
Number of turns	237	572

Although aluminum yields the lighter weight system, the effective aperture diameter is significantly less. For this reason, calculations have been based on the copper, with the realization that a more refined optimization technique will be required in the design of an operational system.

c. Results of Analysis

Figure 31 shows the magnet system weight as a function of resulting plasma signal attenuation (at 250 MHz) for conditions corresponding to a station 1 ft from the apex of 50 and 40-deg wedges for both equilibrium glide and transient trajectories. As previously indicated, these weights are based on a constant magnetic field over that portion of the trajectory during which the unalleviated attenuation exceeds the given value. These results show that a conventional magnet system is promising only if higher signal attenuations can be tolerated.

This observation leads to the consideration of benefits to be gained from a conventional magnet system and increasing the transmitter power. Selected results of this nature are shown in Fig. 32 in terms of total alleviant system weight (magnet system plus additional transmitter) vs additional transmitter weight. Results are shown for two different initial transmitter powers (1 and 10 W) and two different communication link specifications (1 W, 10 dB margin or 10 W, 20 dB margin and 1W, 20 dB margin or 10 W, 30 dB margin). The obvious conclusion here is that it is desirable to increase the transmitter power above that usually employed (between 1 and 10 W).

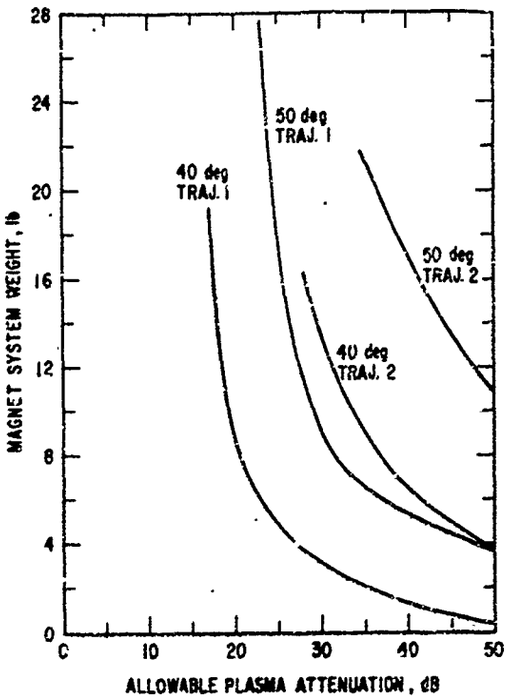

Fig. 31. Theoretical Magnet System Weight for Station 1 ft from Apex of Sharp Wedge (f = 250 MHz)

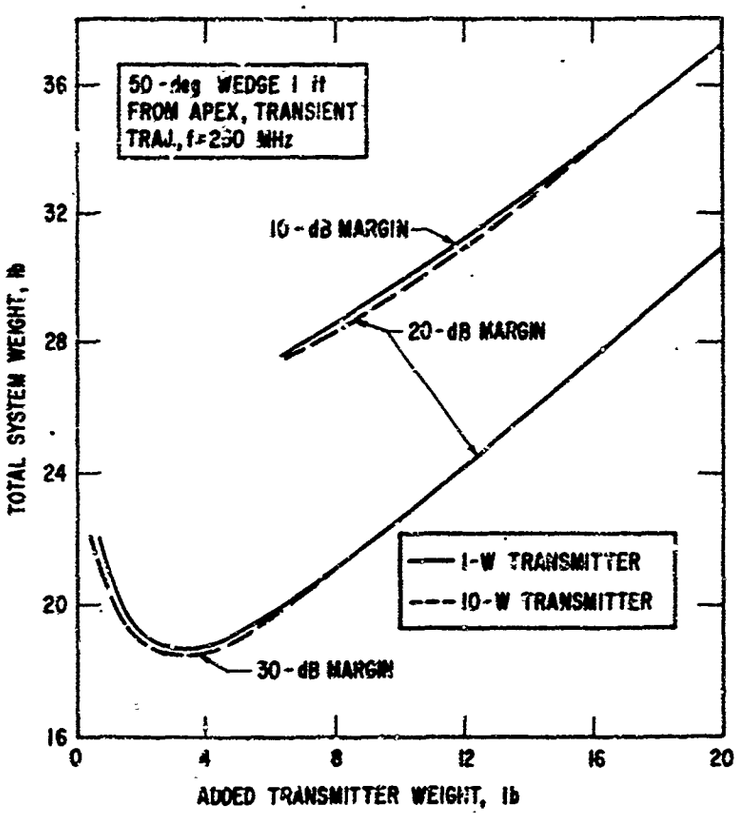

Fig. 32. Total Theoretical Magnet System Weight

In the cases examined, the optimum power level is approximately 20 W. The problem of rf breakdown (Section II-B-4) may become important at these power levels, and more research in this area is indicated. It should also be noted in Fig. 32 that, for a given penalty associated with increasing transmitter power, the potential benefits are greater for systems with lower initial powers and lower system margins. It is mentioned that at lower added transmitter weights the total system weight becomes large and is not shown in the figure

The effect of different lifting trajectories on conventional magnet system weights is presented in Fig. 33 and 34. For a 50-deg wedge at a station 1 ft from the apex, magnet system weight is presented as a function of altitude and velocity for the trajectory point that requires the maximum magnetic field. These weights are based upon maintaining this constant field for a nominal duration of 500 sec; hence, each altitude and velocity may be taken as representative of an entire trajectory. Increasing the velocity or decreasing the altitude increases magnet weights appreciably (e. g. , a decrease of 20, 000 ft in altitude or an increase in velocity from 21, 000 to 26, 000 ft/sec, at lower plasma attenuations, results in a factor of two increase in weight).

A final important result, which emerges directly from the weight estimations is that for the same initial thermodynamic conditions of the sheath, the magnet system weight requirements W scale as

$$W \sim d^2\left(1 + 4\frac{y^2}{d^2}\right)^{3/2}(t)^{1/2}$$

where d is the mean coil diameter, y is the displacement of the coil from the outer edge of the sheath, and t is the duration for which a magnetic field is required (see Volume II, Appendix G). Thus the weight penalty increases roughly as the square of the characteristic vehicle dimension. Since the vehicle weight would be expected to increase at roughly the same rate, the magnet system weight would tend to remain a constant percentage of the gross vehicle weight.

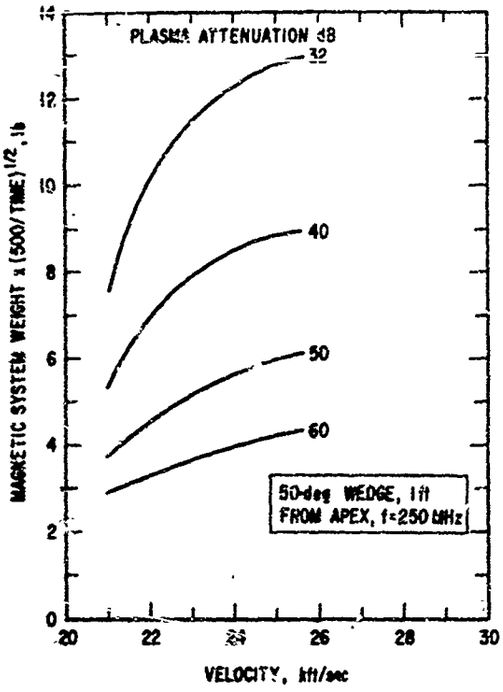

Fig. 33. Velocity Effects on Theoretical Magnet System Weight

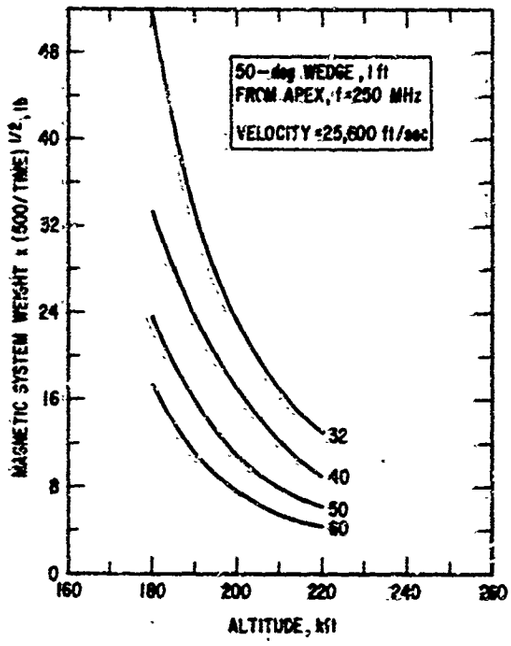

Fig. 34. Altitude Effects on Theoretical Magnet System Weight

4. AREAS REQUIRING FURTHER RESEARCH AND DEVELOPMENT

The most important area requiring further research effort in the development of a conventional magnet system is associated with a more precise determination of plasma attenuation in the inhomogeneous magnetic field produced by a coil. Such a determination will have a large influence on establishing the weight of the coil. It appears that the most promising approach for this determination would be to conduct experiments in the proper coil geometry with a laboratory-produced plasma. The objective would be to obtain the actual attenuation as a function of magnetic field strength (i.e., coil current), displacement of the coil from the plasma slab, as well as coil geometry and plasma conditions. Since it is unlikely that the reentry situation can be exactly simulated in the laboratory, a suitable scaling theory should be developed.

A second area requiring further research, closely related to the preceding one, is the determination of how small the magnetic window aperture can be made and still accommodate an efficient radiator (at an operating frequency in the vicinity of 250 MHz). The most promising approach to this problem is the experimental one of obtaining antenna characteristics in the proper coil geometry in a free-space environment. It should be noted that the importance of this area is governed by whether or not the minimum coil diameter is limited by aperture considerations, as was indeed the case in our previous weight estimates.

A third area requiring further investigation is the rf breakdown level in the presence of a magnetic field. This again requires that emphasis be placed upon producing the proper plasma conditions rather than on producing geometric simulation of the reentry situation. A basic question is whether or not it will be possible to increase the transmitted power to a level of the order of 10 W/cm^2 (400 W incident upon a 2.5-in.-diam circle) without producing breakdown.

5. USE OF SUPERCONDUCTORS

The previous discussions of weight estimates and areas for further research have been concerned solely with conventional magnet systems. A brief discussion of these factors for superconductor systems is presented here.

The major problem is estimating the weight of the coolant required to maintain superconducting temperatures (10°K). The flight system designed in Ref. 44 is not directly applicable here since the heat sinks employed were capable of maintaining these temperatures for only a few hours after launch. The utility of this type of coolant technique seems inadequate for general lifting reentry purposes, although the weight of the system (of the order of 20 lb, heat sinks included), which produces fields of 13,000 G, is certainly reasonable.

A technique of inflight cooling, more appropriate for general purposes, is also discussed briefly in Ref. 44. The tentative design therein requires 1.4 liters/h of liquid helium to maintain the proper temperature. The technique which must therefore be employed is to store liquid helium and cool the apparatus a few hours prior to reentry. The required storage container is estimated to weigh 10 lb for 5 liters of helium stored, and loses 0.5 liter of helium/day.

We therefore conclude that superconductor systems are feasible for alleviation purposes only for relatively short duration missions. Systems utilizing heat sinks as coolants are feasible only for missions of a few hours, and are almost within the state of the art. Systems utilizing inflight cooling are probably feasible for missions of a few days, but require development of flyable storage devices. The major areas requiring further development effort are the thermal design of the coil system and storage containers to minimize coolant requirements, and the problem of radiating through a small aperture.

E. COOLANT INJECTION

1. PRINCIPLE OF OPERATION

Coolant injection into the plasma sheath as a communications alleviation technique has been proposed previously (Refs. 36, 46-49), and the subsequent analysis will be substantially based on these proposals. The basic principle is that if sufficient coolant is injected into the shock layer and if the resulting mixture is brought to thermodynamic equilibrium, the resulting electron density would be low enough so that communication would be possible. It has been proposed to inject coolant into the primary shock layer (Refs. 36 and 46) or to inject it around vehicle appendages (Section II-C-4). In either case, the basic engineering consideration to confine the injectant to the minimum flow area necessary in the localized vicinity of the antenna, in order to reduce coolant requirements. We are concerned only with injection into the primary shock layer, as indicated in Fig. 35, since the use of coolant injection in conjunction with aerodynamic shaping techniques has been treated in Section III-C-4. The aim is then to produce a "window" in the sheath that has at least the dimensions of the radiating aperture.

The quality of communication that would be provided by such a system is excellent in that the operating frequency range is standard. Hence, equipment is available and weather conditions are of no consequence, and the information rate capability is not limited by plasma sheath effects.

2. ESTIMATE OF WEIGHT REQUIREMENTS

a. Coolant Selection

The first problem is the selection of the specific coolant. From a comparison[4] of representative coolants (hydrogen, water, helium, and propane) presented in Ref. 36, the energy per unit mass required to raise the temperature of the coolant from a nominal level (~300°K) to the levels of interest for

[4] Appendix H in Volume II contains this information in more detail, as well as other pertinent calculation details relevant to coolant injection

alleviation (3000° to 4000°K) decreases in the same order as the coolants are listed. Hence, from a pure thermodynamic standpoint, hydrogen is the optimum coolant. However, since gases are more difficult to contain and distribute in a flow field than are liquids, practical considerations indicate that water is probably the best choice (although hydrogen is roughly 6 times better on a unit mass basis). Therefore, we envision water as the coolant; for simplicity the calculation of the weight requirements will be based, however, upon helium. On a purely thermodynamic basis, this approximation overestimates the water requirements by approximately 20%, which is of little consequence for present considerations.

b. Calculation Technique for Minimum Requirement

The calculational technique to obtain the minimum coolant system weight requirement is described as follows. First, the mass flow ratio of injected coolant to air at a given initial state that is required to achieve a given final state of the resulting mixture is calculated. In the final state, it is assumed that the coolant is uniformly distributed in the air stream and completely evaporated, that the mixture is in thermodynamic equilibrium, and that the state has been reached by a quasi one-dimensional mixing process at constant pressure (Volume II, Appendix H). This technique is identical to that used in Ref. 36. Second, the actual amount of air to be cooled is assumed to be that flowing through a cross-sectional area having the dimensions of the inviscid shock layer thickness in the direction normal to the body surface and of one-half the inviscid shock layer thickness in the other direction normal to the flow. With the coolant to air mass flow ratio and the air flow established, the total amount of coolant required for a given body location, trajectory, and desired final mixture state can be determined. Finally, the weight of the coolant system, including storage tank, pipes, valves, etc. is taken to be twice the coolant weight.

In order to accept the results of these calculations when applied to the lifting reentry model, the validity and associated implications of the various assumptions must be assessed. The assumption that the shock layer pressure

is unaffected by coolant injection implies that the flow field geometry is unaffected also. The natural tendency of a jet aligned transverse to the shock layer flow is to raise the pressure and to increase the thickness of the layer; hence, any deviation of the actual physical conditions from those assumed will make alleviation more difficult. It appears that this deviation will be relatively small, since from the results of Ref. 50, atomized liquid jets that are capable of penetrating the shock layer do not introduce large disturbances in the flow field.

The maintenance of thermodynamic equilibrium at the antenna location is of critical importance to the success of the injection technique; it is clear that if the electron density is not reduced sufficiently rapidly, then attenuation will remain severe regardless of how much thermal cooling is accomplished. Whether or not thermodynamic equilibrium is maintained depends upon the reaction rates involved. For our purposes, the only reactions of consequence are those involving electron-ion recombination, since the ionization reaction rates drop sharply with decreasing gas temperature. For pure air recombination rates, the characteristic flow distance required to reduce the electron density to 10^{11} electrons/cc (a density at which communication is possible) is of the order of from 10 to 20 ft for our typical reentry conditions. This distance is far too great for practical purposes, and it is clear that pure air recombination mechanisms will not be sufficient. To obtain an adequate electron recombination rate, some catalytic agent must be employed. As will be more fully discussed in Section III-F, electronegative compounds that possess high electron attachment cross sections are likely candidates as catalysts. For example, calculations (Volume II, Appendix H) indicate that as little as 1% sulfur hexafluoride (or other similar electronegatives) added to the injected water would reduce the characteristic flow distance required to reduce the electron density to 10^{11} electrons/cc to the order of from 5 to 10 in. There is some evidence that the presence of water vapor alone in the air will increase the electron-ion recombination rate by an order of magnitude (Ref. 51). There is also evidence that the presence of water droplets has a catalytic effect on recombination (see Section III-F). Thus water injection

alone may be sufficient to maintain equilibrium electron density levels. In any case, reducing electron densities to their appropriate equilibrium values does not appear to be difficult, although some further research is indicated.

For any liquid coolant to be effectively utilized, it must be largely evaporated at the antenna location. The rate of evaporation is determined by the properties of the coolant, the heat transfer rate to the droplet, and the droplet size. The droplet size was estimated by the correlation of Ref. 52, which was based on experimental results utilizing jets of H_2O, CCl_4, iso-octane, and JP-5 injected transversely into air streams of velocities in the range from 100 to 700 ft/sec. The resulting droplet sizes, corresponding to an orifice diameter of 0.01 in., were in the range from 5 to 10 μ at our typical reentry conditions (Volume II, Appendix H). It should be noted that these results represent a large extrapolation in air stream velocity from the original experimental values. The time required for a given amount of evaporation was computed for initial air conditions corresponding to a 50-deg wedge at 200,000 ft and a velocity of 25,600 ft/sec and final mixture conditions at a temperature of 4000°K (Volume II, Appendix H). The results are as listed:

Evaporation Times for 10-μ Drop, msec			
Evap., %	Free molecular flow		Continuum flow at final rate
	at initial rate	at final rate	
100	0.19	0.55	0.049
90	0.10	0.44	0.038
80	0.078	0.34	0.032
70	0.062	0.27	$\leq$ 0.032

The heat transfer rates were evaluated in both free-molecular and continuum flow regimes since the mean free path is of the same order as the drop diameter. The initial rate corresponds to the rate at initial air conditions and the final rate is that at desired mixture conditions. The time required

for a droplet to traverse a distance of 1 ft in the flow direction has been estimated and results indicate that a typical time is of the order of 0.1 msec (Volume II, Appendix H). Thus it appears from the table that 80% evaporation can be attained in 1 ft, assuming that the distance required for the initial establishment of the droplet spray is of the order of from 2 to 4 in. This distance of 1 ft may be adequate for providing a reasonably well defined, cooled portion of gas over the antenna location. The subsequent calculated coolant requirements are based on the assumption of complete evaporation.

The final and probably most critical assumption involved in this calculation is that the amount of air cooled by the jet can be confined to a small cross-sectional area. To provide a feeling for the magnitudes involved, it is pointed out that results indicate that the mass flow rate of water required is of the order of 10^{-2} lb/sec, and a reasonable orifice diameter to achieve penetration of the shock layer (approximately 1 in. thick) is of the order of 10^{-2} in. Thus, the assumption here is that in a distance of approximately 1 ft in the flow direction, the breakup of the jet into sufficiently small droplets and the subsequent mixing and evaporation processes will yield a reasonably uniform mixture of water vapor and air of lateral dimensions of at least one-half the shock layer thickness. Further, it is assumed that the amount of air flowing in the mixed region is no greater than that flowing in a stream tube of the undisturbed flow having dimensions of the sheath thickness by one-half of the sheath thickness.

To assess the validity of these assumptions, a qualitative description of the flow field is given. This flow field is depicted in Fig. 35 and is based on information contained in Refs. 50 and 53. The jet issues from the orifice in the usual manner, since the coolant velocity is not sufficient to cause immediate breakup of the jet into droplets. The ambient pressure is somewhat greater than the initial vapor pressure of the liquid. The action of the high-velocity air stream on the jet creates the blast wave effect in the shock layer near the vehicle surface, wherein the turbulent wake contains droplets formed by shear on the jet. In the outer portion of the shock layer, the remainder of the jet is broken up into droplets by the air stream. Subsequent to this breakup,

droplet evaporation and mixing occur. Quantitative estimates of the processes are difficult to make. In the inner portion of the shock layer, the width of the turbulent wake can be estimated as that due to flow about a circular cylinder. In the absence of evaporation, this is of the order of 12 jet diam at an axial distance of 100 diam from the orifice (Ref. 54). For our typical situations, this would amount to a lateral spreading of only 0.12 in. at a distance of 10 in. from the orifice. In the outer portion of the shock layer, the trajectory of a single droplet of given initial velocity can be easily estimated, again assuming no evaporation. A typical calculation (Volume II, Appendix H) indicates that a 10-μ drop with an initial lateral velocity of 150 ft/sec in an air stream of 15,000 ft/sec will suffer a lateral deflection of somewhat less than 0.4 in. in traveling 1 ft in the direction of the stream. Neither of these estimates indicates that the lateral spreading of the jet will be more severe than assumed. The largest unknown is, however, the lateral velocities that the droplets are likely to acquire due to the breakup process. This breakup process is quite complex (Ref. 55), but some qualitative evidence exists that the droplets may achieve significant lateral velocities (Ref. 56).

The preceding considerations have neglected the evaporation process. If indeed the pressure field is largely undisturbed by the jet and the process occurs at nearly constant pressure, then the flow area of the air-water vapor mixture will expand by about a factor of ten. This tends to make the assumption regarding the amount of air to be cooled pessimistic. If the mixing process could be confined to an air stream that is initially one-half of the shock layer thickness in lateral extent, subsequent evaporation would cause the resulting mixture to have a lateral extent an order of magnitude greater (approximately), and thus the cooled mixture would cover more area than is necessary. Although allowance has not been made for this effect, it should be partially offset by the assumptions made regarding the lateral extent of the initial liquid spray.

Quantitative evidence regarding the overall jet mixing process is presented in Ref. 50. These data are for both water and liquid nitrogen injected into an air stream of Mach 8 about blunt bodies. The lateral extent

of the liquid drops tends to equal the penetration distance normal to the body. In view of these data, the assumption of one-half of this lateral extent appears optimistic. However, it should be realized that the contemplated geometry and flow conditions are not similar to this experimental situation. Specifically, in the latter situation the effects of vehicle nose bluntness are dominant, and the flow is axisymmetric. Both of these features are appreciably different from the situation to be encountered around lifting vehicles, and it is conceivable that lateral spreading would be less.

The preceding considerations, viewed collectively, help to validate the basis on which the coolant requirements have been estimated. More research is indicated before a better evaluation can be made.

c. Results of Analysis

Figure 36 shows the coolant system weight requirements as a function of resulting plasma signal attenuation (at 250 MHz) for initial plasma conditions corresponding to a station 1 ft from the apex of 50- and 40-deg wedges for both equilibrium glide and transient trajectories. Also shown are the weight requirements for initial plasma conditions corresponding to stagnation point conditions for a 3-in. nose radius for the transient trajectory. A modification in the calculation technique was necessary in that the representative shock layer thickness was taken as twice the shock detachment distance and the air to be cooled was based on a projected area normal to the freestream of 4 in. × 1/2 in. (to accommodate a 6-in. slot antenna). The coolant requirements are based upon a constant flow rate for the time during which the uncooled plasma attenuation exceeds the desired level. This constant rate is taken as the maximum required by any point on the trajectory. This yields a greater coolant requirement than if the flow rate were varied along the trajectory to maintain a fixed level of attenuation at every point; e.g., for the 50-deg wedge on the transient trajectory, the variable flow rate requirement is less than the constant one by a factor of two. Whether the potential weight saving outweighs the increased complexity of a variable flow rate system requires a more detailed evaluation. It is evident from Fig. 36 that the coolant

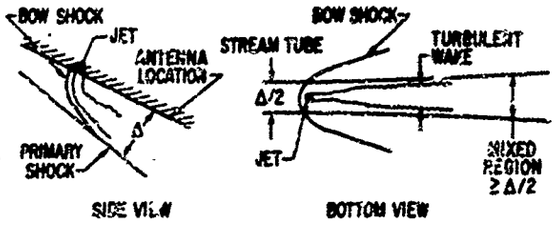

Fig. 35. Schematic Representation of Coolant Injection

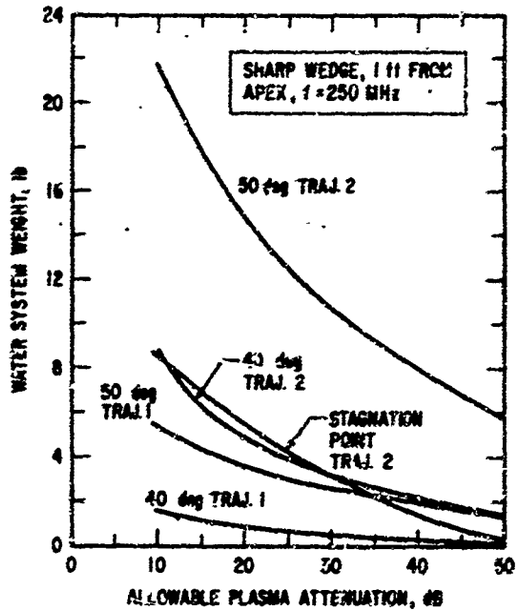

Fig. 36. Coolant System Theoretical Weight Requirements

requirements are quite reasonable from a weight standpoint. The trends exhibited by the different trajectories and shapes follow the expected pattern, with the possible exception of the stagnation point results. These indicate a lesser weight requirement than the 50-deg wedge case because the more forward position of the antenna results in thinner sheaths and less air to be cooled.

The weight requirements for a combination of coolant injection and transmitter power amplification are shown in Fig. 37 in terms of total alleviant system weight (coolant system plus additional transmitter) vs additional transmitter weight. Results are shown for two initial transmitter powers (1 and 10 W) and two communication link specifications (1 W, 10-dB margin or 10 W, 20-dB margin and 1 W, 20-dB margin or 10 W and 30-dB margin). The conclusion is that it is desirable to increase transmitter power above that usually employed (between 1 and 10 W). For the case examined, the optimum power is approximately 50 W. The preceding results all considered a fixed signal frequency of 250 MHz. Figure 38 indicates the effect on the transient trajectory of changing the signal frequency on the coolant system weight requirements for the 50-deg wedge, 1 ft from the apex. The effect of different lifting trajectories on coolant requirements is presented in Figs. 39 and 40. For a 50-deg wedge at a station 1 ft from the apex, coolant system weight is given as a function of the maximum coolant flow rate. These weights are based upon a constant flow rate for a duration of 500 sec; hence, each altitude and velocity may be taken as representative of an entire trajectory. As shown, increasing the velocity or decreasing the altitude increases coolant requirements appreciably (e.g., either increasing the velocity from 21 to 26 kft/sec or decreasing the altitude by 20,000 ft results in roughly an increase by a factor of two in the coolant requirements).

A final result, which emerges directly from the analysis, is that the coolant weight requirements increase approximately as the square of the sheath dimension and the duration of the blackout period. Thus the weight penalty increases rather sharply with vehicle size, so that the coolant system weight penalty tends to remain a constant percentage of the gross vehicle weight.

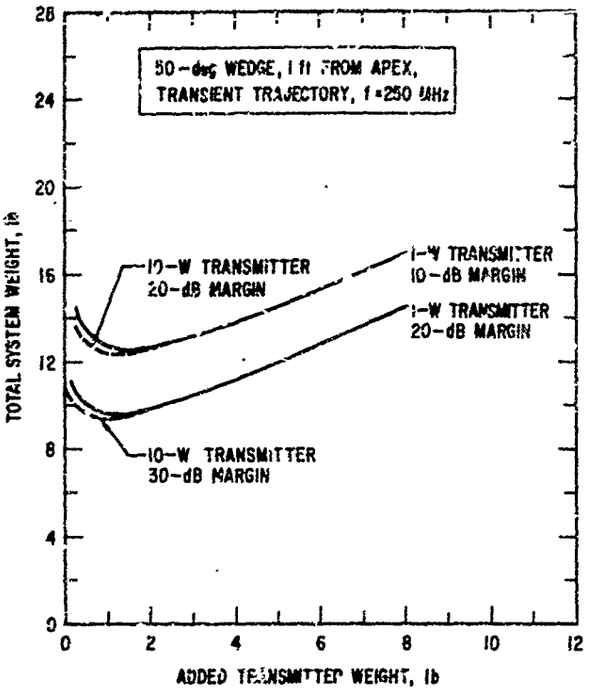

Fig. 37. Total Coolant System Theoretical Weight

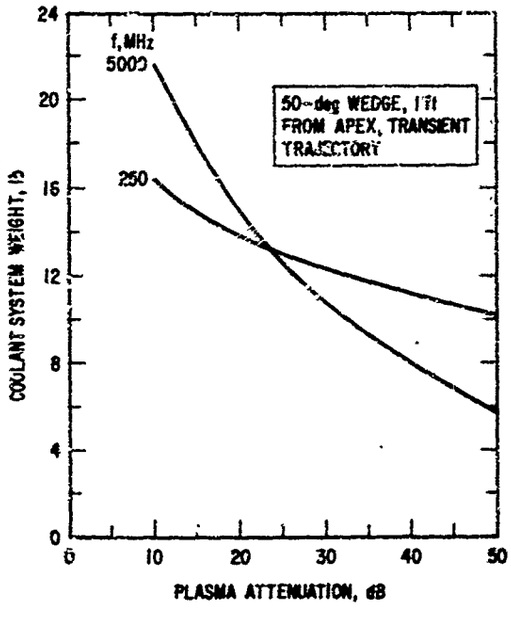

Fig. 38. Coolant System Theoretical Weight at Two Signal Frequencies

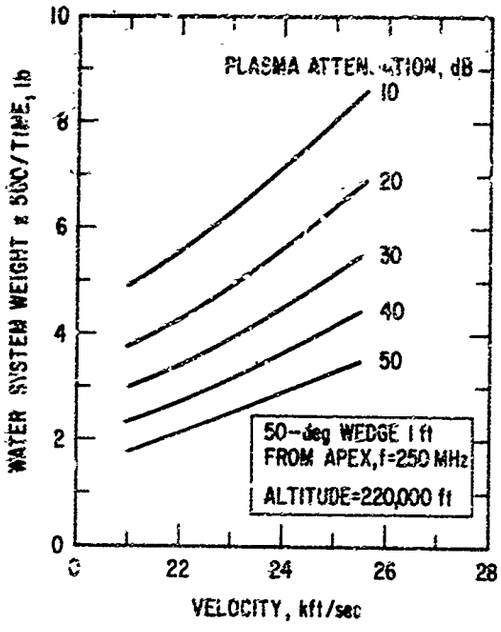

Fig. 39. Velocity Effects on Coolant System Theoretical Weight

Fig. 40. Altitude Effects on Coolant System Theoretical Weight

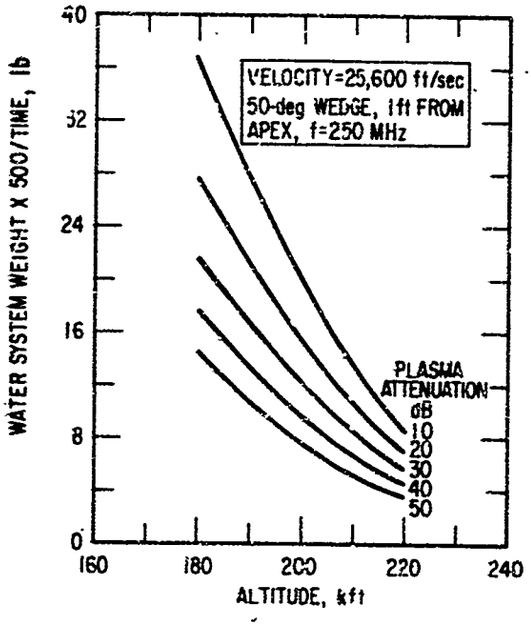

3. AREAS REQUIRING FURTHER RESEARCH AND DEVELOPMENT

As the previous discussion has indicated, the central problems in the development of the coolant injection technique are all associated with obtaining a desirable distribution of the water vapor-air mixture (i.e., a distribution that maximizes the lateral extent of the cool mixture for a given amount of injection) at the antenna location. The following paragraphs contain a discussion of the type of effort required to resolve these problems.

Further effort is required concerning droplet size, velocity, and spatial distribution of the liquid spray in the early stages of the breakup of the jet, since these properties provide the initial conditions for the subsequent evaporation and mixing processes. This information is best obtained by experimental simulation of both geometry and flow conditions. Unfortunately, exact simulation in laboratory facilities does not appear possible. Thus, an investigation such as that reported in Ref. 50, suitably modified to incorporate the correct geometry and expanded to include more definitive measurements of droplet distributions, would be a reasonable approach. In conjunction with this, it would be necessary to develop an adequate scaling theory. An alternative experimental approach would be to simulate the important geometrical properties of the flow field (primarily, an essentially nonexpanding flow) at flow conditions that very closely approximate the desired conditions. This might be accomplished in a shock tube; again, a scaling theory would be required. The points to be emphasized are that the investigation should be centered on experiment and that the geometrical properties of the flow should be properly simulated.

Further research is needed in the study of the evaporation and mixing process that occurs subsequent to the initial formation of the spray. Again, the investigation should be experimentally oriented, and the geometrical properties of the flow field should be simulated. It is in fact very likely that the same experimental facilities could be employed. A subsidiary investigation of the evaporation rate of droplets would be desirable, due to the intermediate nature (i.e., noncontinuum and not free-molecular) of the flow.

In this case, greater emphasis should be placed on simulation of flow conditions than on geometry.

Further effort should be devoted to establishing the time (or distance) required for the electron density to equilibrate in the presence of the injected water. The basic problem is whether the presence of water droplets and vapor is a sufficient catalyst for the recombination process, or if an electronegative additive is necessary. Once again the investigation should be based on an experimental approach and the emphasis should be placed on duplicating thermodynamic conditions rather than flow geometry.

Further investigation is required concerning the size of the alleviated area over the antenna needed for effective transmission; this problem is also common to some other alleviation techniques.

F. OTHER INJECTION TECHNIQUES

1. GENERAL CONSIDERATIONS

Several mechanisms other than cooling have been proposed as bases for injection schemes to reduce plasma attenuation. These include the tendencies of free electrons to precipitate on dust, of electronegative gases to form negative ions by electron attachment, and of certain chemicals to combine with oxygen or nitrogen, thereby reversing the reaction $N + O \rightleftharpoons NO^+ + e$ responsible for the high electron densities in air at reentry conditions. As indicated by aerodynamic analysis (Section II-A-3) we are concerned primarily with nonexpanding flows in thermal equilibrium. In such a situation, these processes can be effective only if they shift the equilibrium composition so that the equilibrium electron density is lower than the blackout level. Consequently, thermodynamic analyses can be used to evaluate these mechanisms.

Of special interest is the case where the electron density is higher than that associated with local thermodynamic equilibrium. This case may occur after coolant injection (Section III-E) or in the flow around the afterbody (Section III-G). In this situation, it may be sufficient for the injectant to merely increase the rate of approach to a desirable equilibrium. The

mechanism for this process is discussed in this Section, and the details of its application as a part of other alleviation techniques are discussed in applicable sections.

2. EQUILIBRIUM FLOWS

a. Dust Injection

It is assumed that the dust consists of micron-sized spherical particles that capture incident electrons and give up electrons to incident ions (Ref. 57). At equilibrium of this "dust plasma," the configuration may be thought of as a collection of floating probes, and the electron density is depleted in spheres with radii larger than the particle radius by a Debye length. Since the Debye length is of the order of or less than a micron at the densities and temperatures of interest, the depleted spheres are at best about 10 times larger in volume than the particles. This indicates that for each 10 cc of quenched plasma 1 cc of dust material is required, with a weight of at least 1 g. This consideration is sufficient to disqualify the scheme without further analysis, since less than a milligram of water has the same effect.[5]

b. Electronegative Gas Injection

The effectiveness of an electronegative atom or molecule in reducing the equilibrium electron density of air is determined by the magnitude of its electron affinity, which is defined as the difference in energy between a free electron and a captured electron in electron volts -- the higher the electron affinity, the higher the probability of electron attachment. Since the highest known electron affinities approach 4 V, we can optimistically evaluate this scheme by calculating concentrations of 4-V electronegative gases required to reduce electron concentrations to satisfactory levels. Calculations of this nature usually involve complicated computer programs, but if the only

[5] Since previous considerations of water as a coolant (Section III-E) indicate that water will quench an amount of air equal to its weight (approximately), 10 cc of air at reentry conditions (weight, 10^{-4} g) can be quenched by 0.1 mg of water.

information required is the electron density reduction factor as a function of electronegative concentration and temperature, it is possible to derive a simple formula. This formula indicates that rather high concentrations are required to achieve significant quenching. The formula is derived in Volume II, Appendix I, and the results for reduction of the plasma frequency by a factor of six are given in the following table. (Note that these results are independent of pressure to a good approximation.)

Temperature, °K	4-V Species Concentration/cc
2200	1×10^{15}
3300	1×10^{18}
4400	5×10^{19}
5500	6×10^{20}
6600	7×10^{21}

The factor of six reduction of the plasma frequency is a reasonable minimum requirement for an alleviation scheme, since the aerodynamic analysis of lifting reentry indicates plasma frequencies of 55 GHz. Considering that reentry temperatures are typically in the 5500 to 6600°K range and that typical coolant requirements to achieve communication are about 10^{16} to 10^{17} particles/cc,[6] we conclude that the electronegative injection scheme is unsatisfactory because its weight requirements are several orders of magnitude higher than those of the coolant scheme discussed in Section III-E.

c. Chemical Injection

The requirement is that the injected material have a high affinity for oxygen or nitrogen if it is to work and that it have a molecular weight of the order

[6]This estimate is based on a typical air density of 10^{16} to 10^{17} particles/cc ($\rho/\rho_0 \approx 10^{-3}$, 10^{-2}).

or less than that of water if it is to be competitive (since at least one molecule will be required for each O atom, and O atoms compose approximately 30% by weight of the air at reentry conditions). On these bases, the leading candidate is carbon. Equilibrium configurations for carbon-air mixtures have been calculated by Clifton (Ref. 58) as part of a program designed to study the effects of ablation products. Typical results are given in Fig. 41. The results for other pertinent pressures are similar. The complete study indicates that carbon does retard the production of NO^+, but this effect is offset by the production of C^+. It is concluded that this injection scheme is unsatisfactory because it is useless above 4000°K.

It should be noted that the preceding analysis is for pure carbon injection. Similar calculations have been made for Teflon (Ref. 59), which is also unsatisfactory because of the production of CF^+. It is difficult to conceive of other candidates for chemical injection schemes, but the considerations listed indicate that such schemes for blackout alleviation are not very promising from even a thermodynamic standpoint, apart from practical injection problems.

3. NONEQUILIBRIUM FLOWS

a. Electronegative Gas Injection

It has been found experimentally (Ref. 60) that relatively small amounts of electronegative gas (SF_6) are capable of rapidly reducing very high electron densities (10^{12}/cc) in argon at low temperatures (700°K). A general theory that is consistent with these specific results is developed in Volume II, Appendix I. The theory indicates that if moderate amounts of electronegative gases are injected into superionized air, the electron density will decay exponentially to its equilibrium value, and the relaxation time is given by the inverse of the product of the effective cross section for attachment, the electron thermal velocity, and the concentration of the electronegative gas. The application of this mechanism to blackout alleviation is discussed in the Sections on coolant injection (Section III-E) and expanding flows (Section III-G).

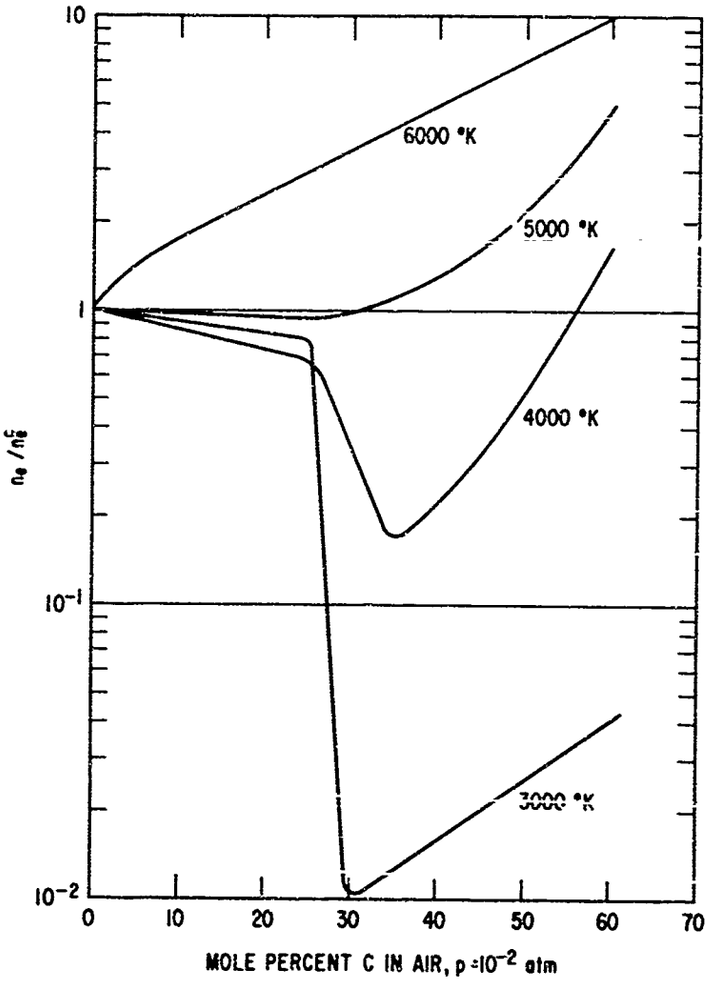

Fig. 41. Relative Electron Concentration in Air as a Function of Carbon Mole Percent

b. Solid or Liquid Particle Injections

Another possible process for driving nonequilibrium flows to equilibrium is the injection of solid or liquid particles to absorb electrons. The effectiveness of such particles, measured by the ratio of effective cross section to weight, is inversely proportional to the particle radius. A reasonable minimum particle size is a micron, indicating an effectiveness of about 2×10^3 cm^2/g if the material is assumed to have a specific density of 1. The cross section for attachment of an SF_6 molecule is about 10^{16} cm^2, and this leads to an effectiveness of about 5×10^5 cm^2/g. It is concluded that electronegative species with high attachment cross sections are orders of magnitude more effective than solid or liquid particles in the reduction of nonequilibrium electron densities.

G. EXPANDING FLOWS

1. BASIC CONCEPT

The previous discussions have emphasized alleviation techniques suitable for nonexpanding flows for reasons detailed in Section II-A-2. In this Section, brief consideration is given to expanding flows, such as occur over the afterbodies of lifting vehicles. For present purposes, an expanding flow is defined by a sequence of two events: the freestream flow is compressed by the bow shock of the vehicle and then it expands isentropically to a lower pressure level determined by the vehicle shape and angle of attack. This definition represents a good approximation for streamlines in the inviscid shock layer.

As previously indicated, the most common occurrence of expanding flows is over the vehicle afterbody, and it is this type that will be examined. Specifically, the situation considered is indicated by the sketch of a typical lifting reentry vehicle shown in Fig. 42. The concept is to locate the antenna on the uppermost, forward position of the vertical stabilizer and to require that the vehicle design be such that the boundary layer flow originating on the windward side of the body will not pass over the antenna location at any angle of attack that the vehicle will assume during reentry ($\leq$50 deg). Some

typical streamlines indicating this situation are sketched in Fig. 42. This requirement is dictated by the desire to eliminate the effect on communication of the contaminated boundary layer formed on the windward side (see Section II-A-3).

As an example of this concept applied to another shape, Fig. 43 shows schematically the different flow regions around a lifting elliptical cone and how stabilizers could be designed to satisfy the communications requirement. The cross-hatched area of the stabilizers indicates the antenna location that will prevent the windward side boundary layer from reaching the antenna.

2. ATTENUATION ESTIMATES FOR EXPANDING FLOWS

a. Equilibrium Flow Results

The plasma conditions representative of the expanded flow region about the stabilizers have been computed on the basis of the freestream flow passing through the shock associated with a 50-deg wedge and expanding isentropically to a pressure between 1 and 10 times the ambient pressure. This ratio of final pressure to ambient pressure (denoted by p_r) is determined by the vehicle shape and attitude; values of 1 and 10 bracket the actual pressure range to be expected. These calculations have been made on the basis of thermodynamic equilibrium, and typical results are indicated in the following table for selected points along the transient trajectory. Attenuation estimates have been made on the basis of a sheath thickness of 2 ft at the antenna location.

Altitude, kft	Velocity, kft/sec	f_p/f				Attenuation, dB			
		f = 250 MHz		f = 5000 MHz		f = 250 MHz		f = 5000 MHz	
		$p_r = 10$	$p_r = 1$	$p_r = 10$	$p_r = 1$	$p_r = 10$	$p_r = 1$	$p_r = 10$	$p_r = 1$
240	25.6	5.6	0.8	0.3	0	150	11	0	0
240	25.6	20.0	2.0	0.9	0.1	550	42	10	0
200	23	12.0	0.6	0.6	0.3	350	0.1	1.3	0
200	21	6.8	0.2	0.3	0	190	0	0	0

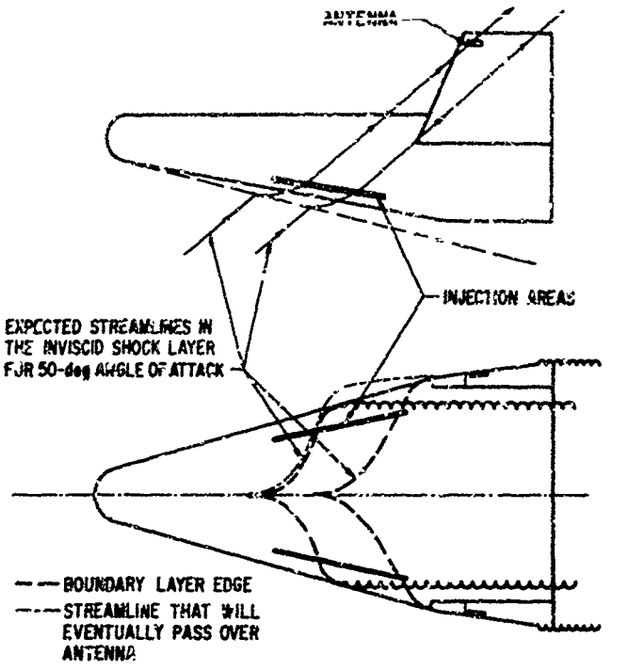

Fig. 42. Typical Lifting Reentry Vehicle

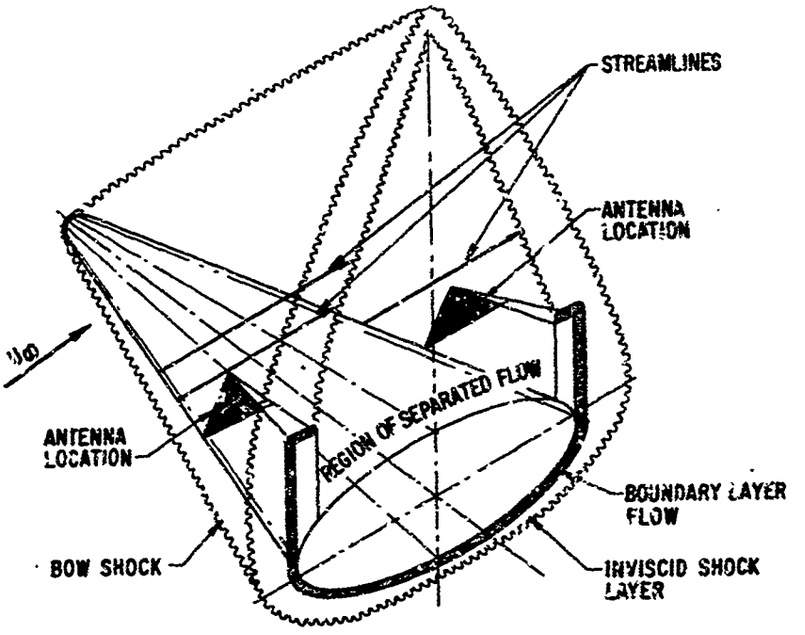

Fig. 43. Three-Dimensional Sketch of Flow Field Around Reentry Vehicle

From these results, it is concluded that communication is possible at frequencies of 5 GHz or higher, provided that the flow is in equilibrium.

b. Nonequilibrium Flow Effects

The importance of chemical nonequilibrium effects in this type of expanded flow has been assessed by a simple recombination rate analysis (detailed in Volume II, Appendix I in connection with electronegative effects). Following a volume element along a streamline, the electron density $n_e(t)$ is given by

$$n_e(t) = \frac{n_e(0)}{1 + \alpha n_e(0) t}$$

where α is the recombination coefficient for air ($2.96 \times 10^{-5}\ T^{-1}\ cm^3/sec$) and $n_e(0)$ is the electron density immediately behind the shock. With an average temperature of approximately 4000°K, over 1 msec will be required for the plasma to reach the equilibrium in the cases cited in the previous table. This time is quite insensitive to the initial electron density. During this time, a volume element will be convected more than 18 ft downstream of the shock, and hence the electron density at the antenna location will be higher than the equilibrium value. An upper bound to this electron density can be estimated by assuming completely frozen flow during the expansion process. The results of such a calculation are tabulated for a final to ambient pressure ratio of 10.

Altitude, kft	Velocity, kft/sec	n_e, particle/cc	f_p, GHz
240	25.6	2.8×10^{11}	5
200	25.6	1.3×10^{12}	11
200	23	9.1×10^{11}	10
200	21	6.1×10^{11}	7

These considerations indicate that for the proposed concept to be generally applicable to lifting reentry, it is necessary to ensure that equilibrium electron densities are obtained.

3. USE OF ELECTRONEGATIVES AS RECOMBINATION CATALYSTS

As has been indicated in Section III-F, electronegatives are effective electron recombination catalysts, and their possible application to the proposed concept has accordingly been examined. Specifically, the amount of sulfur hexafluoride SF_6 required to bring the plasma to equilibrium in a time of the order of 200 μsec (in order that equilibrium prevails at the antenna location) has been estimated. The type of analysis that has been employed is detailed in Volume II, Appendix I. The electron density as a function of time is given by

$$n_e(t) = n_e(0) \exp(-\sigma_a \bar{c}_e n_s t)$$

where $\bar{c}_e$ is the mean thermal speed of the electrons, σ_a is the electron attachment cross section of SF_6 ($\sim 10^{-16}$ cm^2), and n_s is the number density of SF_6. For the points previously selected along the transient trajectory, this relation indicates that a number density of SF_6 molecules of 5×10^{12}/cc should be adequate to produce equilibrium electron densities at the antenna location (again, this value is relatively insensitive to the initial electron density).

The weight of SF_6 required for the trajectory can easily be estimated, knowing the number density required. The following table indicates the mass flow rate of SF_6 required to properly seed 1 ft^2 of the incoming flow at four points along the transient trajectory.

Altitude, kft	Velocity, kft/sec	$\dot{m}_{SF_6}$ lb/ft^2-sec
240	25.6	0.98×10^{-4}
200	25.6	4.0×10^{-4}
200	23.0	2.5×10^{-4}
200	21.0	1.5×10^{-4}

The amount of oncoming flow to be seeded is of course a function of the vehicle size, but the mass flow requirements are sufficiently small to ensure that the total weight is reasonable (less than about 5 lb of SF_6). Hence, the proposed concept is considered feasible.

4. AREAS REQUIRING FURTHER RESEARCH AND DEVELOPMENT

A major aspect of further investigation is the delineation of vehicle requirements that will provide the proper expanding flow field. Wind tunnel testing of stabilizer-body combinations is indicated to establish conditions for a maximum expansion ratio over the fin and proper separation of the vehicle body boundary layer.

Further investigative effort is also required in injection techniques (particularly those involving gases). Configuration testing is therefore also required, since the process is sensitive to vehicle geometry and injection site.

Finally, the chemical kinetics of electronegatives in nonequilibrium high-temperature air should be investigated in order that the total effect may be ascertained both qualitatively and quantitatively.

H. HIGH FREQUENCY BAND COMMUNICATION

1. BASIC CONCEPTS

It has been previously observed that as the signal frequency is lowered, the plasma attenuation at typical reentry conditions approaches an asymptotic value that is appreciably lower than that which exists for conventional

frequencies (Ref. 61). The general frequency dependence of the plasma attenuation in a typical lifting reentry situation is shown in Fig. 44, which has been constructed from the plane wave calculations dicussed in Section II-B-1. The attenuation at low frequencies is anywhere from 40 to 360 dB less than that in the frequency range from 250 to 10,000 MHz. These results suggest the use of a signal frequency in the hf band (3 to 30 MHz) to take advantage of the reduced attenuation. This technique has been proposed previously (Ref. 33).

In this frequency range, the plasma skin depth is of the same order as the sheath thickness (for typical lifting reentry conditions, the skin depth and sheath thickness are approximately equal at a frequency of 1 MHz). This suggests that by a judicious selection of antenna configuration it may be possible to achieve attenuations less than the plane wave values by reducing the amount of reflection and, perhaps, absorption. This consideration has led to the proposal of a loop antenna configuration (Ref. 62).

In this Section, the potential hf band systems will be assessed first by considering the requirements placed on a system assuming that the plane-wave attenuation figures are representative. Then, the accuracy of the plane-wave attenuation will be examined for a typical case to ascertain if substantial improvements in system performance can be expected.

2. PERFORMANCE CONSIDERATIONS

The performance of a state-of-the-art hf band system can be estimated readily from the typical free space system margins discussed in Section II-D. This performance is presented graphically as a function of frequency in Fig. 23. By deducting the plasma attenuation shown in Fig. 44 from the free space margin in Fig. 23, the operating system margin is obtained. The maximum operating system margin that results is -45 dB. This can be increased to zero by increasing the transmitter power, decreasing the receiver bandwidth from the values used in Fig. 23 (1 W and 300 GHz, respectively) or both. The maximum practical transmitter power is approximately 100 W, since the considerations of Section II-B-4 indicate that this is

of the order of the breakdown threshold in the hf band. This improves the operating system margin by 20 dB, and the remaining 25 dB improvement must be obtained by decreasing the receiver bandwidth from 300 to 1 GHz. The resulting curve of hf operating system margin is shown in Fig. 45.

To evaluate the accuracy of the plane-wave attenuation estimates, additional calculations have been performed for a loop antenna with an operating frequency of 10 MHz surrounded by a thin overdense spherical plasma. The spherical plasma has been assumed to be 1 m in diameter and is characterized by $\nu\lambda_0\omega/\omega_p^2 d = 6.9 \times 10^{-3}$ (see Section II-B-1 for definition of symbols), corresponding to plasma conditions at the maximum attenuation point for a station 1 ft from the apex of a 50-deg wedge on the transient trajectory. These calculations (performed by the procedure of Ref. 62) yielded a plasma attenuation of 48 dB, compared with the plane-wave result of 53 dB. Since the calculations neglected changes in antenna impedance, which would add to the attenuation, it would appear that the plane-wave attenuation is an adequate approximation.

From the system margin results shown in Fig. 45, it is concluded that a 100-W hf system can communicate during reentry but at a very limited information rate. This rate, plus the additional considerations that breakdown may be a problem and that the size of the transmitting antenna required precludes the use of any other alleviant technique in combination, indicates that the hf system is not of general applicability for lifting reentry purposes.

I. QUASI-OPTICAL AND OPTICAL SYSTEMS

1. GENERAL CONSIDERATIONS

As indicated in Section II, the signal attenuation due to the plasma can be reduced to negligible levels by using frequencies that exceed the plasma frequency of the ionized air flow. An examination of the ionization levels associated with lifting reentry indicates that such signals must be characterized by frequencies greater than 50 GHz, corresponding to wavelengths considerably less than 1 cm.

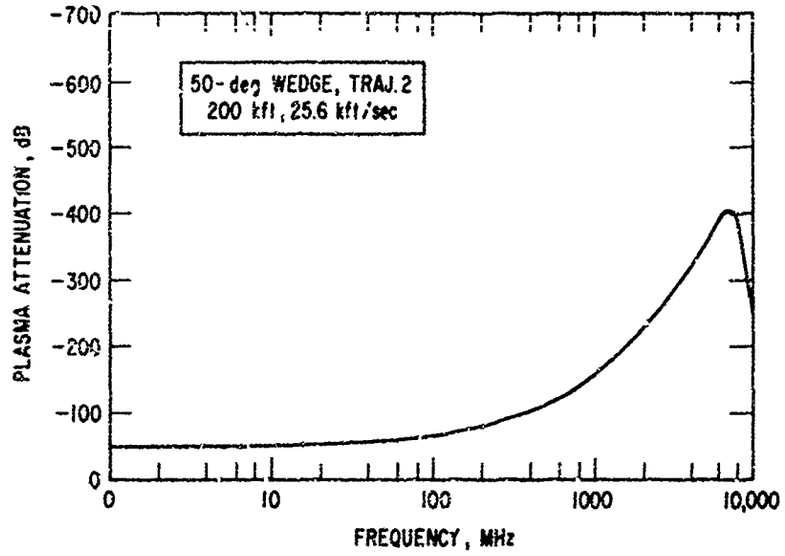

Fig. 44. Plasma Attenuation

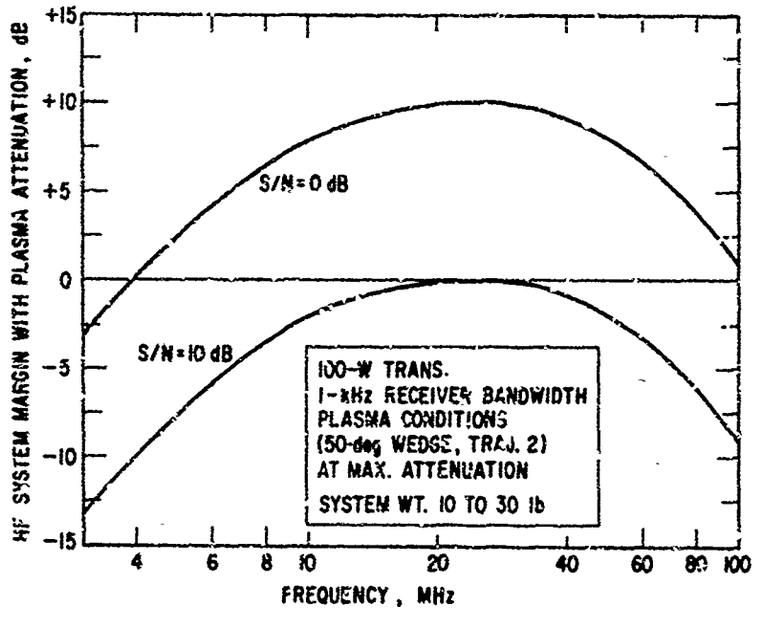

Fig. 45. High Frequency System Margin

Communications systems operating at frequencies above 50 GHz are still in the experimental stage, and device capability does not compare favorably with that of analogous microwave devices. For this reason, a fair evaluation of such systems must allow for considerable improvement in devices in the near future, but it must be tempered by a recognition of permanent obstacles to communication at short wavelengths such as atmospheric absorption, weather sensitivity, and noise. At the present time, the structure of laboratory research activity indicates that the leading candidates for near-future practical systems are those operating in the millimeter range of the spectrum (quasi-optical) and those operating in the micron region of the spectrum (optical). Since different technologies are involved, these two types of systems are treated as separate subjects.

2. QUASI-OPTICAL SYSTEMS

Until recently, the millimeter region of the electromagnetic spectrum has not been explored, probably due to discouraging experiences with water-vapor absorption during World War II. In the past several years, however, the discovery of atmospheric windows and the possibility of space applications have stimulated considerable effort in device development and refinement of knowledge of propagation characteristics in this region of the spectrum. Several reviews of the state of the art have been presented recently (Refs. 63-66), and it appears that the development of practical communications systems is near and that these systems will be competitive with optical systems that are either operational or in the design stages. Although reentry communication is frequently mentioned as a likely application, the requirements for a system have not been defined, but it is now possible to do so to the extent required by our preliminary evaluation criteria.

Current capabilities of receivers in the millimeter region are given in Ref. 63; the present status of millimeter wave sources is described in Ref. 66. These references indicate that the most promising region of the millimeter spectrum for reentry communications is between 50 and 100 GHz, since device capability deteriorates drastically with increasing frequency.

Ambient noise estimates are given in Ref. 63, and atmospheric attenuation data are given in Ref. 67. The noise level is lowest in the vicinity of 95 GHz, which also corresponds to a very sharp minimum in atmospheric attenuation (less than 1 dB). It is concluded that 95 GHz represents a near-optimum operating frequency for a millimeter communications system.

An experimental ground-to-ground communications system operating at 95 GHz has been developed by the Electronics Research Laboratory of the Aerospace Corporation, and it is on the basis of this research that a hypothetical reentry system is evaluated.[7] Systems calculations are presented in Volume II, Appendix J.

The calculations indicate that to obtain an output signal with a signal-to-noise ratio of 10 dB, a state-of-the-art receiving system requires that the signal power intercepted by the antenna be 5×10^{-13} W. This value is based on a bandwidth of 3×10^{5} Hz for the modulated signal, an estimated noise figure of 16 dB, and a noise temperature of 290°K. If there were no losses, a power of 9 mW emitted by an isotropic radiating system on the vehicle is sufficient to achieve a range of 100 miles with a 200-ft^2 receiving aperture. With system and atmospheric losses of 10 dB, the transmitter power required for a clear weather system is 90 mW. Such a transmitting system that could operate in a reentry environment does not now exist, but it is likely that a system could be developed with a weight penalty of less than 20 lb.

The system described is somewhat sensitive to cloud cover (estimated maximum attenuation is 5 dB) and very sensitive to rain (estimated maximum attenuation is from 20 to 30 dB). It is quite conceivable that an advance in the state of the art will result in a capability for an all-weather system. The conclusion is that a 3-mm system is a likely near-future solution to the blackout problem but that at present time the complicated equipment required at receiving sites (Ref. 65), weather sensitivity, and marginal performance of systems based on present technology are important factors to be considered in comparisons with other solutions.

---

[7] Discussions with Dr. B. J. DuWaldt of the System Analysis Laboratory are gratefully acknowledged.

3. OPTICAL SYSTEMS

The recent discovery that gallium-arsenide semiconductor devices (injection lasers) can be used to convert dc currents directly into narrow-band radiation at 8420 Å has stimulated the development of optical communications systems. One system (Ref. 68) using such a device with a 5-mW output has been used to transmit television signals over a distance of 30 miles under advantageous background conditions. Another system (Ref. 69) with a peak power output of 22 W, average power of 1 mW, and a total weight of 6 lb has been designed to transmit voice signals from an orbiting vehicle to a ground station. In the latter system, target acquisition and tracking, which is the major difficulty in the concept of narrow-beam space communication, is handled visually and manually by an astronaut (the required pointing accuracy was ±0.7 mrad). Similar experimental systems are mentioned in a state of the art summary by J. P. Gordon (Ref. 70), who concedes that the potential competition of millimeter systems is strong but without obvious advantages for many applications. At this stage, even crude comparisons may be premature, but we will attempt a comparison for the reentry situation, basing device capability estimates on reported research experience.

The use of injection lasers in space has been discussed in detail by C. M. Johnson (Ref. 71) and B. S. Goldstein and J. D. Welch (Ref. 72). It was stressed that these diodes will be useful because they are of small size and weight, they are capable of emitting hundreds of watts of peak power, they can convert dc power to radiated power with efficiencies approaching 50% at 77°K, and they can be modulated directly by varying the input current. Calculations were presented which indicate that long-distance communication is feasible if the transmitted beam can be pointed with milliradian accuracy. Here, we will investigate the feasibility of optical systems as reentry blackout alleviants. For this purpose, calculations have been made that are similar to those referred to above, except that account has been taken of the background radiation due to the re-entering vehicle and an omnidirectional radiating system has been assumed for the purpose of comparison with other systems.

The optical system calculations are given in Volume II, Appendix J. Considerable range advantage is gained by pulsing, and a pulse-length of 10 nsec has been chosen. A pulse repetition frequency of 10^5/sec provides an information rate comparable with the systems described in previous Sections of this report. To obtain a signal-to-noise ratio of 10 at the output of a photomultiplier circuit, the peak signal power at the input of the receiving system must be 3×10^{-8} W if account is taken of daylight and vehicle noises. It is assumed that the receiving lens has an aperture of 10 ft^2 and a field of view of 10^{-6} sr, and that the radiation from the vehicle is the same as that from a blackbody at 2500°K with a cross-sectional area of 5 m^2. For a range of 100 miles and an atmospheric absorption of 6 dB (clear atmosphere), the source required for an omnidirectional system on the vehicle must deliver a peak power of 50 kW and an average power of 50 W. These requirements exceed the present state of the art (Ref. 69) by a factor of about 10^4 and the predicted near-future state of the art (Ref. 72) by a factor of about 50.

Without a major advance in device technology, a tracking and pointing system is required for a reentry optical system, even in clear weather. If a lower bound of about 10 deg is placed on the transmitted beam width due to vehicle oscillations, the source requirements become about 100 W of peak and 100 mW of average power. It is reasonable to expect that such a transmitting system can be built within a 10-lb weight limit with near-future technology, but the problems of tracking the ground station and pointing the transmitting system are much more imposing. It is doubtful that these can be solved for a reentry environment within reasonable weight limits, unless the trajectory is well known in advance so that pointing information can be stored.

The systems described are extremely vulnerable to weather, require complicated ground equipment, and each requires considerable advances in technology. However, the research required for optical communications systems is likely to continue as an adjunct to the space exploration program, and it is to be expected that better devices and lightweight tracking systems will be developed. We conclude that an optical reentry system is a future possibility but that at the present time it appears to be less promising than millimeter systems.

IV. SUMMARY AND RECOMMENDATIONS

To accomplish the stated objective of defining a program of research and development directed toward solving the lifting reentry communications problem, a comprehensive list of proposed blackout alleviants has been assembled and evaluated. The feasible techniques have been selected and the pertinent problem areas have been delineated. A summary of these conclusions is presented here.

A recommended research program based on the conclusions of this report is described. This program is organized into three phases. Only the first two phases are described in detail, since the design and testing effort of the final phase depends upon the evaluations of the results of the other phases.

A. SUMMARY

1. FEASIBILITY OF PROPOSED SYSTEMS

The following conclusions can be drawn from the feasibility analysis of Section III:

1. The communications fin is the most promising of the aerodynamic shaping techniques. This technique is desirable because it is simple and, therefore, reliable, requires a lower systems margin since the plasma is effectively eliminated from the signal path, and is relatively unaffected by the oscillations of the vehicle. The primary disadvantage of the technique is the aerodynamic design constraint that it introduces.
2. The techniques based on injection of coolant into nonexpanding flows and of electronegative species into expanding flows are the next most promising. These techniques have the disadvantage of requiring the perforation of the vehicle surface and being sensitive to oscillations of the vehicle, particularly in the case of expanding flows.
3. The use of the magnetic window, with conventional magnets, appears feasible, but it may be the heaviest of the feasible alternatives. It is likely that information from future experiments will force a revision of the weight-penalty estimate and,

hence, a reevaluation of the magnetic window feasibility. The use of a superconducting magnet appears feasible only for short missions, since it requires the maintenance of low temperature.

4. Modification of standard communications systems to obtain margins that exceed the plasma attenuation is not feasible because such a technique involves excessive weight and excessive reduction in information transmission rates.

5. Communications systems characterized by signal frequencies outside the standard range are not practicable at the present time. High-frequency band systems are capable of communication only at considerably reduced information rates, whereas, millimeter and optical systems involve equipment specifications that are beyond the present state of the art.

6. Injection of gases, liquids, or solids into the nonexpanding flow to reduce free electron concentration by attachment is not feasible since, in each case, the effect is of insufficient magnitude.

These conclusions are summarized in the following tabulation. As indicated, the systems fall into four separate categories: currently most promising; possible with an advance in state of the art; limited utiiity; and not feasible.

1. CURRENTLY MOST PROMISING

   a. Local Aerodynamic Shaping

   b. Coolant Injection (nonexpanding flows)

   c. Electrophilic Injection (expanding flows)

   d. Magnetic Window (conventional magnet)

2. POSSIBLE WITH AN ADVANCE IN STATE OF THE ART

   a. Millimeter Waves

   b. Injection Lasers

3. LIMITED UTILITY

   a. HF Band Systems

   b. Magnetic Window (superconducting magnet)

4. NOT FEASIBLE

a. Increase in Transmitter Power

b. Decrease in Information Rate

c. Chemical Injection (nonexpanding flows)

d. Electron Absorbing Particles

2. PROBLEM AREAS

The following discussion is limited to systems found to be most promising within the present state of the art.

1. In the case of the communications fin, research must determine the extent to which vehicle stability is affected (and the associated weight penalty), accurate heat transfer rates, and the materials best suited to the construction of the fin.

2. For coolant injection, further research must determine the pertinent properties of the evaporation and mixing processes, the important reaction rates, and the relationship of the window size to its effectiveness.

3. In the case of injection of electronegative species into expanding flows, the effect of vehicle design on the flow field, the details of the chemical kinetics, and the solution to the distribution problem must be determined.

4. For the magnetic window technique, research must determine realistic weight penalties, the effect of aperture size and field inhomogeneities, and the incidence of rf breakdown on system performance.

B. RECOMMENDED RESEARCH PROGRAM

1. INTRODUCTION

The development of any of the apparently feasible systems to the point of flight test can be logically accomplished in three phases:

1. Phase I is research effort aimed toward resolving the most critical problems, that is, those areas where the results could indicate that the estimate of feasibility of any of the systems is grossly in error.

2. Phase II is research and development effort aimed at providing presently unavailable qualitative design information. This implies a partial freeze in the design of the systems that have been selected at the end of Phase I.

3. Phase III is the detailed design of flight systems in conjunction with development testing. At the end of Phases I and II, a comparative evaluation of the various systems is performed, and only the most promising systems are selected for further development.

Figures 46 and 47 give a graphical representation of Phases I and II of the recommended program. It is emphasized that the recommended research and development program is based on the assumption that sufficient funds are available for simultaneous development of the four apparently feasible systems. Should only partial funding be available, further concentration of effort will be required, that is, an a priori selection will have to be made from among the four systems. To this end, and based on our earlier discussions of the relative advantages and disadvantages of the feasible techniques, the following priority order for development has been established:

1. Aerodynamic shaping
2. Coolant injection (nonexpanding flows)
3. Electrophilic injection (expanding flows)
4. Magnetic window

2. PHASE I

Phase I is designed to take advantage of the overlap in the nature of effort required by the various techniques. Hence, the research efforts are grouped by relevant technological areas rather than by effort required for each technique. Four major areas or tasks can be identified.

a. Task I-1: External Flow Fields About Lifting Shapes

This task is relevant to both the aerodynamic shaping technique and the expanding flow technique. The research objectives are

1. Determine stability criteria for typical gliding reentry vehicles fitted with a communication fin. This effort will include finding

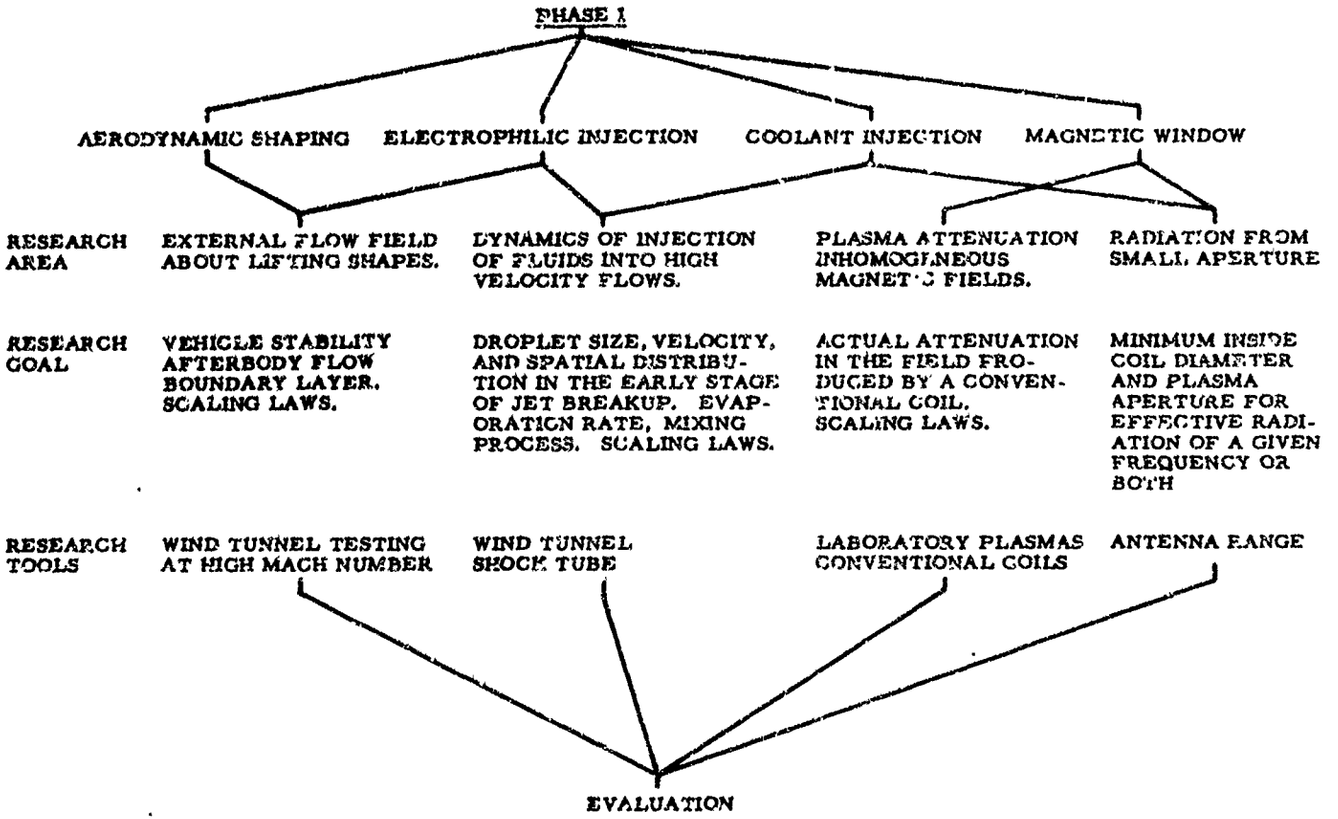

Fig. 46. Recommended Research Program: Phase I

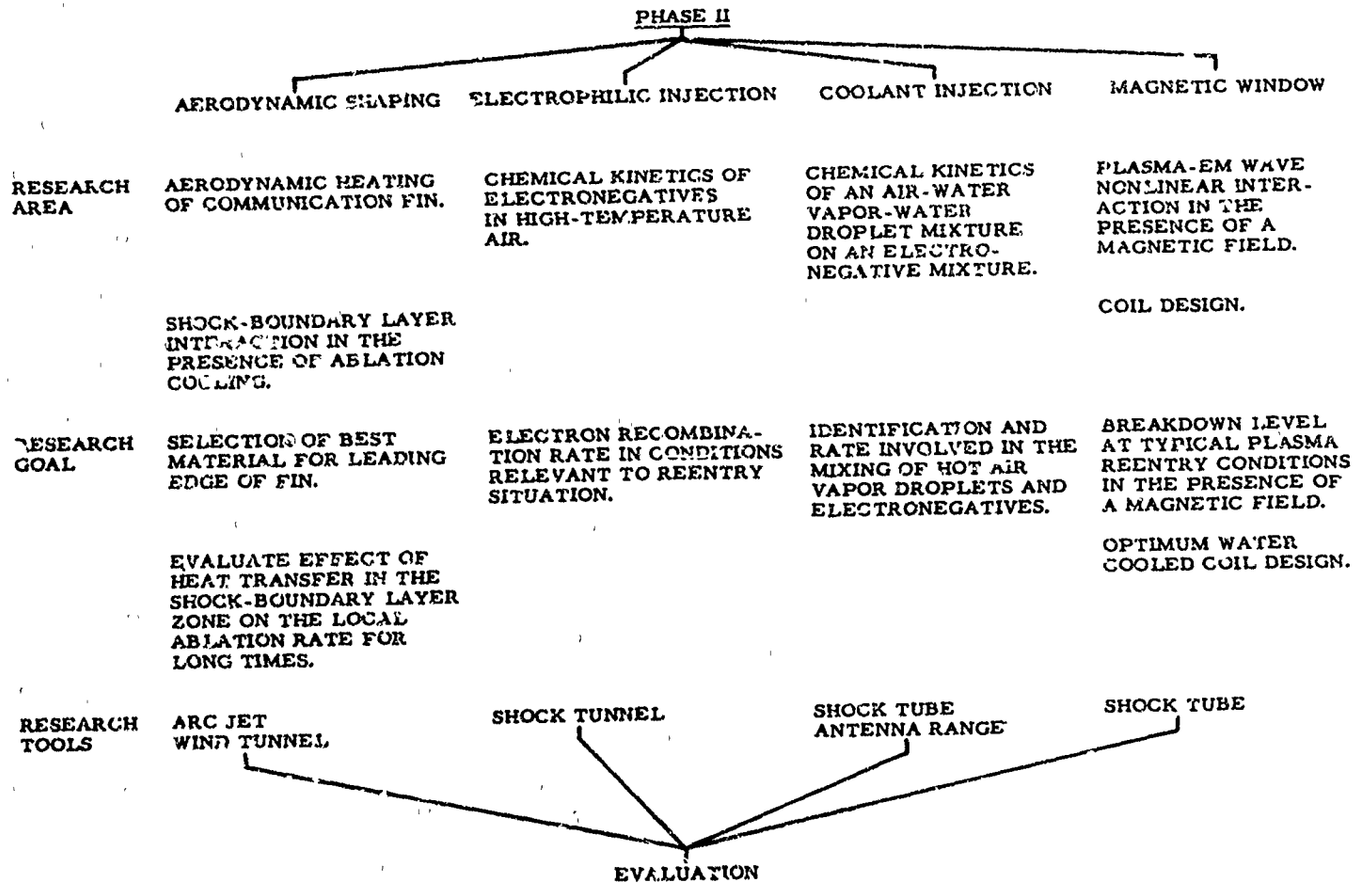

Fig. 47. Recommended Research Program: Phase II

the optimum configuration that will minimize the weight penalty incurred by restoring the aerodynamic stability of the vehicle once it has been disturbed by the addition of the fin.

2. Establish the best body-stabilizer configuration that will achieve proper expanding flow conditions over the stabilizer-antenna location. This will include a partial mapping of the flow field in the area of interest, the investigation of the exact location of the boundary layer separation over the side of the vehicle, and static pressure measurements at the antenna location.

3. Develop scaling laws.

Accomplishment of Task I-1 will require extensive wind tunnel testing at high Mach number, which can be done at existing government facilities.

b. Task I-2: Dynamics of Injection of Fluids into High Velocity Flows

This task is relevant to both the coolant injection technique and the expanding flow technique. The overall objective is the development of a fluid injection technique that will provide the proper distribution of vapor-air mixture at the antenna location. The following research program will be necessary to attain the overall objective:

1. Investigate droplet size, velocity, and spatial distribution in the early stages of the breakup of a liquid jet normal to a high speed flow. An understanding of this phase of the injection process is important in that it provides the initial conditions for the subsequent evaporation and mixing process.

2. Determine evaporation rate of small droplets suspended in high temperature air at pressure level corresponding to reentry conditions. This investigation will lead to a greater knowledge of the evaporation relaxation time and, consequently, of the separation required between the injection point and the antenna.

3. Investigate the mixing process in the wake of the injection jet. This can become a serious problem if the evaporation relaxation time is relatively long. In such a situation, it may not be possible to limit the lateral diffusion of the coolant, which means an inefficient utilization rate and increased coolant weight.

4. Perform analytical studies supporting items 1, 2, and 3 and leading to required scaling laws.

Facilities required to carry out Task I-2 are a high speed wind tunnel and a shock tube. The wind tunnel will be required to simulate the flow geometry necessary for items 1 and 3 of this task. The shock tube is necessary to simulate flow conditions for item 2.

c. Task I-3: Plasma Attenuation in Inhomogeneous Magnetic Fields

Task I-3 is relevant to the magnetic window techniques with conventional magnets. The objective of this task is a precise determination of the plasma attenuation in the presence of the inhomogeneous magnetic field produced by a coil. Such a determination is critical because of its great influence on the weight of the coil. Required are the actual attenuation of the communication signal as a function of magnetic field strengths, the effect of displacement of the coil from the plasma slab, and details of the coil geometry.

The approach to this problem should be experimental, involving an experiment conducted in the proper coil geometry with a laboratory produced plasma slab. Concurrently, a suitable scaling theory should be developed.

d. Task I-4: Radiation from Small Apertures

Task I-4 is relevant to the magnetic window technique and injection cooling. The objective is the determination of the minimum allowable size of the aperture afforded either by the region of alleviated plasma or by the inside diameter of the magnet coil to accommodate an efficient radiator at the telemetry frequency band. This problem is of importance for the magnetic window technique because of the strong dependence of the weight of the magnet as a function of inside diameter for a given magnetic field.

Required are the antenna characteristics of the communication system in the presence of a simulated plasma aperture or of the magnetic coil in a free space environment. An experiment of this nature can be performed on a standard antenna range.

3. PHASE II

In this phase of the recommended program, the various tasks are defined in terms of each particular alleviation technique as there is very little overlap in technological area. Consequently, concentration of effort on each technique is the most effective method of obtaining the desired quantitative design information.

a. Task II-1: Heat Transfer Studies

This task is relevant to the aerodynamic shaping technique. The objective is twofold: (1) evaluation of the material best suited for the leading edge of the fin and its incorporation to the fin structure; (2) evaluation of the effect of localized increase in heat transfer on the ablating bottom surface of the vehicle due to the interaction of the vehicle boundary layer and the fin shock.

The first part of the objective is intended to check the assumption that a fin can be built to withstand the long heating period without losing its original shape. An arc jet facility will be required to simulate the reentry environment.

Part two of the objective is necessary because of a possible catastrophic interaction between the localized increased ablation rate in the vicinity of the shock-boundary layer interaction zone and the flow field. This problem could be best investigated in an arc jet facility.

b. Task II-2: Chemical Kinetics of Electronegative Species in High Temperature Air

This task is relevant to the expanding flow alleviation technique. The objective is a better knowledge of the electron recombination process in an expanding flow of a mixture of high temperature air and electronegative material. Required is the relaxation time for the process at conditions relevant to reentry. An accurate estimate of the relaxation time of the electrons toward equilibrium is of fundamental importance in the prediction of the electron density in the vicinity of the stabilizer antenna.

A suitable experimental program for Task II-2 can be carried out in the expansion nozzle of a small shock tunnel, the electron density being monitored in the nozzle by means of a microwave interferometer.

c. Task II-3: Chemical Kinetics of a Mixture of Water Vapor and Droplets in High Temperature Air

This task is relevant to the coolant injection technique. The objective is knowledge of the rate of electron recombination in a mixture of water vapor and droplets in high temperature air. A secondary objective is the investigation of the acceleration of the recombination process by the addition of electronegative material in the primary mixture. An accurate estimate of the relaxation of the recombination process is necessary to calculate the optimum position of the injection jets with respect to the telemetry antenna.

An experimental program will be necessary to fulfill the objective of this task. A shock tube may be the best research tool for such an investigation, provided the proper suspension of vapor and water droplets can be established in the test gas.

d. Task II-4: Breakdown Studies

This task is relevant to the magnetic window technique. The objective is the determination of the breakdown level at typical reentry conditions in the presence of a magnetic field. The problem arises because, in the magnetic window technique, it is necessary to raise the power of the transmitter to such a level (~10 W/cm^2) that breakdown of the plasma in the vicinity of the antenna may become a problem.

This task requires an experimental approach, with emphasis placed upon producing the proper plasma conditions rather than upon a geometric simulation of the reentry situation. A shock tube will be suitable for such an investigation.

e. Task II-5: Optimum Coil Design Studies

This task is relevant to the magnetic window technique. The objective is the design and development of a boiling-water-cooled magnet coil and its integration into the vehicle structure.

The main problem is the design of a coil that can be mounted very close to the plasma sheath, the coil weight being proportional to the square of the distance between the sheath and the coil. It is possible that some modification of the vehicle skin and associated ablation material will be required to produce a minimum weight system.

4. PHASE III

Phase III of the program is the actual production of flight hardware for specific missions. The information acquired from the first two phases of the recommended research effort should be sufficient for the design and development of communications systems that will function adequately for a wide variety of reentry missions.

REFERENCES

1. Proc. First Symposium on the Plasma Sheath, "Its Effects on Communication and Detection," Boston, 7-9 December 1959, AFCRL-TR-60-108, Air Force Cambridge Research Lab.; also, selected papers, Planetary and Space Sci. 6, (1961).

2. Proc. Second Symposium on the Plasma Sheath, "Its Effect upon Reentry Communication and Detection," Boston, 10-12 April 1962. Unclassified papers, W. Rotman, H. K. Moore, and R. Papa, eds., Electromagnetic Aspects of Hypersonic Flight, Spartan Books, Inc., Baltimore (1964).

3. Proc. Third Symposium on the Plasma Sheath, "Plasma Electromagnetics of Hypersonic Flight," Boston, 21-23 September 1965 (to be published).

4. S. Feldman, Hypersonic Gas Dynamic Charts for Equilibrium Air, RR40, Avco-Everett Research Lab., Everett, Mass. (January 1957).

5. M. F. Romig, Conical Flow Parameters for Air in Dissociation Equilibrium, RR7, Convair Scientific Research Lab., San Diego, Calif. (May 1960).

6. H. M. Musal, Jr., Plasma Frequency and Electron Collision Frequency Charts for Hypersonic Vehicle Equilibrium Flow Fields in Air, TR 62-209C, General Motors Corp. Defense Research Lab., Santa Barbara, Calif. (December 1962).

7. C. E. Witliff and J. T. Curtis, Normal Shock Wave Parameters in Equilibrium Air, Rept. CAL-111, Cornell Aeronautical Lab., Inc., Buffalo, New York (November 1961).

8. J. G. Logan, Jr., and L. E. Treanor, Tables of Thermodynamic Properties of Air from 3000°K to 10000°K at Intervals of 100°K, BE-1007-3-A, Cornell Aeronautical Lab., Inc., Buffalo, New York (January 1957).

9. H. Serbin, "Supersonic Flow Around Blunt Bodies," J. Aerospace Sci. 25, 58-59 (1958).

10. E. Fletcher, Conical Flow FA 013A, ATN 64 (4810-51)-1, Aerospace Corp. (March 1964).

11. R. W. Truitt, Fundamentals of Aerodynamic Heating, Ronald Press Co., New York (1960), Chap. V.

12. E. R. Van Driest, "Investigation of Laminar Boundary Layer in Compressible Fluids Using the Crocco Method," TN 2597, NACA.

13. S. C. Lin, and J. D. Teare, "Rate of Ionization Behind Shock Waves in Air, II. Theoretical Interpretations," Phys. Fluids 6, 355-375 (1963).

14. F. A. Vicente, "Chemistry Effects on r.f. Attenuation During Re-Entry," J. Spacecraft Rockets (to be published).

15. R. H. Edsall, and P. E. Bisbing, "Analysis of Communications Attenuation Data for Blunt and Slender Re-Entry Vehicle." Paper presented Third Symposium on the Plasma Sheath, Boston, Mass. 21-23 September 1965 (S).

16. T. M. Smith, and K. E. Golden, Surface Impedance of a Thin Plasma Sheet, TDR-269(4280-10)-1, Aerospace Corp. (October 1963).

17. R. R. Gold, Reflection and Transmission of Electromagnetic Waves from Inhomogeneous Magnetoactive Plasma Slabs, TDR-169(3230-11)TN-12 Aerospace Corp. (March 1963).

18. K. E. Golden, Radiation from a Waveguide Aperture Covered by a Thin Plasma Layer, TDR-469(5220-10)-5, Aerospace Corp. (September 1965).

19. C. M. Knop, C. T. Swift, and H. Hodara, "Radiation Patterns and Impedance of an Axial Slot on a Plasma Covered Cylinder." Paper presented Third Symposium on the Plasma Sheath, Boston, Mass. 21-23 September 1965.

20. A. T. Villeneuve, "Admittance of Waveguide Radiating into Plasma Environment," IEEE Trans. AP-13 (1), 115-1121 (January 1965).

21. F. J. Tischer, Basic Theory of Space Communications, Van Nostrand and Co., New York (1965), Chap. 19.

22. W. Rotman, "Plasma Simulation by Artificial Dielectrics and Parallel-Plate Media," IRE Trans. AP-10, 82-95 (January 1962).

23. A. Bãnos, unpublished work.

24. M. V. Lopez, A Technique for Foreshortening a Cavity-Backed Slot Antenna, Paper No. 3709, Douglas Aircraft Co., Inc. (October 1965).

25. W. E. Sharfman, and T. Morita, "Power Handling Capability of Antennas at High Altitude," Planetary and Space Sci. 6, 142 (1961).

26. S. C. Brown, Basic Data of Plasma Physics, Technology Press of MIT and John Wiley and Sons, Inc., New York (1959).

27. L. Gould and L. W. Roberts, "Breakdown of Air at Microwave Frequencies," Appl. Phys. 27, 1162 (1956).

28. J. P. Reilly, Microwave Breakdown of the Air Around a Conical Reentry Vehicle, Report 214, Avco-Everett Research Lab. (April 1965).

29. M. Epstein, Antenna Breakdown in a Hypersonic Reentry Environment, TDR-669(6240-20)-1, Aerospace Corp. (September 1965).

30. G. N. Krassner and J. V. Michaels, Introduction to Space Communication Systems, McGraw-Hill Book Co., Inc., New York (1964). Chap. VI, VII.

31. F. T. Sinnott, "RF Telemetry Systems--Part I," Microwave J. (July 1965).

32. T. Juliano, Link Analysis, Tracking, Telemetry and Communications, Report CR-141, Martin Co., Baltimore, Md. (February 1965).

33. E. F. Duryea, E. F. Paski, and W. L. Aseniero, "Re-entry H. F. Transmission Experiment." Paper presented at the American Rocket Society 14th Annual Meeting, Washington, D.C., 16-20 November 1959.

34. G. E. Mueller, "A Pragmatic Approach to Space Communication," Proc. IRE 48, 557 (1960).

35. B. B. Storm and E. A. Sanlorenzo, Analysis of Flow about Protuberant Shapes: Application to E. M. Window, TR-354, General Applied Science Labs., Westbury, New York (June 1963).

36. R. H. Adams and J. J. Rossi, Research of Aerodynamic Methods of Producing Antenna Windows in a Plasma Sheath, Sci. Rep. No. 1, Mithras Inc. (October 1964).

37. H. Marfin and E. Good, "Aerospike Antenna Application for Radio Propagation During Re-entry of Lifting Vehicles," AF33(657)8730 (A-63-3105) (October 1962); also, Tech. Doc. Report ASD-TDR-63-227 (A64-10225) (March 1963).

38. P. Miles, and G. Waldman, Laminar Boundary Layer Skin Friction, Heat Transfer and Displacement Thickness Correlations for Sharp Cones, RAD-TM-62-90, Avco Corp., Research and Advanced Development Div., Wilmington, Mass. (November 1962).

39. H. H. Koelle, ed., Handbook of Astronautical Engineering, McGraw-Hill Book Co., Inc., New York (1961).

40. E. G. Kendall, J. I. Slaughter and W. C. Riley, A New Clan of Hypereutectic Carbide Composites, TDR-469(5250-10)-11, Aerospace Corp. (June 1965).

41. R. A. Newlander, Effect of Shock Impingement on the Distribution of Heat-Transfer Coefficients on a Right Circular Cylinder at Mach Number of 2.65, 3.51 and 4.44, Technical Note D-642, NASA (January 1961).

42. L. G. Siler and H. E. Deskins, Effect of Shock Impingement on the Heat Transfer and Pressure Distributions on a Cylindrical-Leading Edge Model at Mach Number 19, AEDC-TDR-64-228, AEDC (November 1964).

43. Hodara, "The Use of Magnetic Fields in the Elimination of Reentry Radio Blackout," Proc. IRE 49, 1825 (1961).

44. Robert G. De Losh, Antenna Window--A Technique for Propagations Through a Plasma Sheath, AFAL-TR-64-302, Air Force Avionics Labs., Wright-Patterson Air Force Base, Ohio (December 1964).

45. Hodara, "Radiation from a Gyro-Plasma Sheathed Aperture," IEEE Trans. AP-11 (1), 2 (1963).

46. W. F. Cuddihy, I. E. Beckwith, and L. C. Schroeder, "A Solution to the Problem of Communications Blackout of Hypersonic Reentry Vehicles," AMRAC Proceedings, IX (II), 187-231 (19[illegible]).

47. T. E. Sims and R. F. Jones, Flight Measurements of VHF Signal Attenuation and Antenna Impedance for the RAM A1 Slender Probe at Velocities up to 17,800 Feet per Second, TM X-760, NASA (March 1963) (C).

48. W. F. Cuddihy, I. E. Beckwith, and L. C. Schroeder, RAM B2 Flight Test of a Method for Reducing Radio Attenuation During Hypersonic Reentry, TM X-902, NASA (October 1963).

49. W. F. Cuddihy, and J. K. Hughes, Simulated Reentry Tests of a Method for Reducing Radio Blackout by Material Addition to Ionized Flow Fields, TM X-988, NASA (August 1964).

50. I. E. Beckwith and J. K. Huffman, Injection and Distribution of Liquids in the Flow Fields of Blunt Shapes at Hypersonic Speeds, TM X-989, NASA (August 1964).

51. P. W. Kuhns, "Effect of Addition of Impurities on Electron-Ion Recombination Times and on Transmission Through Ionized Layers," Electromagnetic Aspects of Hypersonic Flight, Spartan Books, Inc., Baltimore (1964).

52. R. D. Ingebo and H. H. Foster, Drop-Size Distribution for Cross-current Breakup of Liquid Jets in Airstreams, TN 4087, NACA (October 1957).

53. J. E. Broadwell, "Analysis of the Fluid Mechanics of Secondary Injection for Thrust Vector Control," AIAA J 1, 1067-75(1963).

54. J. O. Hinze, Turbulence, McGraw-Hill Book Co., Inc., New York (1959).

55. A. E. Fuhs, Spray Formation and Breakup, and Spray Combustion, AMF/TD No. 1199, Tech. Note No. 4, Sundstrand Turbo (February 1958).

56. A. R. Hanson, E. G. Domich, and H. S. Adams, "Shock Tube Investigation of the Breakup of Drops by Air Blasts," Phys. Fluids 6, 1070-80 (1963).

57. G. Rosen, "Method for the Removal of Free Electrons in a Plasma," Phys. Fluids 5, 737 (1962).

58. D. G. Clifton, Equilibrium Compositions for Carbon-Air Systems at High Temperatures and Several Pressures, TR65-41E, General Motors Corp., Santa Barbara, Calif. (September 1965).

59. W. Van Tassell, A. Pallone, and H. Schick, A Preliminary Study of the Effect of Ablation Products on Laminar Boundary Layers, RAD-TM-62-74, Avco Corp., Research and Advanced Development Div., Wilmington, Mass. (December 1962).

60. A. L. Caswell and G. G. Cloutier, "Supersonic Plasma Streams Seeded with Electronegative Gases," Phys. Fluids 7, 602 (1964).

61. M. Berkowitz, "Some Factors in Instrumenting a Missile Nose Cone during Re-entry," Proc. 1958 National Symposium on Telemetering, IRE PGTRC, 22-24 September 1958.

62. R. V. Row, "Radiation Efficiency of Electric and Magnetic Dipole Antenna Surrounded by a Small Spherical Shell of Lossy Dielectric," IEEE Trans. AP-12 (5), 646 (1964).

63. J. W. Dees, V. E. Derr, J. J. Gallagher, and J. C. Wiltse, "Beyond Microwaves," Intern. Sci. Technol. (November 1965).

64. G. N. Krassner and J. V. Michaels, op. cit., p. 350.

65. B. J. DuWaldt, "Research on the Suitability of Millimeter Wavelength Systems for Space Applications." Paper presented at Western Electronic Show and Convention, Los Angeles, 25-28 August 1964.

66. D. C. Forster, "Mid-1964 Review of Available Millimeter-Wave Sources." Paper presented at Western Electronic Show and Convention, Los Angeles, 25-28 August 1964.

67. E. S. Rosenblum, "Atmospheric Absorption of 10-400 KMCPC Radiation," Microwave J. (March 1961).

68. R. J. Keyes, T. M. Quist, R. H. Rediker, M. J. Hudson, C. R. Grant, and J. W. Meyer, "Now Out of the Lab--Modulated Infrared Diode," Electronics (April 1963).

69. B. Miller, "Gemini Laser Test May Speed Future Use," Aviation Week and Space Technol. (December 1965).

70. J. P. Gordon, "Optical Communication," Intern. Sci. Technol. (August 1965).

71. C. M. Johnson, "Injection-Laser Systems for Communications and Tracking," Electronics (December 1963).

72. B. S. Goldstein and J. D. Welch, "The Application of Semiconductor Optical Radiators to Space Communication," IEEE Trans. Commun. Electron. 74, 433 (1964).

UNCLASSIFIED

Security Classification

DOCUMENT CONTROL DATA - R&D

(Security classification of title, body of abstract and indexing annotation must be entered when the overall report is classified)

1. ORIGINATING ACTIVITY (Corporate author)	2a. REPORT SECURITY CLASSIFICATION
Aerospace Corporation El Segundo, California	Unclassified
	2b. GROUP

3. REPORT TITLE

LIFTING REENTRY COMMUNICATIONS: VOLUME I. A COMPARATIVE EVALUATION OF POTENTIAL SYSTEMS

4. DESCRIPTIVE NOTES *(Type of report and inclusive dates)*

5. AUTHOR(S) *(Last name, first name, initial)*

Dix, Donald M., Golden, Kurt E., Taylor, Edward C., Kolpin, Marc A., and Caron, Paul R.

6. REPORT DATE	7a. TOTAL NO. OF PAGES	7b. NO. OF REFS
May 1966	126	72

8a. CONTRACT OR GRANT NO.	9a. ORIGINATOR'S REPORT NUMBER(S)
AF 04(695)-669	TR-669(6220-10)-3, Vol I
b. PROJECT NO	
c.	9b. OTHER REPORT NO(S) *(Any other numbers that may be assigned this report)*
d.	SSD-TR-66-73, Vol I

10. AVAILABILITY/LIMITATION NOTICES

This document is subject to special export controls and each transmittal to foreign governments or foreign nationals may be made only with prior approval of SSD(SSTRT).

11. SUPPLEMENTARY NOTES	12. SPONSORING MILITARY ACTIVITY
	Space Systems Division Air Force Systems Command Los Angeles, California

13. ABSTRACT

Aerodynamic and electromagnetic calculations are performed to evaluate quantitatively the magnitude and duration of communications blackout for lifting reentry vehicles. A comprehensive list of proposed alleviation techniques is compiled and evaluated on the bases of communication quality, weight, flexibility, and required research. It is concluded that the techniques of local aerodynamic shaping, injection of coolant into the nonexpanding part of the flow, injection of electronegative species into the expanding part of the flow, and use of magnetic window are apparently feasible. A program of further research, which is required for a solution of the blackout problem, is delineated.

DD FORM 1473 (FACSIMILE)

UNCLASSIFIED

Security Classification

14 KEY WORDS

Communication Systems
Reentry Communications
Lifting Reentry
Antenna Window
Aerodynamics
RF Attenuation
RF Breakdown
Aerodynamic Shaping
Fluid Injection
Magnetic Window
Electrophylic Seeding
Millimeter Waves
Optical Communications Systems
High-Frequency Communications
Communication Blackout

Abstract (Continued)